

RADIAL BASIS FUNCTION BASED FINITE DIFFERENCE METHODS FOR OPTION PRICING PROBLEMS

by

ALPESH KUMAR



Department of Mathematics and Statistics

Indian Institute of Technology, Kanpur

May, 2015

RADIAL BASIS FUNCTION BASED FINITE DIFFERENCE METHODS FOR OPTION PRICING PROBLEMS

A Thesis Submitted

in Partial Fulfilment of the Requirements

for the Degree of

DOCTOR OF PHILOSOPHY

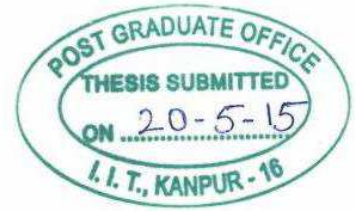
by

ALPESH KUMAR



to the

**Department of Mathematics and Statistics
Indian Institute of Technology, Kanpur
May, 2015**



CERTIFICATE

It is certified that the work contained in the thesis titled “**Radial basis function based finite difference methods for option pricing problems**” by **Alpesh Kumar (Roll No. Y8108062)** has been carried out under my supervision. The results presented in this thesis have not been submitted to any other university or institute for the award of any degree or diploma.

A large, stylized handwritten signature in blue ink, belonging to Mohan K. Kadalbajoo.

Mohan K. Kadalbajoo
Professor

Department of Mathematics and Statistics
Indian Institute of Technology Kanpur
Kanpur, India
May, 2015

Synopsis

Name of the Student	: Alpesh Kumar
Roll Number	: Y8108062
Degree for which submitted	: Ph.D.
Department	: Mathematics and Statistics
Thesis Title	: Radial basis function based finite difference methods for option pricing problems
Thesis Supervisor	: Prof. Mohan K. Kadalbajoo
Month and year of submission	: May, 2015

The Black-Scholes option pricing formula introduced by Black and Scholes, had revolutionized the way financial markets priced, hedge and understood derivatives, and in particular, options. It provides an analytical framework, which on one hand allows to determine how sensitive is price towards various parameters and on the other hand helps to extract price and risk.

Options are a special type of derivative securities because their values are derived from the value of some underlying security. Most options can be grouped into either of the two categories: European options, which can be exercised only on the expiration date, and American options, which can be exercised on or before the expiration date. American options are much harder to deal with than European ones. Since at each time we have

to determine not only the option value but also the location where it should be exercised. This implies that the evaluation of American option is a free boundary value problem. Ever since the seminal work of Black and Scholes, the differential equation approach in pricing options has attracted many researchers.

In the past two decades, researchers have developed state of the art solvers to price these options. Our main focus in this thesis is to develop new numerical analysis tools to solve some partial differential equations arising in option pricing problems. Depending upon the inter-relationship of the financial derivatives, the dimension of the associated problem increases drastically and hence conventional methods (for example, the finite difference methods or finite element methods) for solving them do not provide satisfactory results.

To resolve this issue, a new mesh free method based on Radial Basis Functions (RBFs) is currently undergoing active research. These methods are often better suited to cope with changes in the geometry of the domain of interest than classical discretization techniques. These methods aim to eliminate the structure of the mesh and approximate the solution using a set of random points rather than points from grid discretization. The basic problem with the RBFs based collocation approach is ill conditioning nature of the resulting system, due to use of globally supported radial basis functions.

In this thesis a ‘local’ grid free scheme based on Radial Basis Functions is developed for solving partial differential and partial integro-differential equations. Representing RBF approximation in terms of cardinal functions and restricting the number of supporting nodes in the support domain of each center node, are the two crucial steps in the construction of the new local scheme. The schemes so developed are applied to solve standard and non-standard option pricing problems. The methods in each of these cases are analyzed for stability and thorough comparative numerical results are provided.

The thesis comprises of eight chapters followed by an exhaustive bibliography.

In **Chapter 1**, we provide the brief introduction of option pricing and a literature review for the numerical methods to solve standard and non standard options problems. We also provide the basic feature of Radial basis function interpolation and radial basis function collocation method. We also provide an overview of the computational problem

related to global collocation method.

In **Chapter 2**, we describe the valuation of American option problems. The value of an American option at the time T of expiry of the contract, with strike price E is readily known as a function of the underlying assets s . Let $V(s, \tau)$ is value of American option at time τ with the risk free interest rate by r , and the volatility σ . The price V of the option can be obtained from the solution of the linear complementarity problem

$$\left\{ \begin{array}{rcl} \frac{\partial V}{\partial \tau} + \mathcal{L}V & \leq & 0, \\ V(s, \tau) - \mathcal{G}(s) & \geq & 0, \\ (\frac{\partial V}{\partial \tau} - \mathcal{L}V)(V(s, \tau) - \mathcal{G}(s)) & = & 0, \\ V(s, T) & = & \mathcal{G}(s), \end{array} \right. \quad (0.0.1)$$

for $(s, \tau) \in (0, \infty) \times (0, T]$. Where \mathcal{L} denotes the Black-Scholes operator defined by

$$\mathcal{L}V(s, \tau) = \frac{1}{2}\sigma^2 \frac{\partial^2 V}{\partial s^2} + rs \frac{\partial V}{\partial s} - rV, \quad (0.0.2)$$

and $\mathcal{G}(s)$ is payoff function, define by

$$\mathcal{G}(s) = \max(E - s, 0). \quad (0.0.3)$$

We present a radial basis function based finite difference method to solve American option problems. In this strategy, it is expected that the choice of the shape parameter will not be a critical issue, from stability point of view as in case of global collocation method. We add a small nonlinear penalty term to the classical Black Scholes equation to remove the free and moving boundary and thereby converting a non linear partial differential equation with fixed domain. The numerical discretization is done with the theta method in which the linear part is treated implicitly where as non linear part is treated explicitly. The stability of the proposed numerical scheme is also discussed. It has been shown that the present method is second order convergent. We also provide the comparison of the proposed scheme with radial basis function collocation method and other numerical methods available in the literature.

In **Chapter 3**, we present a radial basis function based operator splitting method to price American option in fixed domain. The numerical discretization is done with the

implicit backward difference method. Numerical experiments for one asset and two assets problems have been carried out. It will be shown that the present method is second order convergent. We also provide the comparison of the proposed scheme with radial basis function collocation method and other numerical methods available in the literature.

In **Chapter 4**, the proposed method has been extended to solve European type Asian call option. The value of an Asian option can be characterized by a two state partial differential equation

$$\frac{\partial V}{\partial \tau} + \frac{1}{2}\sigma^2 S^2 \frac{\partial^2 V}{\partial^2 S} + rS \frac{\partial V}{\partial S} + S \frac{\partial V}{\partial I} - rV = 0 \quad (0.0.4)$$

$$V(S, I, T) = \max\left(\frac{I}{T} - E, 0\right). \quad (0.0.5)$$

Here $S = S(\tau)$ denote the price of underlying asset, σ the volatility of underlying asset, r -the risk free interest rate, which is fixed through out the time period of interest, E is the exercise price of the option, T the time of expiry and $I := I(\tau) = \int_0^\tau S(\varphi)d\varphi$ denotes that the average price of the underlying asset in some time interval.

A one state variable partial differential equation is presented that models the Asian call option. The governing equation is discretized by the well known theta method. The performance of the proposed scheme is investigated for different parameters, by comparing the results with other existing methods available in the literature. It is observed that the proposed method approximates Asian options very nicely.

In **Chapter 5**, we present a numerical method to price an American put option on zero-coupon bond. Let us consider the price of zero coupon bond with face value K and maturity T^* . Then the bond price $B(r, \tau)$, satisfies the following equation:

$$\frac{\partial B}{\partial \tau} + \frac{1}{2}\sigma^2 r^{2\gamma} \frac{\partial^2 B}{\partial r^2} + \kappa(\theta - r) \frac{\partial B}{\partial r} - rB = 0, \quad (0.0.6)$$

$$B(r, T^*) = K. \quad (0.0.7)$$

Now similar to the American put option on stocks, there is unknown optimal interest rate $r^*(\tau)$, called the early interest rate for American put option on bond. It is the smallest value of the interest rate at which the exercise of the put becomes optimal. The American

put option value satisfy the following linear complementarity problem:

$$\begin{cases} \frac{\partial V}{\partial \tau} + \mathcal{L}V \leq 0, \\ V(r, \tau) - g(r, \tau) \geq 0, \\ (\frac{\partial V}{\partial \tau} + \mathcal{L}V)(V(r, \tau) - g(r, \tau)) = 0, \end{cases} \quad (0.0.8)$$

for $(r, \tau) \in (0, \infty) \times (0, T]$ together with initial condition

$$V(r, T) = g(r, T) \quad (0.0.9)$$

and boundary conditions

$$\begin{cases} V(0, \tau) = g(0, \tau), & r \rightarrow 0 \\ V(r, \tau) = g(r, \tau), & r \rightarrow \infty, \end{cases} \quad (0.0.10)$$

where $g(r, \tau) = \max(E - B(r, \tau, T^*), 0)$ and $\mathcal{L} = \frac{1}{2}\sigma^2 r^{2\gamma} \frac{\partial^2}{\partial r^2} + \kappa(\theta - r) \frac{\partial}{\partial r} - r$.

It is worth to be noted that E should be strictly less than $B(0, \tau, T^*)$, otherwise exercising the option would never be optimal.

Using the concept that the American option can be formalized in the form of a linear complementarity problem, we proposed a radial basis function based operator splitting method. The time semi discretization is done by an implicit method and operator splitting method to treat the American constraints and space discretization of the underlying equation is done by using RBF based finite difference method. In numerical experiments, the prices of zero-coupon bond, European bond option and the American put option are given and the optimal early interest rate is also provided.

In **Chapter 6**, we have considered partial integro-differential equation that describes American and European option under jump diffusion model. Let $V(S, \tau)$ represent the value of a contingent claim that depend on the underlying asset price S with current time τ . Then $V(S, \tau)$ satisfy following backward partial integro differential equation

$$\frac{\partial V}{\partial \tau} + \frac{1}{2}\sigma^2 S^2 \frac{\partial^2 V}{\partial S^2} + (r - \lambda\kappa)S \frac{\partial V}{\partial S} - (r + \lambda)V + \lambda \int_0^\infty V(S\eta)g(\eta)d\eta = 0, \quad (0.0.11)$$

for $(S, \tau) \in (0, \infty) \times (0, T]$, where, r is risk free interest rate and $g(\eta)$ is probability density function of the jump with amplitude η with properties that $\forall \eta g(\eta) \geq 0$ and $\int_0^\infty g(\eta)d\eta = 1$.

The value of V at the expiry date is given by,

$$V(S, T) = \mathcal{G}(S), \quad S \in (0, \infty), \quad (0.0.12)$$

where $\mathcal{G}(S)$ is the pay-off function for the option contract. The function $g(\eta)$ is given

$$g(\eta) := \begin{cases} \frac{1}{\sqrt{2\pi}\sigma_J\eta} e^{-\frac{(\ln \eta - \mu_J)^2}{2\sigma_J^2}} & \text{Merton's model,} \\ \frac{1}{\eta} (p\eta_1 e^{-\eta_1 \ln(\eta)} \mathcal{H}(\ln(\eta)) + q\eta_2 e^{\eta_2 \ln(\eta)} \mathcal{H}(-\ln(\eta))) & \text{Kou's model,} \end{cases} \quad (0.0.13)$$

where μ_J and σ_J are the mean and the variance of jump in return and $\eta_1 > 1$, $\eta_2 > 0$, $p > 0$, $q = 1 - p$, and $\mathcal{H}(\cdot)$ is the Heaviside function. We propose an implicit explicit numerical scheme namely IMEX-BDF2 to discretize the equation. The stability of the proposed scheme is also analyzed. The numerical scheme derived for European option is further extended for American option by using operator splitting method. The numerical results for Merton's and Kou's models are given. The efficiency of the proposed IMEX scheme is demonstrated in terms of cpu time and accuracy over other existing numerical methods.

In **Chapter 7**, we have coupled the proposed RBF based scheme with a higher order Padé scheme to solve some non standard option like digital option, butterfly spread and barrier options. Numerical results presented in the chapter prove that the proposed RBF-FD scheme is more efficient than the classical finite difference method.

The outcomes are described briefly in concluding section and some directions of the future work are also outlined in **Chapter 8**. The relevant references are appended in the Bibliography.

Dedicated
To
My Parents

List of Publications

1. Mohan K. Kadalbajoo, Alpesh Kumar, and Lok Pati Tripathi, *Application of radial basis function with L-stable Padé time marching scheme for pricing exotic option*. Computers & Mathematics with Applications, 66(4)(2013), 500-511.
2. Alpesh Kumar, Lok Pati Tripathi, and Mohan K. Kadalbajoo, *A numerical study of Asian option with radial basis functions based finite differences method*. Engineering Analysis with Boundary Elements, 50(2015), 1-7.
3. Mohan K. Kadalbajoo, Alpesh Kumar, and Lok Pati Tripathi, *Application of local radial basis function based finite difference method for pricing American options*. International Journal of Computer Mathematics, 92(8)(2015), 1608-1624.
4. Mohan K. Kadalbajoo, Alpesh Kumar, and Lok Pati Tripathi, *An efficient numerical method for pricing option under jump diffusion model*. International Journal of Advances in Engineering Sciences and Applied Mathematics, 7(3)(2015), 114-123.
5. Alpesh Kumar, Lok Pati Tripathi, and Mohan K. Kadalbajoo, *A numerical study of European options under Merton's jump-diffusion model with radial basis function based finite differences method*. Neural, parallel & scientific computations, 21(3-4) (2013), 293-304.
6. Mohan K. Kadalbajoo, Alpesh Kumar, and Lok Pati Tripathi, *A radial basis function based implicit explicit method for option pricing under jump-diffusion models*, Communicated.

7. Mohan K. Kadalbajoo, Alpesh Kumar, and Lok Pati Tripathi, *A RBF based method for pricing American option on zero coupon bond*, Communicated.
8. Mohan K. Kadalbajoo, Alpesh Kumar, and Lok Pati Tripathi, *A radial basis function based operator splitting method for American option problem*, Communicated.

Acknowledgements

It's my privilege to write a thank you note to everyone who helped me with my dissertation.

To start with, I take this opportunity to express my sincere thanks to my thesis supervisor, **Prof. Mohan K. Kadalbajoo**, for guidance and support throughout my doctoral research. His way of giving complete freedom to the student and providing necessary input when needed,‘ helped me to grow up as a researcher. His expertise, skills, and constant support are major pluses for this research.

I would like to give a heartfelt thanks to **Dr. Usha Kadalbajoo**, for her moral support and encouragement throughout this study.

A good support system is important to survive and staying sane. I was lucky to be part of the Department of Mathematics at IIT Kanpur. I take this opportunity to thank Professor Neeraj Misra and Professor Debasis Kundu who always have been encouraging and accommodative.

I also want to thank all of the faculty members of the department for their support and encouragement. A special thanks goes to Prof. A. K. Lal, Prof. V. Raghvendra, Prof. Manjul Gupta, Prof. B. V. Rathish Kumar and Prof. Rama Rawat for their help and advices given to me during the course work. I thank Prof. Prawal Sinha, Prof. Peeyush Chandra, Prof. Pravir Dutt, Prof. S. Ghorai and Prof. D. Bahuguna for their valuable suggestions on several occasions.

I would like to acknowledge my university teacher Prof. B. Rai, Prof. D. P. Chaudhary, Prof. R. P. Shukla who encouraged me to go for higher studies.

I also extend my thanks to all department staff for their cooperation during this period.

I would also like to gratefully acknowledge CSIR India, for providing me financial support for carrying out my research.

I also want to thank some of my seniors Anuradha Jha, Arjun, Puneet, Vikas and Devendra Kumar and also my fellow PhD students: Abdullah, Indira, Ambuj, Ravi, Aneesh, Arbaz, Lok Pati, Minaxi, Arun, Awanish, Surjit. They each helped make my time in the doctoral program one of the most memorable period of my life. I will cherish their memories for long.

A very special thanks goes to my dear friends, Abhishek, Satyapriya, Lokendra, Balwant, Anurag and Preeti Anurag Shukla for their friendship and support. They always encouraged and believed in me.

I would like to say a big thanks my brothers Manish and Ashish and my sister Priya for their love and support, which is beyond any acknowledgement.

May, 2015

Alpesh Kumar

Contents

Synopsis	i
List of Publications	viii
Acknowledgements	x
Contents	xii
List of Figures	xvi
List of Tables	xviii
1 Introduction	1
1.1 Introduction	1
1.1.1 Option pricing: A brief overview	2
1.1.2 The payoff function	3
1.1.3 A simple model for asset pricing	4
1.1.4 Role of Itô's lemma	5
1.1.5 The Black-Scholes equation	6
1.2 Literature review on methods for option pricing problems	9
1.3 Radial basis functions	15
1.4 Radial basis functions interpolation	16
1.4.1 Radial basis functions interpolation with polynomial precision . . .	17
1.5 RBF based collocation method for PDEs	21

1.5.1	Asymmetric collocation	21
1.5.2	Symmetric collocation	22
1.6	Motivation of the work	23
2	A RBF based finite difference method for American option problem	26
2.1	Introduction	26
2.2	Problem description	28
2.2.1	American multi-asset option problem	28
2.2.2	Penalty Method	30
2.3	Development of the local RBF based finite difference method	31
2.3.1	Lagrange representation of RBF interpolation	32
2.3.2	RBF-FD approximation of operators	33
2.4	Implementation of numerical method	35
2.5	Stability Analysis	36
2.6	Numerical simulation and discussion	38
2.6.1	Numerical results for European options	39
2.6.2	Numerical results for American options	41
2.7	Conclusion	46
3	A RBF based operator splitting method for American option problem	48
3.1	The mathematical model	49
3.2	Numerical scheme	50
3.2.1	Operator splitting method	51
3.3	Numerical simulation and discussion	54
3.3.1	Numerical results for European options	54
3.3.2	Numerical results for American options	59
3.4	Conclusion	62
4	A RBF based finite difference method for Asian option	64
4.1	Introduction	64

4.2	The model formulation for Asian option	65
4.3	RBF approximation and time stepping	67
4.3.1	RBF-FD approximation of space operator	67
4.3.2	Temporal approximation	70
4.4	Stability Analysis	70
4.5	Numerical simulation and discussion	71
4.5.1	European call option	72
4.5.2	Asian option	73
4.6	Conclusion	75
5	A RBF based operator splitting method for pricing American option on zero coupon bond	80
5.1	Introduction	80
5.2	The pricing model of zero coupon bond and option	82
5.3	Numerical scheme	84
5.3.1	Operator splitting method	85
5.4	Numerical simulation and discussion	87
5.5	Conclusion	90
6	A RBF based IMEX method for pricing options under jump-diffusion model	92
6.1	Introduction	92
6.2	The mathematical model	94
6.3	Time semi discretizations	96
6.3.1	Stability Analysis	99
6.4	American Options	102
6.5	Numerical simulation and discussion	104
6.5.1	Numerical results for European options	104
6.5.2	Numerical results for American options	111

6.6	Conclusions	114
7	A RBF based L-stable Padé scheme for pricing exotic option	115
7.1	Introduction	115
7.2	Method of Lines semidiscretization	116
7.3	Time stepping scheme	118
7.3.1	A fourth order L-stable method	119
7.3.2	Partial Fractional form of the schemes	119
7.4	Numerical simulation and discussion	121
7.4.1	A digital call option	121
7.4.2	Two-asset digital call option	123
7.4.3	A butterfly spread option	126
7.4.4	Two-asset butterfly spread option	126
7.4.5	A double barrier option	127
7.5	Conclusion	131
8	Concluding remarks and scope for future research	132
8.1	Conclusions Based on the Thesis	132
8.2	Scope for the Future Work	134
	Bibliography	135

List of Figures

2.1	Global domain X and local domain X_i	33
2.2	A typical stability plot for radial basis function based finite difference method	37
2.3	Analytical and numerical approximation of the delta (Δ) and gamma (Γ) respectively.	42
2.4	American and European put option value, and optimal early exercise boundary.	44
2.5	The payoff function of the two-asset American put option (left).The approximate solution of the two-asset American put option at $T=1$	47
3.1	Analytical and numerical approximation of the delta (Δ) and gamma (Γ) respectively.	57
3.2	The payoff function (left) and the approximate solution of the two-asset European put option (right) at $T=1$	58
3.3	American and European put option value, and optimal early exercise boundary.	60
3.4	The payoff function (left) and the approximate solution of the two-asset American put option (right) at $T=1$	62
4.1	A stability plot for RBF-FD method	72
4.2	Error plot for Asian option for parameters $E = 100$, $r = 0.09$ with maturity year $T = 1$ and $T = 3$	76
4.3	Error plot for Asian option for parameter $E = 100$, $T = 1$ with volatility $\sigma = 0.05$, $\sigma = 0.1$, $\sigma = 0.2$ and $\sigma = 0.3$ respectively.	77

5.1	American put option value, and early exercise boundary for strike price $K = 60$.	90
5.2	American put option and early exercise curve for different value of strike price.	91
6.1	European put option value, Delta and Gamma under the Merton model with parameters as provided in the Example 6.5.1.	106
6.2	European put option value, Delta and Gamma under Kou's model at the last time step. The input parameters are provided in the caption of Table 6.7. . . .	110
6.3	American put option value, and optimal early exercise boundary under the Merton model with parameters as provided in the Example 6.5.5.	113
6.4	American put option value, and optimal early exercise boundary under the Kou model with parameters as provided in the Example 6.5.6.	114
7.1	Space time graph of option value and delta for digital call option using (0,4) Padé scheme.	124
7.2	Space time graph of option payoff and option value for two asset digital call option using (0,4) Padé scheme.	125
7.3	Space time graph of option value and delta for butterfly spread using (0,4) Padé scheme.	128
7.4	Space time graph of option payoff and option value for two asset butterfly spread using (0,4) Padé scheme.	129

List of Tables

1.1	Examples of radial basis functions and their order	16
2.1	Value of absolute and relative error for example 2.6.1 with uniform points for different value of ϵ	40
2.2	European put option values and Greeks for example 2.6.1.	40
2.3	Comparison of numerical solutions of European put option for wide range of asset price for example 2.6.2.	41
2.4	Comparison of numerical solutions of American put option for wide range of asset price for example-2.6.3.	43
2.5	Price of American put option using radial basis function with $E = 100, r = 0.08,$ $\sigma = 0.2, T = 3$ years.	44
2.6	Values of options delta (Δ) of American put using radial basis function with $E = 100, r = 0.08, \sigma = 0.2, T = 3$ years.	45
2.7	Option value for the two asset American option pricing problem at different asset prices.	46
2.8	Error and rate of convergence for two asset American option pricing problem.	46
3.1	Numerical value European put options at different asset price with parameters as given in Example 3.3.1.	55
3.2	Numerical result for Delta of European put options at different asset price with parameters as given in Example 3.3.1.	56

3.3	Numerical result for Gamma of European put options at different asset price with parameters as given in Example 3.3.1.	56
3.4	Comparison of European put option for wide range of asset price for example 3.3.1.	57
3.5	Option value for the two asset European put option at different assets prices. .	58
3.6	Price of American put option at different asset price with parameter given in example 3.3.3.	60
3.7	Values of options delta (Δ) of American put option at different asset price with parameter given in example 3.3.3.	61
3.8	Comparison of American put option for wide range of asset price for example 3.3.4.	61
3.9	Option value for the two asset American put option at different assets prices. .	62
4.1	Absolute error and rate of convergence for European call option with uniform points and different values of ϵ	74
4.2	Comparison of numerical solution of Asian option with $S = 100$, $r = 0.09$, and $T = 1$ for a wide range of volatilities.	75
4.3	Comparison of numerical solution of Asian option with $S = 100$, $r = 0.09$, and $T = 3$ for a wide range of volatilities.	78
4.4	Comparison of numerical solution of Asian call option with $S = 100$, $T = 1$ and different value of E , σ and r	79
5.1	Bond price and bond option prices and respective errors with present method for $T^* = 15$, $T = 10$, $r_0 = 0.05$ and $E = 35$	88
5.2	Bond option prices calculate using CIR exact formula and the present method for $T^* = 10$	88
5.3	Percentage relative mispricings in the zero coupon bond with different maturity.	88
5.4	Bond option prices and respective errors under CKLS with present method for $T^* = 10$, $T = 5$, $r_0 = 0.08$ and $E = 35$	89

5.5	American put option value and error at different values of interest rate under CIR model.	89
6.1	Numerical results for European put options under the Merton model at different asset price with parameters as given in Example 6.5.1.	105
6.2	Numerical results for European call options under the Merton model at different asset price with parameters as given in Example 6.5.1.	105
6.3	Numerical result for Delta of European put options under the Merton model at different asset price with parameters as given in Example 6.5.1.	107
6.4	Numerical result for Gamma of European put options under the Merton model at different asset price with parameters as given in Example 6.5.1.	108
6.5	Comparison of different methods for European put options under the Merton model at strike price with parameters as given in Example 6.5.2.	108
6.6	Comparison of different methods for European call options under the Merton model at strike price with parameters as given in Example 6.5.3.	109
6.7	Numerical results for European call options under the Kou model at different asset price with parameters as given in Example 6.5.4.	111
6.8	Numerical results for European put options under the Kou model at different asset price with parameters as given in Example 6.5.4.	111
6.9	Numerical results for American put options under the Merton model at different asset price with parameters as given in Example 6.5.5.	112
6.10	Numerical results for American put options under the Kou model at different asset price with parameters as given in Example 6.5.6.	113
7.1	Option value, error and rate of convergence for the digital call option at strike price E	122
7.2	Option value, error and rate of convergence for the butterfly spread option at strike price E_2	127
7.3	Option value and error at B_1 & B_2 with various value of ϵ for double barrier option.	130

Introduction

1.1 Introduction

There is a growing interest in pricing financial derivatives that can be used to minimize losses caused by price fluctuation of underlying assets. These assets are generally financial objects whose values are known at present but are liable to change in future. Several financial products like future, swaps, forward and option exist in financial markets. Many mathematical models are developed to price options using quantitative analysis. Many successful methods, including numerical methods and analytical approximations are able to price certain options efficiently. Recently developed numerical methods include the Monte Carlo method, binomial method, finite difference methods and finite element methods.

In this thesis, we develop and analyze a special class of methods based on RBFs for solving a number of different types of option problems. RBF methods have been widely used to solve the problems in science and engineering. We apply these methods to solve some of the option pricing problems arising in computational finance. For further understanding on option pricing and to design suitable numerical method for it, we introduce below some basic concepts on option price theory [117, 61].

1.1.1 Option pricing: A brief overview

An option is the right (but not obligation) to buy or sell an asset at a pre specified fixed price within the specific period. The underlying asset typically is a stock, or a parcel of shares of a company. Other examples may include stock indices, currencies or commodities. Since the value of option depends on the value of the underlying asset, option and other related financial instruments are called derivatives. An option is a contract between two parties about trading an asset at a certain future time. One party is the writer, who fixes the terms of the option contract and sells the option. The other party is the holder, who purchases the option, paying the market price, called the premium. The holder of the option must decide what to do with the rights the option contract grants. The decision will depend on the market situation, and on the type of option. There are two types of the option: call and put. The call option gives the holder the right to buy the underlying asset for an agreed price E (called the strike price) by the date T (called maturity date). The put option gives the holder the right to sell the underlying asset for the price E by the date T . It is important to point out that the holder is not obligated to exercise, that is buying or selling the underlying according to the terms of the contracts. In contrast, the writer of the option has the obligation to deliver or buy the underlying for the price E , in the case holder chooses to exercise. The risk situation of the writer differs strongly from that of the holder. The writer receives the premium when he issues the option and somebody buys it. This upfront premium payment compensates the writer for potential liabilities in the future.

Not every option can be exercised at any time $t \leq T$. For European option, exercise is permitted only at expiration T . However, American option can be exercised at any time up to and including expiration date.

In addition to these standard options, which are traded on many financial exchanges, there is another class of option called exotic option. An exotic option is a derivative which has features making it more complex than commonly traded products (e. g. vanilla options). These products are usually traded over-the-counter (OTC), or are embedded in structured

notes. An exotic options can have feature that its payoff at maturity depend not just on the value of the underlying index at maturity, but at its value at several times during the life of the contract. For examples, it could be an Asian option depending on some average, a look-back option depending on the maximum or minimum, a barrier option which ceases to exist if a certain level is reached or not reached by the underlying asset, a digital option, range options, etc.

In this thesis, we discuss both of these options. To this end, we describe below some important concepts which will be useful throughout the thesis.

The value of the option will be denoted by V . The value V depends on the price per share of the underlying, which is denoted by S . This letter S symbolizes stocks, which are the most prominent examples of underlying assets. The variation of the asset price S with time t is expressed by S_t or $S(t)$. The value of the option also depends on the remaining time to expiry $T - t$. That is, V depends on time t . The dependence of V on S and t is written $V(S, t)$.

1.1.2 The payoff function

At time $t = T$, the holder of a European call option will check the current price $S = S_T$ of the underlying asset. The holder has two alternatives to acquire the underlying asset: either buying the asset on the spot market (costs S), or buying the asset by exercising the call option (costs E). The decision is easy: the costs are to be minimal. The holder will exercise the call only when $S > E$. For then the holder can immediately sell the asset for the spot price S and makes a gain of $S - E$ per share. In this situation the value of the option is $V = S - E$. (This reasoning ignores transaction costs.) In case $S < E$ the holder will not exercise, since then the asset can be purchased on the market for the cheaper price S . In this case the option is worthless, $V = 0$.

In summary, the value $V(S, T)$ of a call option at expiration date T is given by

$$V(S_T, T) = \begin{cases} 0 & \text{in case } S_T \leq E \text{ (option expires worth less),} \\ S_T - E & \text{in case } S_T > E \text{ (option is exercised).} \end{cases} \quad (1.1.1)$$

Hence

$$V(S_T, T) = \max\{S_T - E, 0\}. \quad (1.1.2)$$

This function is the payoff function. The payoff function for put option can be defined in a similar fashion.

1.1.3 A simple model for asset pricing

It is often stated that asset prices must move randomly because of the efficient market hypothesis. There are several different forms of this hypothesis with different restrictive assumptions, but they basically imply two things;

- The past history is reflected in the present price , which does not hold any further information,
- Markets respond immediately to any new information about an asset.

Thus the modeling of asset prices is really about modeling the arrival of the new information which affects the price. With the two assumptions above, unanticipated changes in the asset price are modeled as a Markov process.

With each change in asset price, a return is defined to be the change in the price divided by the original value, i.e., $\frac{dS}{S}$. This relative measure of the change is clearly a better indicator of its size than any absolute error.

Now suppose that at any time t the asset price is S . Let us consider a small subsequent time interval dt , during which S change to $S + dS$. How the corresponding return on the asset $\frac{dS}{S}$ might be modeled? The most common model decomposes this return into two parts. One is a predictable, deterministic and anticipated return akin to the return on money invested in a risk free bank. It gives a contribution μdt to the return $\frac{dS}{S}$, where μ is a measure of average rate of growth of the asset price, also known as drift. In simple models μ is taken to be constant. In more complicated models, for example, for exchange rate , μ can be function of S and t .

The second contribution to $\frac{dS}{S}$ models the random change in the asset price in response

to external effects, such as unexpected news. It is represented by a random sample drawn from a normal distribution with mean zero and adds σdX to $\frac{dS}{S}$. Here σ is a number called the volatility, which measures the standard deviation of the return. The quantity dX is the sample from a normal distribution. Putting these contribution together, we get the stochastic differential equation

$$\frac{dS}{S} = \sigma dX + \mu dt \quad (1.1.3)$$

which is mathematical representation of the simple recipe for generating asset price.

1.1.4 Role of Itô's lemma

In real life, asset prices are quoted at discrete intervals of time. There is thus a practical lower bound for the basic time step dt of the random walk (1.1.3). If we use this time step in practice of value options, we would find that we must deal with unmanageably large amount of data. Instead, we set up our mathematical models in the continuous time limit $dt \rightarrow 0$; it is much more efficient to solve the resulting differential equations than it is by direct simulation of the random walk on the practical timescale. In order to do this, Itô's lemma is the most important result about the manipulation of random variables. First we need the following, with probability 1,

$$dX^2 \rightarrow dt \quad \text{as} \quad dt \rightarrow 0. \quad (1.1.4)$$

thus the smaller dt becomes, the more certainly dX^2 is equal to dt .

Suppose that $f(S)$ is smooth function of S and temporarily forget that S is stochastic. If we vary S by small amount dS then clearly f also varies by a small amount provided we are not close to singularities of f . From the Taylor series expansion we can write

$$df = \frac{df}{dS}dS + \frac{1}{2} \frac{d^2f}{dS^2}dS^2 + \dots, \quad (1.1.5)$$

where the dots denote the reminder which is smaller than any of the terms we have retained. Now recall that dS is given by (1.1.3). Squaring it we find that

$$dS^2 = (\sigma S dX + \mu S dt)^2$$

$$= \sigma^2 S^2 dX^2 + 2\sigma\mu S^2 dt dX + \mu^2 S^2 dt^2. \quad (1.1.6)$$

We now examine the order of magnitude of each of terms in (1.1.6). Since

$$dX = O(\sqrt{dt}), \quad (1.1.7)$$

the first term is the largest for small dt and dominates on the other two terms. Thus to leading order

$$dS^2 = \sigma^2 S^2 dX^2 + \dots$$

Since $dX^2 \rightarrow dt$, we get

$$dS^2 \rightarrow \sigma^2 S^2 dt.$$

We substitute this into (1.1.5) and retain only those terms that are at least as large as $O(dt)$. Using also the definition of dS from (1.1.3), we find that

$$\begin{aligned} df &= \frac{df}{dS} (\sigma S dX + \mu S dt) + \frac{1}{2} \sigma^2 S^2 \frac{d^2 f}{dS^2} dt \\ &= \sigma S \frac{df}{dS} dX + \left(\mu S \frac{df}{dS} + \frac{1}{2} \sigma^2 S^2 \frac{d^2 f}{dS^2} \right) dt. \end{aligned} \quad (1.1.8)$$

This is Itô lemma relating the small change in a function of random variable to the small change in variable itself. The result (1.1.8) can be further generalized by considering a function of the random variable S and of time, $f(S, t)$. This entails the use of partial derivatives since there are now two independent variables, S and t . We can expand $f(S + dS, t + dt)$ in a Taylor series about (S, t) to get

$$df = \frac{\partial f}{\partial S} dS + \frac{\partial f}{\partial t} dt + \frac{1}{2} \frac{\partial^2 f}{\partial S^2} dS^2 + \dots$$

Using expression (1.1.3) for dS and (1.1.4) for dX^2 we find that the new expression for df is

$$df = \sigma S \frac{\partial f}{\partial S} dX + \left(\mu S \frac{\partial f}{\partial S} + \frac{1}{2} \sigma^2 S^2 \frac{\partial^2 f}{\partial S^2} + \frac{\partial f}{\partial t} \right) dt. \quad (1.1.9)$$

1.1.5 The Black-Scholes equation

Let us start this section with the discussion of the concepts of arbitrage. One of the fundamental concept in the theory of option pricing is the absence of arbitrage possibilities,

called no arbitrage principle. Let us consider an illustrative example of an arbitrage opportunity. Suppose the price of given stock in exchanges A and B are listed at \$100 and \$102, respectively. Assuming there is no transaction cost, one can lock in riskless profit of \$2 per share by buying at \$100 in exchange A and selling \$102 in exchange B. The trader who engaged in such transaction is called an arbitrageur. If the financial market functions properly, such an arbitrage opportunity can not occur since traders are well aware of the differential in the stock prices and they immediately compete away the opportunity. However, when there is transaction cost, which is common form of market friction, the small difference in prices may persist. For example, if the transaction costs for buying and selling per share in Exchanges A and B are both \$1.50, then the total transaction costs of \$3 per share will discourage arbitrageurs.

More precisely, an arbitrage opportunity can be defined as a self-financing trading strategy requiring no initial investment, having zero probability of negative value at expiration, and yet having some possibility of a positive terminal payoff.

Before describing the Black-Scholes analysis which leads to the value of an option we will use the following assumptions.

- The asset price follows the lognormal random walk (1.1.1).

Other models do exist, and in many cases it is possible to perform the Black-Scholes analysis to derive a differential equation for the value of an option.

- The risk free interest rate r and the asset volatility σ are known function of time over the life of the option.
- There is no transaction cost associated with hedging portfolio.
- The underlying asset pays no dividends during the life of option.

This assumption can be dropped if dividends are known beforehand. They can be paid either at discrete intervals or continuously over the life of the option.

- There are no arbitrages.

The absence of arbitrage opportunities means that all risk free portfolios must earn

the same return.

- Trading of underlying asset can take place continuously.

This is clearly an idealization, but becomes important in the case of transaction cost.

- Short selling is permitted and the assets are divisible. By this assumption, we can buy and sell any portion of the underlying asset, and we may sell assets that we do not own.

Suppose that we have an option whose value $V(S, t)$ depends only on S and t . It is not necessary at this stage to specify whether V is a call or a put; indeed, V can be the value of a whole portfolio of different options. Using Itô lemma, equation (1.1.9) can be written as

$$dV = \sigma S \frac{\partial V}{\partial S} dX + \left(\mu S \frac{\partial V}{\partial S} + \frac{1}{2} \sigma^2 S^2 \frac{\partial^2 V}{\partial S^2} + \frac{\partial V}{\partial t} \right) dt, \quad (1.1.10)$$

which gives the random walk followed by V .

Now construct a portfolio consisting of one option and a number $-\Delta$ of the underlying asset. This number is unspecified as yet. The value of this portfolio is

$$\Pi = V - \Delta S. \quad (1.1.11)$$

The jump in the value of this portfolio in one time-step is

$$d\Pi = dV - \Delta dS.$$

Here Δ is held fixed during the time step; if it were not then $d\Pi$ would contain terms in $d\Delta$. Putting (1.1.3), (1.1.10) and (1.1.11) together, we find that Π follows the random walk

$$d\Pi = \sigma S \left(\frac{\partial V}{\partial S} - \Delta \right) dX + \left(\mu S \frac{\partial V}{\partial S} + \frac{1}{2} \sigma^2 S^2 \frac{\partial^2 V}{\partial S^2} + \frac{\partial V}{\partial t} - \mu \Delta S \right) dt. \quad (1.1.12)$$

The random component in this random walk can be eliminated by choosing

$$\Delta = \frac{\partial V}{\partial S} \quad (1.1.13)$$

This results in a portfolio whose increment is wholly deterministic, i.e.,

$$d\Pi = \left(\frac{\partial V}{\partial t} + \frac{1}{2}\sigma^2 S^2 \frac{\partial^2 V}{\partial S^2} \right) dt. \quad (1.1.14)$$

We now appeal to the concepts of arbitrage and supply and demand, with the assumption of no transaction costs. The return on an amount Π invested in riskless assets would see a growth of $r\Pi dt$ in a time dt . If the right-hand side of (1.1.14) were greater than this amount, an arbitrageur could make a guaranteed riskless profit by borrowing an amount Π to invest in the portfolio. The return for this risk-free strategy would be greater than the cost of borrowing. Conversely, if the right-hand side of (1.1.14) were less than $r\Pi dt$ then the arbitrageur would short the portfolio and invest Π in the bank. Either way the arbitrageur would make a riskless, no cost, instantaneous profit. The existence of such arbitrageur with the ability to trade at low cost ensures that the return on the portfolio and on the riskless account are more or less equal. Thus, we have

$$r\Pi dt = \left(\frac{\partial V}{\partial t} + \frac{1}{2}\sigma^2 S^2 \frac{\partial^2 V}{\partial S^2} \right) dt. \quad (1.1.15)$$

Substituting (1.1.11) and (1.1.13) into (1.1.15) and dividing throughout by dt we arrive at

$$\frac{\partial V}{\partial t} + \frac{1}{2}\sigma^2 S^2 \frac{\partial^2 V}{\partial S^2} + rS \frac{\partial V}{\partial S} - rV = 0 \quad (1.1.16)$$

This is the famous Black-Scholes partial differential equation. By deriving the partial differential equation for a quantity, such as an option price, we have made an enormous step towards finding its value. The main aim of this thesis is to develop new, stable, and faster techniques to find this value by solving the equation. The value of an option should be unique (otherwise, arbitrage possibilities would arise), and so, to find the solution, specifies the behavior of the required solution at some part of the solution domain. This would mostly be achieved by appropriate initial (final) and boundary conditions.

1.2 Literature review on methods for option pricing problems

There are two main approaches to study the problems in finance: a statistical approach and a differential equation approach. Our research is focused on the differential equation

approach and therefore most of the literature that we present in this thesis will be based on this approach.

Brennan and Schwartz [11] were the first to describe finite-difference methods for option pricing. Vazquez [128] presented an upwind scheme for solving the backward parabolic partial differential equation problem in the case of European options. Geske and Shastri [50] compared the efficiency of various finite-difference and other numerical methods for option pricing. In [74, 75] spline based techniques are developed to solve option price problem.

The earliest work on American options is by McKean [91], where a free-boundary problem for the price function and the optimal exercise boundary (the free boundary) is derived. The price function is expressed in terms of the optimal exercise boundary. Moerbeke [95] further extended the analysis and studied the properties of the optimal exercise boundary. Courtadon [25] and Schwartz [116] developed numerical methods to solve the free-boundary problem.

Cho et al. [20] considered a free boundary problem arising in the pricing of an American call option. The free boundary represents the optimal exercise price as a function of time before a maturity date. They developed a parameter estimation technique to obtain the optimal exercise curve of an American call option and its price. For the numerical solution of problem, they adopted a time marching finite element method.

Choi et al. [21] considered the valuation of options written on a foreign currency when interest rates are stochastic and the matrix of the diffusion representing the global economy is strongly coercive. They solved the associated variational inequality for the value function numerically by the finite element method. In the European case, a comparison is made with the exact solution. They also presented a corresponding result for the American option.

Engström and Nordén [32] estimated the value of the early exercise premium in American put option prices using Swedish equity options data. They found the value of the premium as the deviation of the American put price from European put-call parity, and computed a theoretical estimate of the premium. They also used the empirically found premium in

a modified version of the control variate approach to value American puts. Their results indicate a substantial value of the early exercise premium, where the premium derived from put-call parity is higher than the theoretical premium.

Zhao et al. [146] gave three ways of combining compact finite difference methods for American option price on a single asset with methods for dealing with this optimal exercise boundary. The first one is the compact finite difference method which uses the implicit condition that solutions of the transformed partial differential equation be nonnegative to detect the optimal exercise value. The second one is the compact finite difference method that solves an algebraic nonlinear equation obtained by Pantazopoulos [101] at every time step. The third one is the compact finite difference method that refines the free boundary value by a method developed by Adesi [6].

The approach of Lindset and Lund [86] for the valuation of an American put option under stochastic interest rates consists of a combination of a Monte Carlo simulation approach for the valuation of Bermudan options and the valuation technique for American options proposed by Geske and Johnson [48].

Some of the other popular numerical methods that are used so far for pricing American options are the front-fixing method (Wu and Kwok [134] and Nielsen [99]) and the penalty method (Nielsen [99]). Front-fixing methods apply a non-linear transformation to fix the boundary and solve the resulting non-linear problem. Penalty methods on the other hand eliminate the free-boundary by adding a non-linear penalty term to the PDE. Both these methods boil down to solving a set of non-linear equations, the computational speed and accuracy of which largely depends on the initial guess, the problem size and the underlying non-linear solver used.

Brennan and Schwartz [93] approximated the partial derivatives by finite differences. Their algorithm is based on transforming a tridiagonal system to a lower bidiagonal system and then solving this system while enforcing the American constraint.

In [62] Ikonen and Toivanen proposed a technique known as operator splitting for time discretization for solving the linear complementarity problems arising from the pricing of American options. The spacediscretization is done using a central finite difference scheme.

The operator splittings are based on the Crank-Nicolson method and the two-step backward differentiation formula.

Tangman et al. [124] described a new finite difference algorithm for the American option problem which is an improvement of the method proposed by Han and Wu [54]. They used an optimal higher-order compact scheme [120] instead of the Crank-Nicolson scheme used in [54].

The Black Scholes model for the American option problem take the form of moving boundary problem. For this, Forsyth and Vetzal [42], Nielsen [99], Khaliq et al. [80] approximate the model by adding a penalty term yielding a nonlinear partial differential equation on a fixed domain. Nielsen [99] treated the penalty term implicitly and resulting non linear system is solved using a Newton iteration method. Khaliq et al. [80] used the well known θ method with second order central differencing applied to the diffusion operator and upwind differencing of the transport term to avoid oscillation due to spatial discretization. They treat the penalty term explicitly. The corresponding linear implicit scheme then has the form which does not require a nonlinear iteration solver.

In [53], the radial basis function based technique is used to evaluate European, barrier, and Asian options. The governing equation is discretized by Crank-Nicolson scheme and the option price is approximated by the radial basis function based collocation method. Based on an idea of quasi-interpolation and radial basis functions approximation, a fast and accurate numerical method is developed in [58] for solving the Black-Scholes equation for valuation of American options prices. Since this method does not require solving a resultant full matrix, the ill-conditioning problem resulting from using the radial basis functions as a global interpolant can be avoided. It is shown that the method is effective in solving problems with free boundary condition. In [119], the radial basis function collocation method is used to solve several standard and non standard options.

More relevant numerical works dealing with pricing American options include Allegretto et al. [1], Clift and Forsyth [24], Israel and Rincon [65], Kallast and Kivinukk [69], Markolefas [90], Zvan et al. [150], and some of the references there in. Some other works pertaining to the standard options will be discussed further in the respective chapters.

Exotic options are widely used in the field of finance (see Bormetti et al. [9], Lasserre et al. [85], and Zhang [145]). Exotic options are particularly challenging for traditional numerical methods which can perform inaccurately due to the discontinuities in the payoff function (or its derivatives). Large errors may also occur in estimating the hedging parameters e.g., delta, vega, and gamma values, even though the prices appear to be correct. The non-smooth data can further lead to serious degradation in the convergence of the numerical schemes.

Explicit schemes are easy to implement but suffer from stability problems noticed by Heston and Zhou [56]. The fully implicit Backward Euler method may be used to accurately solve the Black-Scholes PDE due to its strong stability properties. Giles and Carter [51], Pooley et al. [103] utilized a smoothing scheme developed by Rannacher [106] which uses a finite number of steps of the fully implicit Backward Euler method followed by the Crank-Nicolson method.

In [5], Arciniega and Allen analyzed the fully implicit and Crank-Nicolson difference schemes for solving option prices. They proved that the error expansions for the difference methods have the correct form for applying Richardson extrapolation to increase the order of accuracy of the approximations. They applied the difference methods to European, American, and down-and-out knock-out call options. Their computational results indicated that Richardson extrapolation significantly decreases the amount of computational work in estimation of option prices.

Zvan et al. [151], proposed to use an implicit method which has superior convergence (when the barrier is close to the region of interest) and stability properties as well as offering additional flexibility in terms of constructing the spatial grid. Their method also allows to place grid points either near or exactly on barriers. In particular, they presented an implicit method which can be used for PDE models with general algebraic constraints on the solution. Examples of constraints can include early exercise features as well as barriers. Also in their method, barrier options with or without American constraints can be handled. Either continuously or discretely monitored barriers can also be accommodated, as can time-varying barriers.

Wade et al. [129], developed smoothing strategy for the Crank-Nicolson method which is unique in achieving optimal order convergence for barrier option problems. They extended their smoothing strategy to higher order methods using diagonal (m, m) -Padé main schemes under a smoothing strategy of using as damping schemes the $(0, 2m - 1)$ subdiagonal Padé schemes.

Khaliq et al. [78] developed a strongly stable (L-stable) and highly accurate method for pricing exotic options. Their method is based on Padé schemes and also utilizes partial fraction decomposition to address issues regarding accuracy and computational efficiency. In [138], Yousuf presented an improved smoothing strategy for smoothing the A-stable Crank-Nicolson scheme at each time when a barrier is applied. Further in [140], he extend the results to develop a fourth order smoothing scheme for pricing barrier options under stochastic volatility. Partial differential equation approach is utilized for the valuation of complex option pricing models under stochastic volatility which brings major mathematical and computational challenges for estimation of stability of the estimates. Efficient parallel version of the scheme is constructed using splitting technique. Rambeerich et al. [105] considered exponential time integration schemes for fast numerical pricing of European, American, barrier and butterfly options when the stock price follows a dynamics described by a jump-diffusion process. The resulting pricing equation which is in the form of a partial integro-differential equation is approximated in space using finite elements. Their methods required the computation of a single matrix exponential. They demonstrated the method using a wide range of numerical tests that the combination of exponential integrator and finite element discretizations with quadratic basis functions. They made Comparisons with other time-stepping methods to illustrate the effectiveness of their methods. In [109], a new the radial basis functions algorithm for pricing financial options under Merton's jump-diffusion model is described. The method is based on a differential quadrature approach, that allows the implementation of the boundary conditions in an efficient way. The semi-discrete equations obtained after approximation of the spatial derivatives, using RBFs based on differential quadrature are solved, using an exponential time integration scheme [105], they provide several numerical tests which show the superi-

ority of this method over the popular Crank-Nicolson method.

Some other works related to the option price theory would be reviewed inside the chapters.

1.3 Radial basis functions

Radial basis functions (RBFs) are well known for approximating multivariate function, which are known only at a finite number of points. Failure to obtain accurate approximation using multivariate polynomial and also non existence of unique interpolation in \mathbb{R}^d for $d > 1$ (see Mairhuber [89]), Hardy [55] developed a method to approximate a topographic surface from given scattered data using multiquadric function referred as MQ, which has the form

$$\Phi := \sqrt{c^2 + (x^2 + y^2)}, \quad c > 0, \quad (x, y) \in \mathbb{R}^2. \quad (1.3.1)$$

In the literature the multiquadric is also represented in the form $\Phi := \sqrt{1 + \epsilon^2 r^2}$, where $\epsilon = 1/c$ with appropriate normalization. He also proposed another class of basis function called inverse multiquadric (IMQ) which is reciprocal of MQ. Another function which has been found useful is the thin plate spline (TPS) given by $\|x\|^2 \log(\|x\|)$, and Gaussian which has the form $e^{(-\epsilon\|x\|)^2}$ where $\epsilon \neq 0$.

Franke [45] provides a very important contribution in this direction. He made a comprehensive comparison of several interpolation methods on different sets of functions and found that performance of MQ is better in term of accuracy. The superiority of MQ based method on other different approximation methods, attract the researchers to look towards the development of radial basis functions based methods.

Definition 1.3.1. *A function $\Phi : \mathbb{R}^d \rightarrow \mathbb{R}$ is called radial provided there exists a univariate function $\phi : [0, \infty) \rightarrow \mathbb{R}$ such that $\Phi(x) = \phi(r)$, where $r = \|x\|$ and $\|\cdot\|$ is some norm on \mathbb{R}^d .*

These functions can be broadly classified into two classes, infinitely smooth and piecewise smooth radial basis functions. Classical choices of RBF are given in Table 1.1 with their order, where for any $x \in \mathbb{R}$, the symbol $\lceil x \rceil$ denotes as usual the smallest integer greater than or equal to x . The gaussian and inverse multiquadric are positive definite

functions where as thin plate spline and multiquadric are conditionally positive definite functions of order $m > 0$.

Table 1.1: Examples of radial basis functions and their order

R.B.F.	$\phi(r), r > 0$	Order
Multiquadric (MQ)	$(1 + (\epsilon r)^2)^v, v > 0, v \notin \mathbb{N}$	$m = \lceil v \rceil$
Inverse multiquadric (IMQ)	$(1 + (\epsilon r)^2)^v, v < 0, v \notin \mathbb{N}$	$m = 0$
Gaussian (GA)	$e^{-(\epsilon r)^2}$	$m = 0$
Polyharmonic spline	$\begin{cases} r^v, v > 0 \text{ if } v \in 2\mathbb{N} - 1 \\ r^v \log(r), \text{ if } v \in 2\mathbb{N} \end{cases}$	$m = \begin{cases} \lceil \frac{v}{2} \rceil \\ \frac{v}{2} + 1 \end{cases}$

1.4 Radial basis functions interpolation

In the RBF interpolation, a function is approximated as a linear combination of translate of particular radial basis function $\phi(\|\cdot\|)$, which is radially symmetric about its center. In other words, for a given set of distinct nodes $\Omega := \{x_i \in \mathbb{R}^d; i = 1, 2, \dots, n\}$ and corresponding function values $f(x_i), i = 1, 2, \dots, n$, the RBF interpolant is of the form

$$f(x) \approx s(x) = \sum_{j=1}^n \lambda_j \phi(\|x - x_j\|), \quad x \in \mathbb{R}^d, \quad (1.4.1)$$

where $\phi(\|\cdot\|)$ is some radial function.

Applying the interpolation condition on (1.4.1) leads to a symmetric linear system

$$\Phi \lambda = f \quad (1.4.2)$$

where $\Phi := (\phi\|x_i - x_j\|)_{1 \leq i, j \leq n}$, $\lambda := [\lambda_1, \dots, \lambda_n]^\top$ and $f := [f_1, \dots, f_n]^\top$.

The main advantage of radial basis functions interpolation is its insensitivity on the space dimension d . That is, the complexity of the developed algorithm does not increase substantially with respect to the space dimension of the problem, which is not possible for other multivariate function like polynomials. Since each basis function is the translation of a single radial function with respect to each center x_i , hence it is symmetric with respect to x_i .

Schoenberg [115] characterized radial functions by relating positive definite radial function to completely monotone functions.

Definition 1.4.1. *A real valued continuous function $\phi : \mathbb{R}^+ \rightarrow \mathbb{R}$ is strictly positive definite, if and only if, it is even and*

$$\sum_{j=1}^n \sum_{k=1}^n c_j c_k \phi(\|x_j - x_k\|) > 0, \quad (1.4.3)$$

for any n distinct points $x_1, \dots, x_n \in \mathbb{R}^d$, and $[c_1, \dots, c_n]^\top \neq 0 \in \mathbb{R}^n$.

Definition 1.4.2. *A function $\phi : \mathbb{R}^+ \rightarrow \mathbb{R}$ which is in $C[0, \infty) \cap C^\infty(0, \infty)$ and that satisfies*

$$(-1)^l \phi^{(l)}(r) \geq 0, \quad r > 0, \quad l = 0, 1, \dots \quad (1.4.4)$$

is called completely monotone on $[0, \infty)$.

We have the following characterization due to Schoenberg [115]:

Theorem 1.4.3. *If the function $\phi : \mathbb{R}^+ \rightarrow \mathbb{R}$ is completely monotone, but not constant, then $\phi(\|\cdot\|^2)$ is strictly positive definite and radial on \mathbb{R}^d , for any d .*

Example of strictly positive definite function include IMQs and Gaussian. For these functions, the interpolation system (1.4.2) is uniquely solvable. But it can not be generalized to conclude the invertibility of the interpolation matrix for other famous functions like multiquadric and polyharmonic splines. The generalization of these results by considering the notion of conditionally positive definite functions for more classes of functions was done by Michelli [94]. Now the RBF interpolation problem is redefined in more general form.

1.4.1 Radial basis functions interpolation with polynomial precision

Given a set of n distinct data points (x_i, f_i) , $i = 1, 2, \dots, n$, RBF interpolant in (1.4.1) can be modified to,

$$f(x) \approx s(x) = \sum_{j=1}^n \lambda_j \phi(\|x - x_j\|) + \sum_{j=1}^l \gamma_j p_j(x), \quad x \in \mathbb{R}^d \quad (1.4.5)$$

where $\phi(\|\cdot\|)$ is some radial function and $\{p_j(x)\}_{j=1}^l$ denote basis of \prod_{m-1}^d (space of all d -variate polynomials of total degree $\leq m-1$) and l is the dimension of \prod_{m-1}^d .

Here m represents the order of the radial function, which represents the minimum degree of the polynomial to be appended to the interpolation matrix to ensure the non singularity of interpolation matrix. To take care of extra degree of freedom in (1.4.5), l extra conditions are necessary along with the interpolation conditions. The extra l condition are chosen the coefficient vector $\lambda \in \mathbb{R}^d$ orthogonal to $\prod_{m-1}^d|_{\Omega}$ i.e.,

$$\sum_{j=1}^n \lambda_j p_k(x_j) = 0 \quad \forall 1 \leq k \leq l. \quad (1.4.6)$$

Imposing the interpolation condition and orthogonality condition give a linear system

$$\begin{pmatrix} \Phi & P \\ P^t & O \end{pmatrix} \begin{pmatrix} \lambda \\ \gamma \end{pmatrix} = \begin{pmatrix} f|_{\Omega} \\ O \end{pmatrix} \quad (1.4.7)$$

where $\Phi := (\phi\|x_i - x_j\|)_{1 \leq i, j \leq n}$, $P := (p_j(x_i))_{1 \leq i \leq n \text{ \& } 1 \leq j \leq l}$, $\lambda := [\lambda_1, \dots, \lambda_n]^T$ and $\gamma := [\gamma_1, \dots, \gamma_l]^T$. The coefficient matrix in (1.4.7) will be denoted by ‘ A ’ for future reference.

To investigate whether the augmented system matrix (1.4.7) is non singular, consider the definition,

Definition 1.4.4. *A real valued continuous even function Φ is called strictly conditionally positive definite of order m on \mathbb{R}^d , if*

$$\sum_{j=1}^n \sum_{k=1}^n c_j c_k \Phi(x_j - x_k) > 0, \quad (1.4.8)$$

for any n pairwise distinct points $x_1, \dots, x_n \in \mathbb{R}^d$, and $[c_1, \dots, c_n]^T \neq 0 \in \mathbb{R}^n$ and satisfying

$$\sum_{j=1}^n c_j p(x_j) = 0, \quad (1.4.9)$$

for all real valued d variate polynomials of degree at most $m-1$.

The matrix A in the system (1.4.6) can be interpreted as being on the space of vectors $[c_1, \dots, c_n]^T$ perpendicular to \prod_{m-1}^d . The example of conditionally positively definite function are multiquadric function ($m=1$) and thin plate spline ($m=2$).

Michelli [94] generalized the results for the interpolation problem based on the modified form (1.4.5) with mild restriction on the location of the data points given by,

Definition 1.4.5. *The points $\Omega := \{x_1, \dots, x_n\} \subseteq \mathbb{R}^d$, with $n \geq 1$ are called $m -$ unisolvent if the zero is the only polynomial from \prod_m^d that vanishes on all of the points in Ω .*

Any three points in \mathbb{R}^2 are $m -$ unisolvent if and only if they are not collinear.

We have following theorem due to Michelli [94],

Theorem 1.4.6. *Suppose $\phi : \mathbb{R}^+ \rightarrow \mathbb{R} \in C[0, \infty) \cap C^\infty(0, \infty)$ is given. Then the function $\Phi := \phi(\|\cdot\|^2)$ is strictly conditionally positive definite function of order m on every \mathbb{R} , if and only if, $(-1)^m \phi^{(m)}$ is completely monotone on $(0, \infty)$.*

Now the solvability of the system (1.4.6) is ensured from the following theorem,

Theorem 1.4.7. *If the real valued even function Φ is strictly conditionally positive definite function of order m on \mathbb{R}^d and the points x_1, \dots, x_n form an $(m - 1) -$ unisolvent set, then the system of the linear equation (1.4.6) is uniquely solvable.*

The stability and convergence rate of interpolation method have been studied by many researchers. These properties can be classified for both infinitely smooth and piecewise smooth radial functions because the value of shape parameter ϵ play important role in the case of infinitely smooth function where as order of smoothness and the space dimension in the latter case.

In the case of infinitely smooth function, it has been shown (Madych and Nelson [88], Yoon [137], Schaback [114]) that radial basis function interpolation converges as a spectral rate. Madych [87] shows that accuracy of method depends on value of shape parameter ϵ and can be improved by decreasing ϵ . However the cost of instability of the corresponding system will be high for this. It is also observed that condition number increase when the number of data points increases, for a fixed value of shape parameter ϵ (Narcowich and Ward [97]) due to denseness of data points.

For piecewise smooth functions, the rate of convergence is proved to be algebraic (if the underlying function is sufficiently smooth). The rate is directly proportional to both the smoothness of the radial function (Wu and Schaback [135]) and the space dimension (Powell [104]). However, the linear system gets ill-conditioned as the smoothness or the closeness of the points are increased.

The choice of optimal value of shape parameter is another area in which considerable efforts have been made and are still undergoing. A few algorithms (for example Carlson et al. [15], Rippa [107], Sanyasiraju et al. [112], Davydov [28] and references there in) have been developed for the selection of a good value of shape parameter. However the choice of the optimal value of shape parameter is still an open problem. Fornberg and Wright [37] provide a stable algorithm for computation with all values of shape parameter ϵ including zero, on a small number of data points. In [31], Driscoll and Fornberg show that one dimensional RBF interpolation converges to polynomial interpolation when $\epsilon \rightarrow 0$. Several variable shape parameter methods have been successfully used in radial basis function approximation methods. Kansa and Carlson [72], Sarra and Sturgill [113], Bayona et al. [7], Sanyasiraju et al. [110, 111, 112], Fornberg et al. [38] have shown that in many cases variable shape parameter strategies produced more accurate results than if a constant shape parameter had been used.

In many branches of science and engineering it is desirable to interpolate not only function value but its derivatives and this type of approximation is known as Hermite Interpolation. Wu [148] deals with Hermit-Birkhoff interpolation in \mathbb{R}^d , his method is limited in the sense that one can have only one interpolation condition per data points. Sun [122] does eliminate this restriction. Iske [64] discussed Hermite interpolation for positive definite functions. Fasshauer [34] discussed Hermite interpolation on spheres.

Consider the given set of data points $\{x_i, \mathcal{L}_i\}$, $i = 1, 2, \dots, n$, $x_i \in \mathbb{R}^d$, where $\{\mathcal{L}_1, \dots, \mathcal{L}_n\}$ is a linear independent set of continuous functional, then the generalized Hermite interpolation is of the form

$$f(x) \approx s(x) = \sum_{j=1}^n \lambda_j \mathcal{L}_j^2 \phi(\|x - x_j\|), \quad (1.4.10)$$

where the notation \mathcal{L}^2 indicates that the functional \mathcal{L} now act on ϕ viewed as a function of its second arguments. The interpolation condition

$$\mathcal{L}_i s(x) = \mathcal{L}_i f(x) \quad (1.4.11)$$

leads to a linear system

$$A^H \lambda = f_{\mathcal{L}} \quad (1.4.12)$$

with matrix entries $A^H := \mathcal{L}_i \mathcal{L}_j^2 \phi(\|x_i - x_j\|)$ and right hand side $f_{\mathcal{L}} := [\mathcal{L}f_1, \dots, \mathcal{L}f_n]^t$.

Another track for looking the radial basis function interpolation problem is through compactly supported radial basis function, these are developed and investigated by Wendland[130, 131], Floater et al. [36], Wu [136].

1.5 RBF based collocation method for PDEs

The mesh free nature, dimension independent and exponential convergence properties of radial basis function attract the scholars to look at the use of RBF in numerical solution of PDE. It was Kansa [70, 71] who first used RBFs for numerical approximation of PDEs. He was motivated by the success of RBF based interpolation method, and used RBF in direct collocation approach. The method developed by Kansa is known as asymmetric collocation and can be described as follows.

1.5.1 Asymmetric collocation

Consider a linear boundary value problem

$$\mathcal{L}u(x) = f(x), \quad x \in \Omega \quad (1.5.1)$$

$$\mathcal{B}u(x) = g(x), \quad x \in \partial\Omega, \quad (1.5.2)$$

where \mathcal{L} and \mathcal{B} are linear operators. Let $n = n_I + n_B$ denote total number of collocation points, among which n_I are interior nodes and n_B lie on boundary.

For Kansa's collocation method, the approximated solution is represented the same as RBF interpolation (1.4.1). For sake of simplicity, consider RBF interpolation without

polynomial precision. Applying the operator \mathcal{L} and \mathcal{B} on (1.4.1) at interior and boundary nodes respectively gives,

$$\sum_{j=1}^n \lambda_j \mathcal{L}\phi(\|x_i - x_j\|) = f(x_i), \quad x_i \in \Omega, \quad i = 1, \dots, n_I, \quad (1.5.3)$$

$$\sum_{j=1}^n \lambda_j \mathcal{B}\phi(\|x_i - x_j\|) = g(x_i), \quad x_i \in \partial\Omega, \quad i = n_I + 1, \dots, n_I + n_B. \quad (1.5.4)$$

In matrix form system (1.5.3)-(1.5.4) can be written as

$$\begin{pmatrix} L[\Phi] \\ B[\Phi] \end{pmatrix} \begin{pmatrix} \lambda_I \\ \lambda_B \end{pmatrix} = \begin{pmatrix} f \\ g \end{pmatrix} \quad (1.5.5)$$

where $L[\Phi]_{i,j} := \mathcal{L}\phi(\|x_i - x_j\|)$, $i = 1, \dots, n_I$ & $j = 1, \dots, n$, $B[\Phi]_{i,j} := \mathcal{B}\phi(\|x_i - x_j\|)$, $i = 1, \dots, n_B$ & $j = 1, \dots, n$, $f_i = f(x_i)$ and $g_i = g(x_i)$.

Kansa specifically proposed to use multiquadrics radial function, it can be seen that Kansa collocation method is very simple in terms of implementation. He suggests the use of varying shape parameter which improved the accuracy and stability of method when compared to using only one constant value of ϵ . Kansa assumes that the non singularity results established by Micchelli would carry over to this PDE collocation method, but this is not so. It has been shown by Hon and Schaback [57] by using a counter example. So it is now interesting question to find sufficient condition on the center location that guaranteed invertibility of interpolation matrix. The collocation matrix is dense as in the case of interpolation. The symmetry nature of the matrix is also lost.

Another approach, known as symmetric collocation approach is based on generalized Hermite interpolation method, due to Fasshaure [33].

1.5.2 Symmetric collocation

For a given boundary value problem (1.5.1)-(1.5.2), Fasshaure [33] proposed symmetric collocation approach, in which the solution is represented as

$$u(x) \approx \sum_{j=1}^{n_I} \lambda_j \mathcal{L}^2\phi(\|x - x_j\|) + \sum_{j=n_I+1}^n \lambda_j \mathcal{B}^2\phi(\|x - x_j\|). \quad (1.5.6)$$

After enforcing collocation condition at interior and boundary nodes respectively, leads to a linear system, given by

$$\begin{pmatrix} L[L^2\Phi] & L[B^2\Phi] \\ B[L^2\Phi] & B[B^2\Phi] \end{pmatrix} \begin{pmatrix} \lambda_I \\ \lambda_B \end{pmatrix} = \begin{pmatrix} f \\ g \end{pmatrix}. \quad (1.5.7)$$

Here the four blocks can be defined as follows:

$$\begin{aligned} L[L^2\Phi]_{i,j} &= \mathcal{L}[\mathcal{L}^2\phi(\|x_i - x_j\|)], \quad i, j = 1, \dots, n_I, \\ L[B^2\Phi]_{i,j} &= \mathcal{L}[\mathcal{B}^2\phi(\|x_i - x_j\|)], \quad i = 1, \dots, n_I \text{ \& } j = 1 + n_I \dots, n, \\ B[L^2\Phi]_{i,j} &= \mathcal{B}[\mathcal{L}^2\phi(\|x_i - x_j\|)], \quad i = n_I + 1, \dots, n \text{ \& } j = 1 \dots, n_I, \\ B[B^2\Phi]_{i,j} &= \mathcal{B}[\mathcal{B}^2\phi(\|x_i - x_j\|)], \quad i, j = n_I + 1, \dots, n. \end{aligned}$$

The advantage of Hermite based approach is that the collocation matrix is symmetric and the invertibility of the coefficient matrix is ensured. The convergence rate and error estimate for symmetric collocation approach have been provided in Franke and Schaback [43, 44]. The error estimates established by Franke and Schaback [43, 44] require the solution of PDE to be very smooth.

1.6 Motivation of the work

The RBF based collocation methods are used to solve several option price problems [58, 59, 102, 52, 35]. In all these investigations, it is required to invert a highly ill-conditioned dense collocation matrix due to the use of global supported radial basis function. To resolve such a type of problem, there are many strategies developed in the literature. More recently Wright et al.[133] proposed radial basis function finite difference method, the idea is to use radial basis functions with a local collocation as in finite difference mode thereby reducing number of nodes and hence producing a sparse matrix. Wright et al.[133] examine the accuracy and efficiency of the method for Poisson type problems.

The local mesh free approach possess certain advantage over global collocation approach:

- It reduces the ill-conditioning nature of collocation matrix due to use of small local support.
- Easy in direct implementation as in the case of classical finite difference methods.
- Flexibility in the choice of supporting domain for each nodal points due to mesh free nature of RBF.
- Possibility of improvement in accuracy by varying shape parameter ϵ .
- Easy extension of RBF based schemes to higher dimension problems, due to insensitivity of radial functions on the space dimension d .

In the present work the local RBF schemes have been extended to solve the option price problems like American option, Asian option, American Bond option, Merton and Kou jump diffusion model and some exotic options.

We have organized the rest of the thesis as follows.

In Chapter 2, we develop efficient mesh free methods based on the local radial basis functions (RBFs) to solve European and American option pricing problems in computational finance. The application of RBFs leads to a system of differential equations, which are then solved by a time integration scheme. This is done by using a θ -method. The main difficulty in pricing the American options is that it is a free boundary problem. We use a small penalty term to remove the free boundary. The method is analyzed for stability. Numerical results describing the option values are presented.

In Chapter 3, we present a radial basis function based operator splitting method to price American option in fixed domain. The numerical discretization is done with the implicit backward difference method. Numerical experiments for one asset and two assets have been carried out. It has been shown that the present method is second order convergent.

In Chapter 4, we extend the method presented in Chapter 2 to solve problems for pricing European style Asian options. A one state variable partial differential equation which characterizes the price of European type Asian option is discussed. The resulting

method is analyzed for stability. Comparative numerical results are presented at the end of the chapter.

In chapter 5, we present a numerical method to price an American put option on zero-coupon bond. Using the concept that American option can be formalized in form of linear complementarity problems, we proposed a radial basis function based operator splitting method. The time semi discretization is done by an implicit method and operator splitting method to treat the American constraints and space discretization of underlying equation is done by using RBF based finite difference method. In numerical experiment, the prices of zero-coupon bond, European bond option and American put option are given and the optimal early interest rate is also provided.

In Chapter 6, the method was extended for pricing European and American option under Merton's and Kou jump diffusion models. We present an implicit explicit numerical scheme called IMEX-BDF2. Numerical comparison in terms of accuracy and cpu time with other existing method are carried out.

In Chapter 7, we discuss the application of local radial basis function method for special discretization in conjunction with L-stable time stepping scheme for pricing exotic option.

Finally in Chapter 8, we provide some concluding remarks and discuss some issues, problems and improvements that could be pursued in the future.

A RBF based finite difference method for American option problem

In this chapter, we discuss a local radial basis function based finite difference method to solve European and American option price problems. Time discretization is achieved by a linearly implicit θ method. The spatial discretization is done by radial basis function based local grid free method. Numerical study with multiquadric radial basis function is carried out and the results obtained are compared with existing one. Stability of the scheme is also discussed.

2.1 Introduction

In the financial world, there are different types of options for various purposes, for example, vanilla options (European call or put option, American call or put option etc.), Bermudan options, exotic options, barrier options, Asian options etc. American derivatives are one of the popular trading instruments in financial markets. The pricing of an American option is complicated, since at each time we have to determine not only the option value but also the location where it should be exercised. This implies that the evaluation of American

option is a free boundary value problem.

For derivative with simple payoff, the analytical solution for the price is available, but for more complex derivatives, possibility of early exercise, efficient and accurate numerical algorithms are required. A standard method for solving the Black-Scholes PDE is the finite difference method. Geske and Shastri [49] compared the efficiency of various finite difference and other numerical methods for option pricing, Vázquez [128] presented a upwind scheme for solving the backward parabolic partial differential equation problem in the case of European options. Zhao et al. [146] developed three compact finite difference methods for American option on a single asset.

Another method for solving multidimensional problems is the Monte Carlo method and sparse grid methods, Monte Carlo methods have the advantage of scaling linearly with the number of dimensions but have the disadvantage of converging very slowly.

Nielsen et al. [100] investigate performance of various schemes based on theta method for temporal discretization and finite difference for spacial discretization to solve one and two asset American option. Khaliq et al. [77] consider numerical solution of American option problems using a penalty approach followed by semi-discretization of resulting equation on a fixed domain. In their work they used a second order linearly implicit time stepping method for computing option value. Khaliq et al. [80] used implicit adaptive method for pricing American options.

Nielsen et al. [100] presented a penalty method for solving multi-asset American option problems. They added a small nonlinear penalty term to the classical Black Scholes equation to remove the free and moving boundary. They derived several explicit, semi implicit and fully implicit finite difference method. A new mesh free method for partial differential equations based on radial basis function is currently ongoing active research. These methods aim to eliminate the structure of the mesh and approximate the solution using a set of random points rather than points from grid discretization.

Application of RBF in one dimension European and American options are done by Hon et al. [58] where for developing numerical method he used concept of quasi interpolation and radial basis function. Fasshauer et al. [35] solve multi-asset American option problem

using penalty method. They constructed a penalty method which allows the removal of the free and moving boundary by adding a small and continuous penalty term to Black Scholes equation. Pettersson [102] proposed a method for multidimensional option pricing, and Larsson et al. [84] used generalized Fourier transform to reduce memory requirement and computation cost of RBF methods.

In the present work, a new grid free ‘local’ RBF scheme is developed based on the localizing concept proposed by Wright and Fornberg [133] to solve the Black-Scholes model for American basket option with non linear penalty source term. In the penalty approach as suggested by Nielsen et al. [100], the free boundary is removed by a small continuous penalty terms to Black-Scholes equation, that leads the resulting equation to be solved in a fixed domain.

In this strategy, it is expected that the choice of the shape parameter will not be a critical issue for stability point of view as in case of global collocation method.

We will now describe the content of the chapter more precisely. In section 2.2 we present the generalized version of the American multi-asset option problem. The development of the scheme to solve resulting equation is given in sections 2.3 and 2.4. Numerical results are presented in section 2.6. Finally, conclusion are given in section 2.7.

2.2 Problem description

Pricing option on several underlying stock prices is of great interest for the financial industry. Since in the American option early exercise is allowed this problem is normally formulated as moving boundary value problem.

2.2.1 American multi-asset option problem

The value $V(S, \tau)$ of American put option can be determined by the Black-Scholes equation for multi-asset problem:

$$\frac{\partial V(S, \tau)}{\partial \tau} + \mathcal{L}V(S, \tau) = 0, \quad s_i > \bar{s}_i(\tau), i = 1, 2, \dots, d, 0 \leq \tau < T \quad (2.2.1)$$

where

$$\mathcal{L}V(S, \tau) = \frac{1}{2} \sum_{i=1}^d \sum_{j=1}^d \rho_{ij} \sigma_i \sigma_j s_i s_j \frac{\partial^2 V}{\partial s_i \partial s_j} + \sum_{i=1}^d (r - q_i) s_i \frac{\partial V}{\partial s_i} - rV \quad (2.2.2)$$

where T the time of expiry, σ_i the volatility of i^{th} underlying asset, q_i the dividend paid by asset i , r the risk free interest rate, which is fixed through out the time period of interest, ρ_{ij} denotes the correlation between the assets i and j , $\bar{S}(\tau) = (\bar{s}_1(\tau), \bar{s}_2(\tau), \dots, \bar{s}_d(\tau))$ the moving boundary and d denotes the number of assets, which have the following prices at time τ : $S(\tau) = (s_1(\tau), s_2(\tau), \dots, s_d(\tau))$.

The American put option has following payoff function

$$\mathcal{G}(S) = \max(E - \sum_{i=1}^d \alpha_i s_i, 0) \quad (2.2.3)$$

where E is the exercise price of the option and α_i are given constants.

The terminal condition for equation (2.2.1) is given by

$$V(S, T) = \mathcal{G}(S), \quad S \in \Omega = \{(s_1, s_2, \dots, s_d) | s_i > 0, 1 \leq i < d\}. \quad (2.2.4)$$

To ensure that the exercise value and the continuation value of the option are the same along the exercise boundary, the following conditions are prescribed;

$$V(\bar{S}(\tau), \tau) = \mathcal{G}(\bar{S}(\tau)) \quad (2.2.5)$$

$$\mathcal{G}(\bar{S}(T)) = 0. \quad (2.2.6)$$

The smooth pasting condition for a smooth transition is given as

$$\frac{\partial V(\bar{S}, \tau)}{\partial s_i} = -\alpha_i. \quad (2.2.7)$$

The American option problems leads to the linear complementarity form of the problem;

$$\begin{aligned} \frac{\partial V}{\partial \tau} + \mathcal{L}V &\leq 0 & \Omega \times [0, T], \\ V(S, \tau) - \mathcal{G}(S) &\geq 0 & \Omega \times [0, T], \\ (\frac{\partial V}{\partial \tau} + \mathcal{L}V)(V(S, \tau) - \mathcal{G}(S)) &= 0 & \Omega \times [0, T], \\ V(S, T) &= \mathcal{G}(S) & S \in \Omega. \end{aligned} \quad (2.2.8)$$

The boundary conditions are given as

$$\lim_{s_i \rightarrow \infty} V(S, \tau) = 0, \quad S \in \Omega, i = 1, 2, \dots, d \quad (2.2.9)$$

$$V(S, \tau) = g_i, \quad S \in \Omega_i, i = 1, 2, \dots, d \quad (2.2.10)$$

where Ω_i denote the boundary of Ω along which the price s_i vanish.

The Black-Scholes equation assumes a lognormal distribution model for the changes in asset prices, so it allows that if any one of asset price is zero at any time τ^* then asset will be meaningless for any time $\tau \geq \tau^*$. Typically the function g_i is assigned the value on the boundary, which is determined by solving the associated $(d - 1)$ dimension American put option problem. In the case of put option, the contract become meaningless as the price of any underlying asset increases unboundedly, therefore the right hand side of equation (2.2.9) is zero

2.2.2 Penalty Method

The American put option involves an unknown boundary. We can approximate the governing model by adding a penalty term and thereby converting a non linear partial differential equation with fixed domain. The choice of the penalty term are such that the solution stay above the payoff function as solution approaches expiry and small enough so that resulting PDE still resembles the Black-Scholes equation very closely. Nelson et al.[100] motivate the choice of a penalty term in the following form

$$\frac{\mu C}{V + \mu - q} \quad (2.2.11)$$

where $0 < \mu \ll 1$ is a small regularization parameter, $C \geq rE[100]$ is a positivity constant and the barrier function is given by

$$q(S) = E - \sum_{i=1}^d \alpha_i s_i, \quad (2.2.12)$$

after adding penalty term (2.2.11) to equation (2.2.1), the PDE become

$$\frac{\partial V(S, \tau)}{\partial \tau} + \mathcal{L}_\mu V(S, \tau) = 0, \quad S \in \Omega, 0 \leq \tau \leq T, \quad (2.2.13)$$

where

$$\mathcal{L}_\mu V(S, \tau) = \frac{1}{2} \sum_{i=1}^d \sum_{j=1}^d \rho_{ij} \sigma_i \sigma_j s_i s_j \frac{\partial^2 V}{\partial s_i \partial s_j} + \sum_{i=1}^d (r - q_i) s_i \frac{\partial V}{\partial s_i} - rV + \frac{\mu C}{V + \mu - q}. \quad (2.2.14)$$

The terminal and boundary condition on a fixed domain is

$$V(S, T) = \mathcal{G}(S), \quad S \in \Omega, \quad (2.2.15)$$

$$V(S, \tau) = g_i(S), \quad S \in \Omega_i, i = 1, 2, \dots, d, \quad (2.2.16)$$

$$\lim_{s_i \rightarrow \infty} V(S, \tau) = 0, \quad S \in \Omega, i = 1, 2, \dots, d. \quad (2.2.17)$$

Before solving the penalized partial differential equation (2.2.13), we transform it from a final value problem into a initial value problem. The transformation of time variable has the advantage that standard text on time integration are applicable. Using the transformation $t = T - \tau$, leads to

$$\frac{\partial V}{\partial t} = \mathcal{L}_\mu V(S, t). \quad (2.2.18)$$

The initial condition becomes

$$V(S, 0) = \mathcal{G}(S), \quad S \in \Omega. \quad (2.2.19)$$

It is important that the penalty term define in (2.2.11) is of order μ in regions where $V(S, \tau) \gg q(S)$, and hence the Black-Scholes equation is approximately satisfied. On the other hand, as $V(S, \tau)$ approaches $q(S)$ this term is approximately equal to C assuring that the early exercise constraint is not violated. Thus the penalty term is chosen so that the solution stays above the payoff function as the solution approaches expiry.

From a numerical point of view the domain Ω is usually truncated by introducing relatively large value of $s_{i\infty}$ indicating the price of i^{th} asset for which the option is meaningless. The usual rule of taking $s_{i\infty}$ to be about three or four times the value of exercise price.

2.3 Development of the local RBF based finite difference method

To derive the local RBF based finite difference method, we require Lagrange form of RBF interpolant.

2.3.1 Lagrange representation of RBF interpolation

In Lagrange form of RBF interpolant, the interpolant is represented in the following form,

$$s(x) = \sum_{j=1}^n \psi_j(x) u(x_j) \quad (2.3.1)$$

where $\psi_j(x)$ are Lagrange functions that satisfy the cardinal conditions,

$$\psi_j(x_k) = \delta_{jk}, j, k = 1, 2, \dots, n.$$

Approximation of each $\psi_j(x)$ in terms of RBF's can be obtained by posing another set of RBF interpolation problems for which data can be obtained from cardinal conditions on $\psi_j(x)$; i.e.

$$\psi_j(x) = \sum_{k=1}^n \lambda_{j,k} \phi(\|x - x_k\|) + \sum_{k=1}^l \gamma_{j,k} p_k(x). \quad (2.3.2)$$

The weights $\lambda_{j,k}$, and $\gamma_{j,k}$ can be obtained by imposing cardinality condition and orthogonality conditions. Thus for each j there will be a linear system, which can be expressed in the following form;

$$\begin{pmatrix} \phi_{11} & \cdots & \phi_{1n} & p_{11} & \cdots & p_{1l} \\ \cdots & \cdots & \cdots & \cdots & \cdots & \cdots \\ \phi_{j1} & \cdots & \phi_{jn} & p_{1j} & \cdots & p_{lj} \\ \cdots & \cdots & \cdots & \cdots & \cdots & \cdots \\ \phi_{n1} & \cdots & \phi_{nn} & p_{1n} & \cdots & p_{ln} \\ p_{11} & \cdots & p_{1n} & 0 & 0 & 0 \\ \cdots & \cdots & \cdots & \cdots & \cdots & \cdots \\ p_{l1} & \cdots & p_{ln} & 0 & 0 & 0 \end{pmatrix} \begin{pmatrix} \lambda_{j1} \\ \cdots \\ \lambda_{jn} \\ \gamma_{j1} \\ \cdots \\ \gamma_{jl} \end{pmatrix} = \begin{pmatrix} \psi_j(x_1) = 0 \\ \cdots \\ \psi_j(x_j) = 1 \\ \cdots \\ \psi_j(x_n) = 0 \\ 0 \\ \cdots \\ 0 \end{pmatrix} \quad (2.3.3)$$

where $\phi_{ij} = \phi(\|x_i - x_j\|)$, $i, j = 1, \dots, n$ and $p_{ij} = p_i(x_j)$, $i = 1, \dots, l, j = 1, \dots, n$.

Certain properties of determinants and Cramer's rule on (2.3.2)-(2.3.3) yield [39]

$$\psi_j(x) = \frac{|A_j(x)|}{|A|}, j = 1, 2, \dots, n \quad (2.3.4)$$

where matrix ‘ A ’ is same as defined in (1.4.7) and $A_j(x)$ is same as the matrix ‘ A ’, except that j^{th} row is replace by vector,

$$B(x) = [\phi(\|x - x_1\|) \ \phi(\|x - x_2\|) \ \dots \ \phi(\|x - x_n\|) \mid p_1(x) \ p_2(x) \ \dots \ p_l(x)] \quad (2.3.5)$$

where $p_k(x) \in \prod_{m=1}^d$.

2.3.2 RBF-FD approximation of operators

To derive a local RBF-FD approximation of operators \mathcal{L} at the node x_i in the discretized domain containing n number of nodes, we consider any local support X_i , containing $n_i (< n)$ neighborhood of x_i , given by $X_i = \{x_1, x_2, \dots, x_{n_i}\}$. Let $\mathcal{L}u(x_i)$ be approximated by linear combination of value of the function u at the point x_i contained in X_i i.e.

$$\mathcal{L}u(x_i) \approx \sum_{j=1}^{n_i} c_j u(x_j). \quad (2.3.6)$$

Then computing the weights c_j , we will get required formula for $\mathcal{L}u(x_i)$. Now application

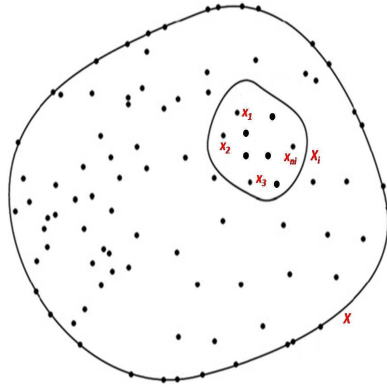


Figure 2.1: Global domain X and local domain X_i

of the operator \mathcal{L} on the Lagrange representation of RBF interpolant gives us;

$$\mathcal{L}u(x_i) \approx \mathcal{L}s(x_i) = \sum_{j=1}^{n_i} \mathcal{L}\psi_j(x_i)u(x_j). \quad (2.3.7)$$

From equation (2.3.6 -2.3.7), c_j can be written as,

$$c_j = \mathcal{L}\psi_j(x_i).$$

Now using definition of ψ_j , c_j can be rewritten as follows;

$$c_j = \mathcal{L} \frac{|A_j(x)|}{|A|} \Big|_{x=x_i}, j = 1, 2, \dots, n_i. \quad (2.3.8)$$

Now taking advantage of the symmetric nature of interpolation matrix and applying Cramer's rule to (2.3.7), c_j can be obtained by solving the following linear system;

$$\begin{pmatrix} \Phi & P \\ P^t & O \end{pmatrix} \begin{pmatrix} c \\ \xi \end{pmatrix} = (\mathcal{L}B(x))^T \Big|_{x=x_i} \quad (2.3.9)$$

where $B(x)$ is the vector defined by (2.3.5), ξ is dummy vector corresponding to the vector γ in (2.3.2). From this onwards we will concentrate on multiquadric RBF and the case $m = 1$. Constraint(1.4.6) enforces the condition

$$\sum_{j=1}^{n_i} c_j = 0 \quad (2.3.10)$$

which ensures that the stencil is exact for all constants. It was shown by Wright et al.[133] that in the case of uniform point distribution weights of RBF-FD formula converge to weights of the corresponding classical finite difference formula.

It is obvious from the final linear system (2.3.9) that, its size is only $n_i + l$, which is very much smaller than the size $n + l$ of global RBF collocation. That is why the proposed method provides a more stable system for wide range of ϵ . Further the right hand side in (2.3.9) depends only on the operator \mathcal{L} for which weights are to be computed. This property optimizes the computational time when weights are to be computed for many operators with the same distribution of nodes. It is interesting to point out here that using the above argument, that the rate of convergence may decrease for very large grids and for very small value of ϵ due to the ill-conditioning of the resulting system. To resolve these problems various algorithm were developed by Fornberg et al.[37, 40, 41].

Algorithm-

For the solution strategy of steady state problem, consider a linear boundary value problem

$$\mathcal{L}u(x) = f(x), \text{ in } \Omega$$

$$u(x) = g(x), \text{ on } \partial\Omega. \quad (2.3.11)$$

Compute the weights using (2.3.9), for each $\mathcal{L}u(x_i)$, $i \in \{1, 2, \dots, n\}$ and $x_i \notin \partial\Omega$. Assemble the weights at proper location to form global matrix L .

The RBF-FD solution can be obtained by solving the linear system.

$$Lu = f + g \quad (2.3.12)$$

where g contains contribution from boundary $\partial\Omega$. It is important to point out that weights depend only on the choice of RBF and the surrounding nodes considered in the neighborhood of the main node. Hence, implementation of the method is as simple as classical finite difference method.

2.4 Implementation of numerical method

The numerical solution of multi-asset problems, using any implicit technique, requires the generation of a modified PDE operator through a finite difference approximation of the time derivative. We will do above thing using weighted θ -method.

Consider the following initial-boundary value problem

$$\begin{aligned} \frac{\partial V(S, t)}{\partial t} &= \mathcal{L}_\mu V(S, t) \quad S \in \Omega, 0 \leq t \leq T \\ V(S, 0) &= V_0 \\ V(S, t) &= g(S, t) \quad S \in \partial\Omega \end{aligned} \quad (2.4.1)$$

a finite difference approximation made for the time derivative with notation $V^n = V(S, t^n) = V^n(S)$, and $t^n = t^{n-1} + \delta t$, we obtain

$$\frac{V^{n+1} - V^n}{\delta t} = \theta \mathcal{L}_\mu V^{n+1} + (1 - \theta) \mathcal{L}_\mu V^n. \quad (2.4.2)$$

After simplification we will get

$$\frac{V^{n+1} - V^n}{\delta t} = \theta \mathcal{L} V^{n+1} + (1 - \theta) \mathcal{L} V^n + \theta \frac{\mu C}{V^n + \mu - q} + (1 - \theta) \frac{\mu C}{V^{n+1} + \mu - q}. \quad (2.4.3)$$

The nonlinear penalty term gives rise to a nonlinear system of equations whose solution can be obtained by the modified Newton method. However by replacing V^{n+1} by V^n in

the above equation (2.4.3), the corresponding linear implicit scheme become;

$$\frac{V^{n+1} - V^n}{\delta t} = \theta \mathcal{L}V^{n+1} + (1 - \theta) \mathcal{L}V^n + \frac{\mu C}{V^n + \mu - q}. \quad (2.4.4)$$

For each fixed point $S_i \in \Omega$ the above equation is linear system of ODEs. The price one pays for this simplification is that the method is limited to first-order accuracy in time. Now using radial basis function based finite difference method discussed through (2.3.6) to (2.3.9) for spacial discretization of operator $\mathcal{L}V$ leads to;

$$[I - \theta \delta t L]V^{n+1} = [I - (1 - \theta) \delta t L]V^n + \delta t Q(V^n), \quad (2.4.5)$$

where L is matrix of weights for corresponding differential operator \mathcal{L} and I is an identity matrix. The vector Q has components

$$Q_i = \frac{\mu C}{V_i + \mu + q(S_i)}.$$

2.5 Stability Analysis

In this section, we present an analysis of the stability of the radial basis function based finite difference method using the matrix method. A small perturbation at n^{th} time level $e^n = V^n - \tilde{V}^n$ is introduced in the equation (2.4.5) for corresponding European option problem, where V^n is the numerical solution in exact arithmetic and \tilde{V}^n is perturbed solution. The equation for the error e^{n+1} can be written as

$$e^{n+1} = K e^n$$

where the amplification matrix $K = [I - \theta \delta t L]^{-1} [I - (1 - \theta) \delta t L]$. The numerical scheme will be stable if as $n \rightarrow \infty$, the error $e^n \rightarrow 0$. This can be ensured provided $\rho(K) < 1$, where $\rho(K)$ denote the spectral radius of K .

It can be seen that the stability is assured if all eigenvalues of the matrix $[I - \theta \delta t L]^{-1} [I - (1 - \theta) \delta t L]$ satisfy the following condition

$$\left| \frac{1 + (1 - \theta) \delta t \lambda}{1 - \theta \delta t \lambda} \right| \leq 1 \quad (2.5.1)$$

where λ is eigenvalue of the matrix L . For the case of Crank-Nicolson scheme ($\theta = 0.5$) the inequality (2.5.1) is always satisfied provided $Re(\lambda) \leq 0$. This shows that scheme is unconditionally stable. It can be seen from the inequality that the stability of the scheme highly depends on the minimum distance between two nodes ' h ' in the domain and the shape parameter ' ϵ '. In the case of global collocation, it is found that the condition number of the collocation matrix becomes very large and the system leads to ill-conditioning, when ' ϵ ' and ' h ' become very small. The present local RBF approximation is free from these complexities. Since there is currently no explicit relationship among the eigenvalues of the matrix L , the number of nodes and the shape parameter ' ϵ ', we investigate this dependence numerically and this is given in Figure 2.2.

Figure 2.2 show how the maximum eigenvalue of L varies as a function of ' ϵ ' and ' h '

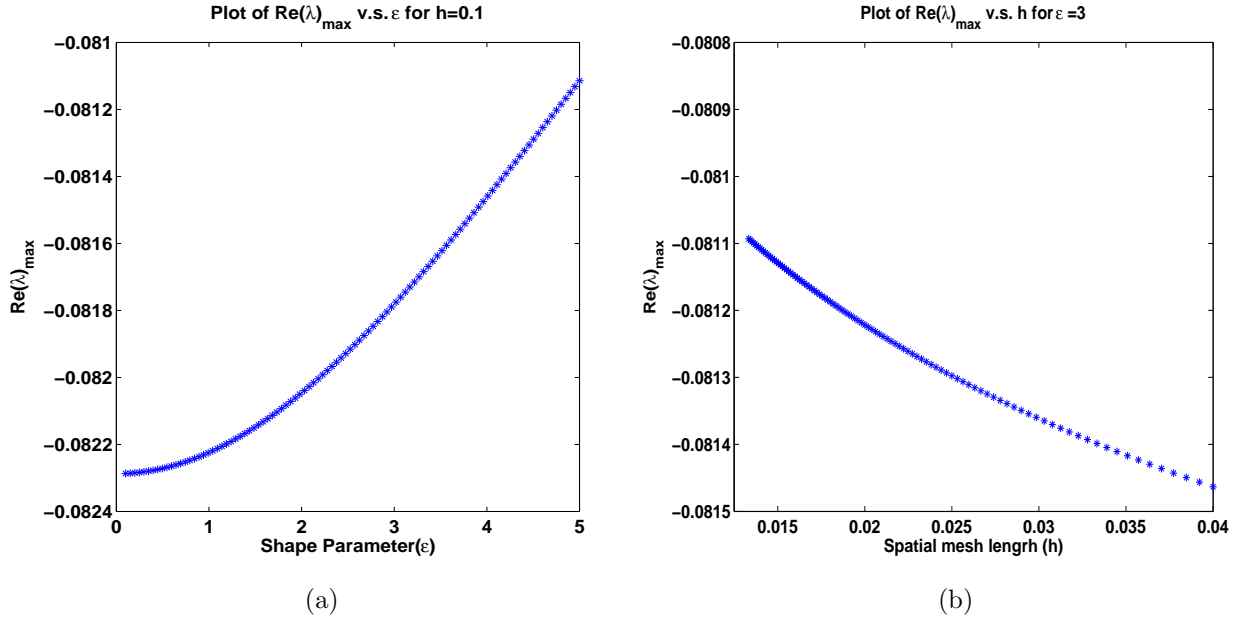


Figure 2.2: A typical stability plot for radial basis function based finite difference method

(keeping another parameter as constant) respectively. It can be seen that in both cases, the scheme satisfies the stability condition for a wide range of these parameters.

2.6 Numerical simulation and discussion

In this section, we are going to present numerical results for one and two dimension Black-Scholes equation to evaluate proposed mesh-less approaches. Although the scheme works for all radial basis function but we will use multi-quadric ($\sqrt{1 + (\epsilon r)^2}$) radial basis function on different experimental setup. It was found that accuracy of RBF method highly depends on the value of shape parameter ϵ . The choice of optimal value of this shape parameter is still an interesting problem for many researchers. Considerable effort has been made in this direction. More detail can be found in Davydov et al. [27], Sanyasiraju et al. [112] and references therein. We will choose value of ϵ on error and trial basis. The computational domain Ω are discretized by M space nodes and the temporal domain are divided into N equispaced intervals $t_n = n\delta t$ for $n = 0, 1, \dots, N$ with $\delta t = \frac{T}{N}$. In all numerical experiments a fixed stencil size $n_i = 3$ for one dimension and $n_i = 5$ for two dimension problems are used.

By keeping the shape ϵ fixed, the computational error produced by the numerical schemes was measured against the value of analytical solution or reference solution using maximum norm as

$$E_\infty = \max_{1 \leq i \leq M} |u(x_i, t_N) - U(x_i, t_N)|$$

$$E_{rms} = \left(\frac{1}{M} \sum_{i=1}^M |u(x_i, t_N) - U(x_i, t_N)|^2 \right)^{1/2}$$

where $u(x, t)$ is analytical or reference solution and $U(x, t)$ are numerical solution.

Using the RBF approach, the resulting problems for European and American put option with dividend and without dividend paying asset are solved via the Crank-Nicolson's method.

2.6.1 Numerical results for European options

To illustrate the accuracy and convergent trend of the proposed method, we consider European put option governing equation and payoff;

$$\frac{\partial V}{\partial \tau} + \frac{1}{2}\sigma^2 S^2 \frac{\partial^2 V}{\partial S^2} + (r - q)S \frac{\partial V}{\partial S} - rV = 0, \quad (V, \tau) \in (0, \infty) \times (0, T] \quad (2.6.1)$$

$$V(S, T) = \max(E - S, 0) \quad (2.6.2)$$

with the boundary condition given as

$$V(S, \tau) = \begin{cases} Ee^{-r(T-\tau)} & \text{for } S = 0, \\ 0 & \text{for } S \rightarrow \infty. \end{cases} \quad (2.6.3)$$

The exact solution of the above differential equation (2.6.1) with the initial condition (2.6.2) and boundary condition (2.6.3) is given by;

$$V(S, \tau) = Ee^{-r(T-\tau)}\mathcal{N}(-d_2(S, \tau)) - e^{-q(T-\tau)}S\mathcal{N}(-d_1(S, \tau)) \quad (2.6.4)$$

where $\mathcal{N}(\cdot)$ is the cumulative distribution of the standard normal distribution function with

$$d_1(S, \tau) = \frac{\ln(\frac{S}{E}) + (r - q + \frac{1}{2}\sigma^2)(T - \tau)}{\sigma\sqrt{T - \tau}}$$

$$d_2(S, \tau) = d_1(S, \tau) - \sigma\sqrt{T - \tau}.$$

For illustration of the performance of the method the numerical experiments for some model problem was carried out.

Example 2.6.1. *European put option; the interest rate r has been fixed at 0.08, the volatility σ have the value 0.2, dividend $q = 0.04$, strike price $E = 1$, and the exercise time used was $T = 0.50$ years.*

Numerical computation are done in domain $[0, 4]$ with fixed time length $\delta t = 0.001$ and results obtained from proposed method for example 2.6.1 is reported in Table 2.1 for different value of ϵ and compared with classical finite difference method. From these tables

2.6.1. Numerical results for European options

Table 2.1: Value of absolute and relative error for example 2.6.1 with uniform points for different value of ϵ .

M	FD		$\epsilon = 1.0$		$\epsilon = 2.0$	
	E_∞	E_{rms}	E_∞	E_{rms}	E_∞	E_{rms}
21	1.5962e-02	3.4965e-03	1.4662e-02	3.2089e-03	1.1584e-02	2.5395e-03
41	3.9245e-03	7.7494e-04	3.6011e-03	7.0480e-04	2.6989e-03	5.1343e-04
81	8.7922e-04	1.8757e-04	8.0381e-04	1.7003e-04	5.8170e-04	1.1985e-04
161	2.1566e-04	4.6663e-05	1.9702e-04	4.2270e-05	1.4192e-04	2.9545e-05
321	5.3891e-05	1.1660e-05	4.9276e-05	1.0561e-05	3.5448e-05	7.3658e-06

we can observe that the proposed method has good agreement with the classical finite difference method all value of ϵ considered, however the accuracy of the method can be improved by choosing suitable value of shape parameter.

Since radial basis function is infinitely differentiable, the value of derivative of the options is promptly available from the derivative of basis function, we also calculate value of delta(Δ) of an option which is the rate of change of the option value with respect to the asset price and gamma(Γ) of a portfolio of options on a underlying asset which is the rate of change of portfolio's delta with respect to the price of the underlying asset.

We extended same numerical experiments for strike price $E = 100$ with $S_{\min} = 0$, $S_{\max} = 180$ and the value of European Put option at different asset price are reported in Table 2.2, Table 2.2 gives the analytical and numerical value of the option price, delta and gamma at different asset price at respective column with shape parameter $\epsilon = 0.05$.

Table 2.2: European put option values and Greeks for example 2.6.1.

S	Value of option's		Values of option's Δ		Values of option's Γ	
	Analytical	Numerical	Analytical	Numerical	Analytical	Numerical
80	18.0774	18.0775	-0.8959	-0.8959	0.0136	0.0136
90	10.0414	10.0414	-0.6890	-0.6890	0.0266	0.0266
100	4.5549	4.5549	-0.4077	-0.4077	0.0270	0.0270
110	1.6814	1.6814	-0.1840	-0.1840	0.0169	0.0169
120	0.5142	0.5142	-0.0653	-0.0653	0.0074	0.0074

Example 2.6.2. *European put option with parameter $r = 0.05$, $\sigma = 0.2$, $q = 0$, $E = 10$ and maturity time $T = 0.5$ years with $S_{\min} = 0$, $S_{\max} = 30$ as considered by Goto et al.[53].*

The value of European put option at different asset price for example 3.3.2 with $M = 121$ spatial points are reported in Table 2.3 and compared with what result obtained by other radial basis function based method proposed by Goto et al.[53]. From the Table

Table 2.3: Comparison of numerical solutions of European put option for wide range of asset price for example 2.6.2.

S	Analytical	Goto-MQ	Goto-RMQ	Present	Error
2	7.75310	7.75310	7.75310	7.75310	1.56031e-05
4	5.75310	5.57310	5.75310	5.75310	3.12056e-05
6	3.75318	3.75318	3.75318	3.75316	1.65979e-05
8	1.79871	1.79823	1.79823	1.79871	4.20080e-07
10	0.44197	0.44055	0.44055	0.43994	2.02376e-03
12	0.04834	0.04780	0.04780	0.04799	3.52587e-04
14	0.00277	0.00271	0.00271	0.00282	4.76999e-05
16	0.00010	0.00010	0.00010	0.00010	9.05167e-06
18	0.00000	0.00008	0.00008	0.00000	6.31382e-07

2.3 we observe that proposed method have good agreement with analytical result and and radial basis function based collocation method. In Figure 2.3a and 2.3b we plot the analytical and numerical value of Delta and the Gamma. These figures show that the Greeks are very stable and no spurious oscillation at or around the strike price.

2.6.2 Numerical results for American options

Single Asset case

For a single asset whose price is denoted by S , the penalty formulation of the Black-Scholes equation is given by

$$\frac{\partial V}{\partial \tau} + \frac{1}{2}\sigma^2 S^2 \frac{\partial^2 V}{\partial S^2} + (r - q)S \frac{\partial V}{\partial S} - rV + \frac{\mu C}{V + \mu - q(S)} = 0 \quad (2.6.5)$$

the boundary conditions corresponding to (2.2.16) and (2.2.17) are usually given as

$$V(0, \tau) = E$$

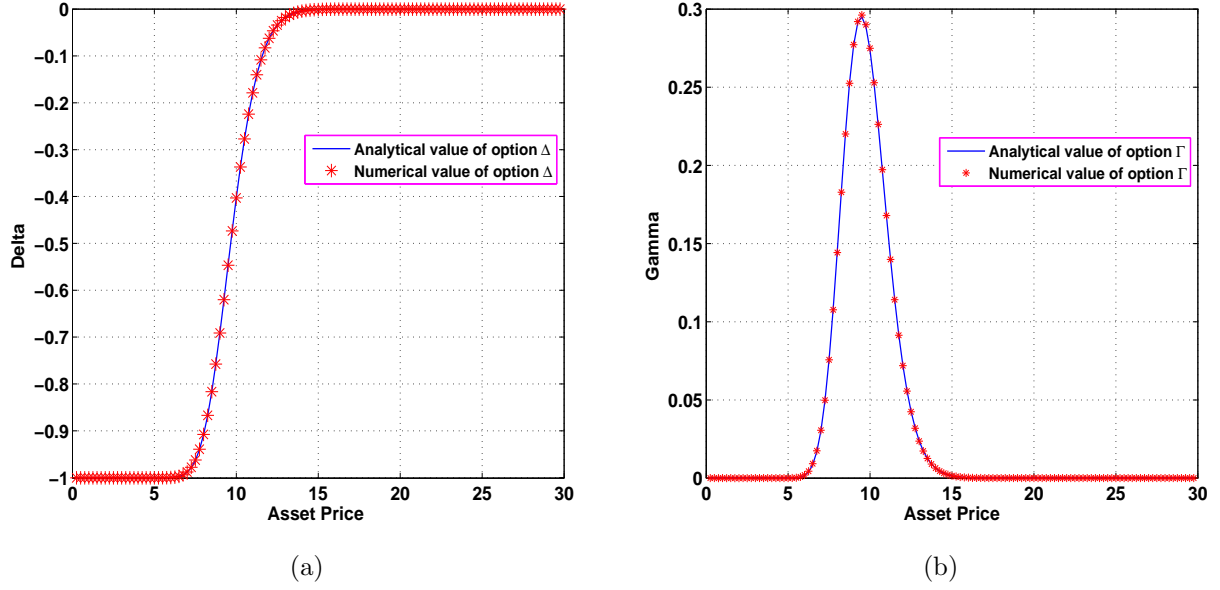


Figure 2.3: Analytical and numerical approximation of the delta (Δ) and gamma (Γ) respectively.

$$\lim_{S \rightarrow \infty} V(S, \tau) = 0.$$

Example 2.6.3. American put option with parameter $r = 0.1$, $\sigma = 0.2$, $q = 0$, $E = 1$, $T = 1.0$. The above parameter are adopted from Fasshauer et al. [35].

The value of American Put option at different asset price for example 3.3.4 with $\delta t = 0.01$, $\mu = 0.01$, $S_{\min} = 0$ and $S_{\max} = 2$ as considered by Fasshauer et al. [35] with shape parameter $\epsilon = 0.1$ are reported in Table 2.4. The reference solution for corresponding asset price is adopted from Fasshauer et al. [35] and compared with what result obtained by method proposed. From the tabulated data one can observe that we got reasonable accurate result using local radial basis function based method, in the sense that it is very close to the result obtained by Fasshauer et al. [35] using global collocation method.

Example 2.6.4. American put option with parameter $r = 0.08$, $\sigma = 0.2$, $q = 0, 0.04$, $E = 100$, $T = 3.0$. The above parameter is considered by Ju [67] and Chung et al. [23].

Table 2.4: Comparison of numerical solutions of American put option for wide range of asset price for example-2.6.3.

S	Reference price	M=21		M=41	
		Fasshauer[35]	Present	Fasshauer[35]	Present
0.6	0.4000037	0.4000176	0.4000185	0.4000012	0.4000068
0.7	0.3001161	0.3001007	0.3002333	0.3001120	0.3001480
0.8	0.2020397	0.2019901	0.2022428	0.2020191	0.2020871
0.9	0.1169591	0.1165422	0.1154885	0.1168706	0.1165987
1.0	0.0602833	0.0597033	0.0580422	0.0601659	0.0597749
1.1	0.0293272	0.0287648	0.0276763	0.0291898	0.0289261
1.2	0.0140864	0.0136840	0.0132349	0.0139888	0.0138704
1.3	0.0070408	0.0068192	0.0066983	0.0069832	0.0069502
1.4	0.0038609	0.0037485	0.0037539	0.0038313	0.0038316

The comparison of proposed method with existing ones for American option at different asset price, numerical experiment with $S_{\min} = 0$ $S_{\max} = 300$ is carried out and reported in Table 2.5. For comparison purpose data are taken from the [67]. From the table, we can observe that proposed method has nice agreement with previous one. The numerical experiment was carried out with $h = \delta t = 0.1$, shape parameter $\epsilon = 0.1$. From the table, we can observe that the proposed method has nice agreement with the previous one and we get relatively small error in the asset value, however by decreasing value of h , δt and optimal value of shape parameter can improve the accuracy of method. Figure 2.4a show the comparison of European and American option value where as Figure 2.4b show the optimal exercise curve for American option. The numerical values of option delta are reported in Table 2.6, it is clear from the result presented in the table that the numerical value of option delta lie between -1 to 0 which is in nice agreement with what is mentioned in Hull [61].

Two Asset Case

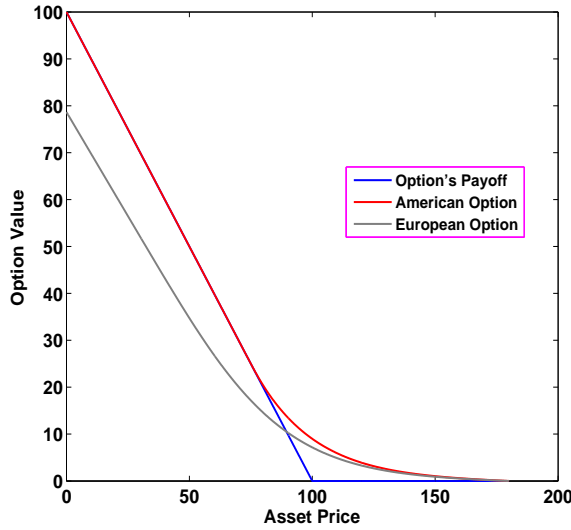
The penalty formulation of an American put option with two underlying assets is given by

$$\frac{\partial V}{\partial t} + \frac{1}{2}\sigma_1^2 s_1^2 \frac{\partial^2 V}{\partial s_1^2} + \frac{1}{2}\sigma_2^2 s_2^2 \frac{\partial^2 V}{\partial s_2^2} + \frac{1}{2}\rho\sigma_1\sigma_2 s_1 s_2 \frac{\partial^2 V}{\partial s_1 \partial s_2} + (r - q_1)s_1 \frac{\partial V}{\partial s_1}$$

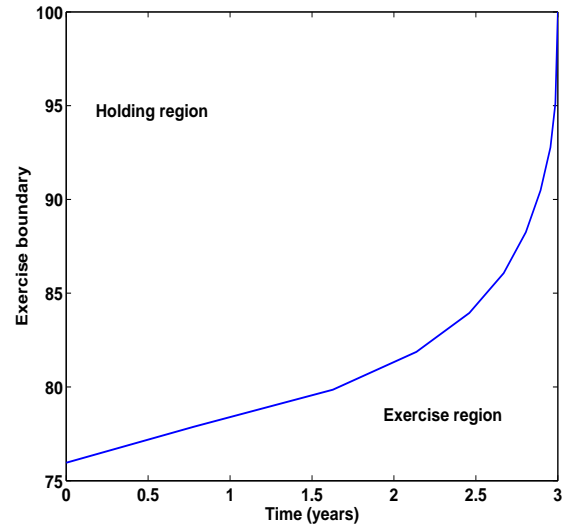
2.6.2. Numerical results for American options

Table 2.5: Price of American put option using radial basis function with $E = 100$, $r = 0.08$, $\sigma = 0.2$, $T = 3$ years.

(S, q)	Binomial	LUBA[13]	MGJ [14]	HSY4[60]	HSY6[60]	EXP3[67]	RBF-FD
(80,0.04)	20.3500	20.3335	20.0000	20.5225	20.3932	20.3511	20.4010
(90,0.04)	13.4968	13.4982	14.0246	13.3784	13.4602	13.5000	13.5207
(100,0.04)	8.9438	8.9424	9.1086	8.8038	8.9891	8.9474	8.9460
(110,0.04)	5.9119	5.9122	5.9310	5.9186	5.9269	5.9146	5.9026
(120,0.04)	3.8975	3.8980	3.8823	3.9778	3.8834	3.8997	3.8939
(80,0.08)	22.2050	22.1985	22.7106	22.2445	22.1493	22.2084	22.2854
(90,0.08)	16.2071	16.1986	16.5305	16.1340	16.2578	16.2106	16.2557
(100,0.08)	11.7037	11.6988	11.8106	11.7175	11.7237	11.7066	11.7263
(110,0.08)	8.3671	8.3630	8.4072	8.4355	8.3563	8.3695	8.3712
(120,0.08)	5.9299	5.9261	5.9310	5.9881	5.9323	5.9323	5.9229



(a)



(b)

Figure 2.4: American and European put option value, and optimal early exercise boundary.

$$+(r - q_2)s_2 \frac{\partial V}{\partial s_2} - rV + \frac{\mu C}{V + \mu - q(S)} = 0 \quad s_1, s_2 \geq 0, t \in [0, T) \quad (2.6.6)$$

$$V(s_1, s_2, T) = \mathcal{G}(s_1, s_2), \quad s_1, s_2 \geq 0 \quad (2.6.7)$$

2.6.2. Numerical results for American options

Table 2.6: Values of options delta (Δ) of American put using radial basis function with $E = 100$, $r = 0.08$, $\sigma = 0.2$, $T = 3$ years.

(S, q)	Binomial	LUBA[13]	MGJ [14]	HSY4[60]	HSY6[60]	EXP3[67]	RBF-FD
(80,0.04)	-0.8374	-1.0000	-0.8570	-0.8500	-0.8338	-0.8372	-0.8384
(90,0.04)	-0.5541	-0.5939	-0.5754	-0.5472	-0.5547	-0.5540	-0.5568
(100,0.04)	-0.3691	-0.3853	-0.3568	-0.3664	-0.3689	-0.3691	-0.3706
(110,0.04)	-0.2456	-0.2571	-0.2328	-0.2508	-0.2455	-0.2456	-0.2462
(120,0.04)	-0.1628	-0.1645	-0.1606	-0.1630	-0.1628	-0.1628	-0.1630
(80,0.08)	-0.6878	-0.3540	-0.7164	-0.6788	-0.6887	-0.6877	-0.6996
(90,0.08)	-0.5189	-0.5439	-0.5152	-0.5150	-0.5168	-0.5190	-0.5219
(100,0.08)	-0.3871	-0.4043	-0.3779	-0.3929	-0.3869	-0.3872	-0.3893
(110,0.08)	-0.2847	-0.2897	-0.2831	-0.2847	-0.2846	-0.2847	-0.2861
(120,0.08)	-0.2064	-0.2092	-0.2091	-0.2048	-0.2064	-0.2064	-0.2072

$$V(s_1, 0, t) = g_1(s_1), \quad s_1 \geq 0, t \in [0, T] \quad (2.6.8)$$

$$V(0, s_2, t) = g_2(s_2), \quad s_2 \geq 0, t \in [0, T] \quad (2.6.9)$$

$$\lim_{s_2 \rightarrow \infty} V(s_1, s_2, t) = G_1(s_1, t), \quad s_1 \geq 0, t \in [0, T] \quad (2.6.10)$$

$$\lim_{s_1 \rightarrow \infty} V(s_1, s_2, t) = G_2(s_2, t), \quad s_2 \geq 0, t \in [0, T] \quad (2.6.11)$$

where

$$q(s_1, s_2) = E - (\alpha_1 s_1 + \alpha_2 s_2), \quad \phi(s_1, s_2) = \max(q(s_1, s_2), 0). \quad (2.6.12)$$

Since we are interested in American put option, the contract becomes worthless as the price of either of the respective asset tends to infinity, so for two factor problem the boundary value G_1 and G_2 are identical become zeros. The boundary condition g_1 and g_2 in (2.6.8) and (2.6.9) are the solution of associated single-asset American put option problems.

Example 2.6.5. For two asset case we use $r = 0.1$, $\sigma_1 = 0.2$, $\sigma_2 = 0.3$, $\alpha_1 = 0.6$, $\alpha_2 = 0.4$, $q_1 = 0.05$, $q_2 = 0.01$, $E = 1$, $T = 1$, $s_{1,\infty} = s_{2,\infty} = 4$ as considered by Fasshauer et al. [35].

Approximate solution values of the two assets American option pricing problem with uncorrelated assets at different asset prices for different numbers of node points are displayed in Table 2.7. The parameter for numerical simulation are $\delta t = 0.01$, shape parameter $\epsilon = 0.1$, and penalty parameter $\mu = 0.01$. Finally in Table 2.8 the E_∞ and E_{rms} error and rate of converges are reported. The option value and the payoff function of two assets American put option are plotted in the Figure 2.5.

Table 2.7: Option value for the two asset American option pricing problem at different asset prices.

	V(0.9,1.0)	V(1.0,0.9)	V(1.0,1.0)	V(1.1,1.0)	V(1.0,1.1)	cpu(s)
11×11	0.112332	0.101563	0.082479	0.052626	0.063395	0.685
21×21	0.096163	0.080511	0.057458	0.039551	0.044247	1.073
31×31	0.094389	0.082234	0.062122	0.038502	0.046022	1.565
41×41	0.091664	0.079117	0.059028	0.036638	0.043629	2.333

Table 2.8: Error and rate of convergence for two asset American option pricing problem.

	E_∞	rate	E_{rms}	rate
6×6	1.161293e-02	-	2.946099e-03	-
11×11	7.487033e-03	0.6	1.007292e-03	1.5
21×21	2.360894e-03	1.7	2.416444e-04	2.0
41×41	5.031772e-04	2.2	6.006923e-05	2.0

2.7 Conclusion

In this chapter, a local radial basis function based grid free method for numerical solution of multi-dimension option price has been developed. The method of lines has been used to dissociate the space and time variable. The complete derivation of the grid free scheme for the space discretization of a general time dependent differential operator has been discussed. Numerical studies for both one and two dimensional problem are carried out. To compare the method with the standard finite difference scheme and other existing

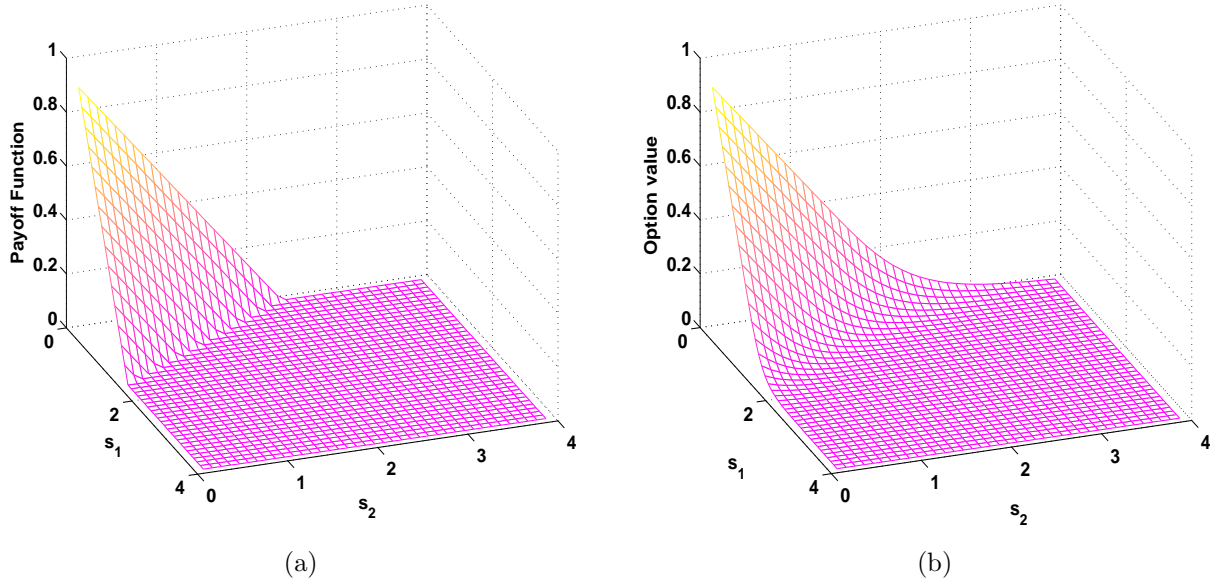


Figure 2.5: The payoff function of the two-asset American put option (left). The approximate solution of the two-asset American put option at $T=1$.

method, uniform distribution of nodal points has been chosen, though the method can be used on any scattered nodal distribution. The radial basis functions turns out to be an extremely flexible interpolation method because it does not depend on the locations of the approximation nodes, avoiding most of the frequently arising problems in computational finance such as the unstable or slow convergent numerical solutions, multi-asset valuation, complexity of computation domain. Numerical study with one and two dimension problems are carried out with accurate results that are in good agreement with those obtained by other numerical and analytical methods in literature. It has been shown that method is second order accurate in space.

Suitable choice of penalty parameter is a serious issue in penalty based numerical method for solving American option problems. So in the next chapter we propose a radial basis function based operator splitting method to solve an American option problem.

A RBF based operator splitting method for American option problem

In this chapter, we discuss a local radial basis function based operator splitting finite difference method to solve European and American option price problems. Time semi discretization is achieved by a linearly implicit backward difference method. The spatial discretization is done by radial basis function based local grid free method. The numerical scheme derived for European option is extended for American option by using operator splitting method. Numerical study with multiquadric radial basis function is carried out and the results obtained are compared with existing one.

We will now describe the content of the chapter more precisely. In section 3.1 we present the generalized version of the American multi-asset option problem. The development of the scheme to solve resulting equation is given in sections 3.2. Numerical results are presented in section 3.3. Finally, conclusion are given in section 3.4.

3.1 The mathematical model

The value $V(S, \tau)$ of European put option can be determined by the Black-Scholes equation for multi-asset problem:

$$\frac{\partial V(S, \tau)}{\partial \tau} + \mathcal{L}V(S, \tau) = 0, \quad s_i \geq 0, i = 1, 2, \dots, d, 0 \leq \tau < T \quad (3.1.1)$$

where

$$\mathcal{L}V(S, \tau) = \frac{1}{2} \sum_{i=1}^d \sum_{j=1}^d \rho_{ij} \sigma_i \sigma_j s_i s_j \frac{\partial^2 V}{\partial s_i \partial s_j} + \sum_{i=1}^d (r - q_i) s_i \frac{\partial V}{\partial s_i} - rV \quad (3.1.2)$$

where d denotes the number of assets, which have the following prices at time τ : $S(\tau) = (s_1(\tau), s_2(\tau), \dots, s_d(\tau))$, T the time of expiry, σ_i the volatility of i^{th} underlying asset, q_i the dividend paid by asset i , r the risk free interest rate, which is fixed through out the time period of interest, ρ_{ij} denotes the correlation between the assets i and j .

The value of an option at the time T of expiry of the contract is readily known as a function of the underlying assets, called payoff function. For most of the multi-asset European put option models the payoff function at expiry is

$$\mathcal{G}(S) = \max(E - \sum_{i=1}^d \alpha_i s_i, 0) \quad (3.1.3)$$

where E is the exercise price of the option and α_i are given constants.

The terminal condition for equation (3.1.1) is given by

$$V(S, T) = \mathcal{G}(S). \quad (3.1.4)$$

The following asymptotic boundary conditions are employed at the near and far field boundaries respectively

$$V(S, \tau) = \begin{cases} Ee^{-r(T-\tau)} - \sum_{i=1}^d \alpha_i s_i & \text{for } S \rightarrow 0, \\ 0 & \text{for } \|S\| \rightarrow \infty. \end{cases} \quad (3.1.5)$$

In the case of American options, the solution domain can be divided into two parts. In one region the price of the option satisfies the Black-Scholes equation and in the second

sub domain it equals the payoff function \mathcal{G} . This leads to the linear complementarity form of the problem.

$$\begin{cases} \frac{\partial V}{\partial \tau} + \mathcal{L}V \leq 0, \\ V(S, \tau) - \mathcal{G}(S) \geq 0, \\ (\frac{\partial V}{\partial \tau} + \mathcal{L}V)(V(S, \tau) - \mathcal{G}(S)) = 0, \end{cases} \quad (3.1.6)$$

By using change of variables $x_i = \ln(\frac{s_i}{E})$, $t = T - \tau$ and introducing a time-value function $u(x, t) = V(Ee^x, \tau)$, the linear complementarity problem(LCP) (3.1.6) is transformed as

$$\begin{cases} \frac{\partial u}{\partial t} - \mathcal{L}u \geq 0, \\ u(x, t) - \mathcal{G}(x) \geq 0, \\ (\frac{\partial u}{\partial t} - \mathcal{L}u)(u(x, t) - \mathcal{G}(x)) = 0, \end{cases} \quad (3.1.7)$$

where

$$\mathcal{L}u(x, t) = \frac{1}{2} \sum_{i,j=1}^d \rho_{ij} \sigma_i \sigma_j \frac{\partial^2 u}{\partial x_i \partial x_j} + \sum_{i=1}^d (r - q_i - \frac{1}{2} \sigma_i^2) \frac{\partial u}{\partial x_i} - ru \quad (3.1.8)$$

$$\mathcal{G}(x) = \max(E - \sum_{i=1}^d \alpha_i e^{x_i}, 0). \quad (3.1.9)$$

For applying the numerical method, we truncate the infinite domain into Ω by introducing relatively large values x_i . Generally upper bound of the computational domain for the asset price is typically three or four times the strike price.

3.2 Numerical scheme

In this section we shall construct an implicit time semi discretization for following PIDE on truncated domain $\Omega \times [0, T)$,

$$\frac{\partial u(x, t)}{\partial t} = \mathcal{L}u(x, t), \quad (x, t) \in \Omega \times [0, T) \quad (3.2.1)$$

$$u(x, 0) = \mathcal{G}(x), \quad x \in \bar{\Omega} \quad (3.2.2)$$

where \mathcal{L} is the partial differential operator on the right side of (3.1.8).

Let $\{0 = t_0 < t_1 < \dots < t_N = T; t_n - t_{n-1} = \delta t, 1 \leq n \leq N\}$ be a partition of the interval

$[0, T]$. Let us use the notation $u^n := u(x, t_n)$ then equation (3.2.1) will be discretized by following implicit scheme,

$$\frac{1}{\delta t} \left(\frac{3}{2}u^{n+1} - 2u^n + \frac{1}{2}u^{n-1} \right) = \mathcal{L}u^{n+1}, \quad n \geq 1. \quad (3.2.3)$$

The above discretization method of the operator $\mathcal{L}u$ is called implicit backward difference of order two method with three time levels. In order to use the proposed method we need two initial values on the zeroth and first time level. The value u^0 at the zeroth time level is given by initial condition on the model problem, and the value u^1 can be obtained by applying the implicit backward difference method of order one.

We solve the resulting time semi discrete scheme by using radial basis function based finite difference method discussed in previous section.

The approximated value of the solution $u_m^n = u(x_m, t_n)$ denoted by U_m^n can be obtained by following time stepping problem:

```

for  $n = 0 : N - 1$ 
  if  $n = 0$ 
     $\frac{U_m^{n+1} - U_m^n}{\delta t} = \mathcal{L}_\Delta U_m^{n+1}$ 
  else
     $\frac{1}{\delta t} \left( \frac{3}{2}U_m^{n+1} - 2U_m^n + \frac{1}{2}U_m^{n-1} \right) = \mathcal{L}_\Delta U_m^{n+1}$ 
  end
end
end

```

Where $\mathcal{L}_\Delta U$ is local RBF based space discretization of differential operator $\mathcal{L}u$, obtained by using procedure described in previous chapter.

3.2.1 Operator splitting method

The RBF based scheme discussed for pricing European option can be combined with operator splitting method to solve the linear complementarity problem (LCP) (3.1.6) for the American option. The operator splitting method was introduced by Ikonen and Toivanen [62] to evaluate the American put option. The main concept behind the operator splitting

method is the formulation with the auxiliary variable ψ such that $\psi = u_t - \mathcal{L}u$. Now the reformulated LCP (3.1.6) is

$$\left\{ \begin{array}{rcl} \frac{\partial u}{\partial t} - \mathcal{L}u & = & \psi, \\ (u(x, t) - \mathcal{G}(x)) \cdot \psi & = & 0, \\ u(x, t) - \mathcal{G}(x) & \geq & 0, \\ \psi & \geq & 0, \end{array} \right. \quad (3.2.4)$$

in the region $\Omega \times [0, T)$.

Now in operator splitting method we split the governing equation $u_t - \mathcal{L}u = \psi$ on the $(n+1)^{th}$ time level into two discrete equations as

$$\frac{1}{\delta t} \left(\frac{3}{2} \tilde{U}_m^{n+1} - 2U_m^n + \frac{1}{2} U_m^{n-1} \right) - \mathcal{L}_\Delta \tilde{U}_m^{n+1} = \Psi_m^n, \quad (3.2.5)$$

$$\frac{1}{\delta t} \left(\frac{3}{2} U_m^{n+1} - 2U_m^n + \frac{1}{2} U_m^{n-1} \right) - \mathcal{L}_\Delta \tilde{U}_m^{n+1} = \Psi_m^{n+1}. \quad (3.2.6)$$

Now the corresponding discrete problem for equation (3.2.4) is to seek a pair $(U_m^{n+1}, \Psi_m^{n+1})$, which satisfy the discrete equations (3.2.5)-(3.2.6) as well as the constrains

$$\left\{ \begin{array}{rcl} U_m^{n+1} & \geq & \mathcal{G}(x_m) \\ \Psi_m^{n+1} & \geq & 0, \\ \Psi_m^{n+1}(U_m^{n+1} - \mathcal{G}(x_m)) & = & 0, \end{array} \right. \quad (3.2.7)$$

respectively.

The first step is concerned with computing an intermediate approximation \tilde{U}_m^{n+1} by solving the discrete equation (3.2.5) on n^{th} time level with known auxiliary term Ψ_m^n .

Now the second step is to derive a relationship in (3.2.6) between U_m^{n+1} and Ψ_m^{n+1} . To obtain the desire relationship, rewrite the equation (3.2.6) using equation (3.2.5), together with the constrains in (3.2.7) as a problem to find the pair $(U_m^{n+1}, \Psi_m^{n+1})$, such that

$$\left\{ \begin{array}{rcl} \frac{3}{2} \frac{U_m^{n+1} - \tilde{U}_m^{n+1}}{\delta t} & = & \Psi_m^{n+1} - \Psi_m^n, \\ \Psi_m^{n+1}(U_m^{n+1} - \mathcal{G}(x_m)) & = & 0, \end{array} \right. \quad (3.2.8)$$

with the constrains

$$U_m^{n+1} \geq \mathcal{G}(x_m) \quad \text{and} \quad \Psi_m^{n+1} \geq 0. \quad (3.2.9)$$

Now by solving the problems (3.2.8)-(3.2.9), we get

$$(U_m^{n+1}, \Psi_m^{n+1}) = \begin{cases} (\mathcal{G}(x_m), \Psi_m^n + \frac{3}{2} \frac{\mathcal{G}(x_m) - \tilde{U}_m^{n+1}}{\delta t}) & \text{if } \tilde{U}_m^{n+1} - \frac{2\delta t}{3} \Psi_m^n \leq \mathcal{G}(x_m), \\ (\tilde{U}_m^{n+1} - \frac{2\delta t}{3} \Psi_m^n, 0) & \text{otherwise.} \end{cases} \quad (3.2.10)$$

Thus, the second step can be done not by solving the discrete equation in (3.2.6), but with updating the formula in (3.2.10) with a few counts of operations. Thus, we observe that the computational cost for the American option generally depends on solving the first step in (3.2.6).

The initial pair (U_m^0, Ψ_m^0) on zeroth time level can be obtained by using initial condition and assign value $\Psi_m^0 = 0$. To find the pair (U_m^1, Ψ_m^1) at first level, the first step is to compute the intermediate value \tilde{U}_m^1 as follow

$$\frac{\tilde{U}_m^1 - U_m^0}{\delta t} - \mathcal{L}_\Delta \tilde{U}_m^1 = \Psi_m^0. \quad (3.2.11)$$

Now the second step is to find the pair (U_m^1, Ψ_m^1) such that

$$(U_m^1, \Psi_m^1) = \begin{cases} (\mathcal{G}(x_m), \Psi_m^0 + \frac{\mathcal{G}(x_m) - \tilde{U}_m^1}{\delta t}) & \text{if } \tilde{U}_m^1 - \delta t \Psi_m^0 \leq \mathcal{G}(x_m), \\ (\tilde{U}_m^1 - \delta t \Psi_m^0, 0) & \text{otherwise.} \end{cases} \quad (3.2.12)$$

Algorithm to evaluate an American option

```

for  $n = 0 : N - 1$ 
  if  $n = 0$ 
     $\frac{\tilde{U}_m^{n+1} - U_m^n}{\delta t} - \mathcal{L}_\Delta \tilde{U}_m^{n+1} = \Psi_m^n$ 
     $U_m^{n+1} = \max(\tilde{U}_m^{n+1} - \delta t \Psi_m^n, \mathcal{G}(x_m))$ 
     $\Psi_m^{n+1} = \Psi_m^n + \frac{U_m^{n+1} - \tilde{U}_m^{n+1}}{\delta t}$ 
  else
     $\frac{1}{\delta t} \left( \frac{3}{2} \tilde{U}_m^{n+1} - 2U_m^n + \frac{1}{2} U_m^{n-1} \right) - \mathcal{L}_\Delta \tilde{U}_m^{n+1} = \Psi_m^n$ 
     $U_m^{n+1} = \max(\tilde{U}_m^{n+1} - \frac{2\delta t}{3} \Psi_m^n, \mathcal{G}(x_m))$ 
     $\Psi_m^{n+1} = \Psi_m^n + \frac{3}{2} \frac{U_m^{n+1} - \tilde{U}_m^{n+1}}{\delta t}$ 
  end
end
    
```

Usually option pricing problems have non smooth payoff functions. Hence, it may be possible to have solutions oscillating on the final time level. To overcome this problem, the solutions on a few initial time levels are estimated by the implicit Euler method.

3.3 Numerical simulation and discussion

In this section, we are going to present numerical results for one and two dimension Black-Scholes equation to evaluate proposed mesh-less approaches. We will use multi-quadric ($\sqrt{1 + (\epsilon r)^2}$) radial basis function on different experimental setup. The computational domain Ω are discretized by M space nodes and the temporal domain are divided into N equispaced intervals $t_n = n\delta t$ for $n = 0, 1, \dots, N$ with $\delta t = \frac{T}{N}$. In all numerical experiments a fixed stencil size $n_i = 3$ for one dimension and $n_i = 5$ for two dimension problems are used.

3.3.1 Numerical results for European options

To illustrate the accuracy and convergent trend of the proposed method, we consider European put option governing equation and payoff;

$$\frac{\partial V}{\partial \tau} + \frac{1}{2}\sigma^2 S^2 \frac{\partial^2 V}{\partial S^2} + (r - q)S \frac{\partial V}{\partial S} - rV = 0, \quad (V, \tau) \in (0, \infty) \times (0, T] \quad (3.3.1)$$

$$V(S, T) = \max(E - S, 0) \quad (3.3.2)$$

with the boundary condition given as

$$V(S, \tau) = \begin{cases} Ee^{-r(T-\tau)} & \text{for } S = 0, \\ 0 & \text{for } S \rightarrow \infty. \end{cases} \quad (3.3.3)$$

The exact solution of the above differential equation (3.3.1) with the initial condition (3.3.2) and boundary condition (3.3.3) is given by;

$$V(S, \tau) = Ee^{-r(T-\tau)}\mathcal{N}(-d_2(S, \tau)) - e^{-q(T-\tau)}S\mathcal{N}(-d_1(S, \tau)) \quad (3.3.4)$$

where $\mathcal{N}(\cdot)$ is the cumulative distribution of the standard normal distribution function with

$$d_1(S, \tau) = \frac{\ln(\frac{S}{E}) + (r - q + \frac{1}{2}\sigma^2)(T - \tau)}{\sigma\sqrt{T - \tau}}$$

$$d_2(S, \tau) = d_1(S, \tau) - \sigma\sqrt{T - \tau}.$$

For illustration of the performance of the method the numerical experiments for some model problem was carried out.

Example 3.3.1. *European put option; the interest rate r has been fixed at 0.05, the volatility σ have the value 0.2, dividend $q = 0$, strike price $E = 100$, and the exercise time used was $T = 0.50$ years.*

These parameters are adopted from Goto et al.[53] and Hon[58]. Numerical simulation are done in the computation domain $x_{\min} = -1.5$ and $x_{\max} = 1.5$. The numerical results for put option are listed in Tables 3.1 for shape parameter $\epsilon = 1.0$. The option value and absolute error are given at different asset prices. From the Table, we can observe that the discretization scheme is convergent with quadratic rate, since the ratio in respective error is approximately four.

Since radial basis function function is infinitely differentiable, the value of derivative of

Table 3.1: Numerical value European put options at different asset price with parameters as given in Example 3.3.1.

M	N	$S = 90$		$S = 100$		$S = 110$	
		Value	Error	Value	Error	Value	Error
129	25	9.869511	1.0908e-02	4.400779	1.8941e-02	1.593611	1.2764e-02
257	50	9.877705	2.7141e-03	4.415003	4.7165e-03	1.603178	3.1971e-03
513	100	9.879742	6.7790e-04	4.418542	1.1776e-03	1.605572	8.0328e-04
1025	200	9.880246	1.7332e-04	4.419420	2.9993e-04	1.606169	2.0670e-04
2049	400	9.880364	5.5148e-05	4.419628	9.1987e-05	1.606310	6.4953e-05
4097	800	9.880406	1.3790e-05	4.419697	2.2997e-05	1.606359	1.6240e-05

the options is promptly available from the derivative of basis function. We also calculate value of delta(Δ) of an option which is the rate of change of the option value with respect to the asset price and gamma(Γ) of a portfolio of options on a underlying asset which is the rate of change of portfolio's delta with respect to the price of the underlying asset.

Using the same parameter values which is employed for results in Table 3.1, we computed

3.3.1. Numerical results for European options

two Greeks viz Delta and Gamma at different asset prices and results obtained are reported in Table 3.2 and 3.3 respectively. From these tables we can observe that convergence rate of the proposed scheme is quadratic for computing Greeks as well.

These parameters are also used by Goto et al.[53] with RBF based collocation method

Table 3.2: Numerical result for Delta of European put options at different asset price with parameters as given in Example 3.3.1.

M	N	$S = 90$		$S = 100$		$S = 110$	
		Value	Error	Value	Error	Value	Error
129	25	-0.690953	3.6233e-04	-0.402382	1.1693e-04	-0.178287	1.2519e-04
257	50	-0.690682	9.1441e-05	-0.402295	2.9198e-05	-0.178380	3.2464e-05
513	100	-0.690613	2.2876e-05	-0.402273	7.2994e-06	-0.178404	8.5250e-06
1025	200	-0.690596	6.0381e-06	-0.402267	1.8342e-06	-0.178410	2.4612e-06
2049	400	-0.690593	2.4668e-06	-0.402266	4.8548e-07	-0.178411	1.2257e-06
4097	800	-0.690591	6.1584e-07	-0.402266	1.2051e-07	-0.178412	3.0733e-07

Table 3.3: Numerical result for Gamma of European put options at different asset price with parameters as given in Example 3.3.1.

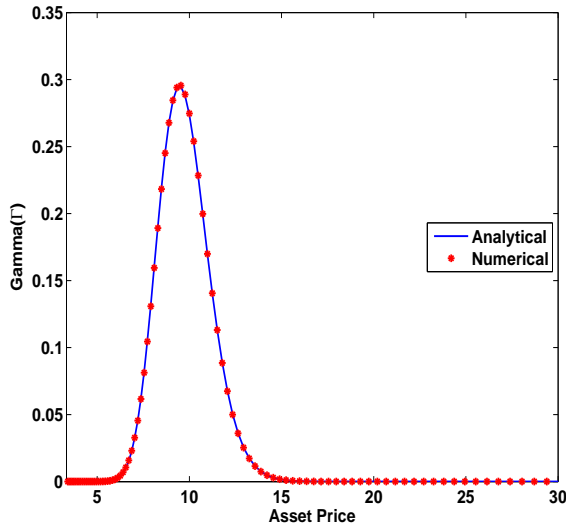
M	N	$S = 90$		$S = 100$		$S = 110$	
		Value	Error	Value	Error	Value	Error
129	25	0.027722	2.7215e-05	0.027476	1.1733e-04	0.016800	2.6443e-05
257	50	0.027700	5.2632e-06	0.027388	2.9211e-05	0.016780	6.4907e-06
513	100	0.027696	1.3072e-06	0.027366	7.3069e-06	0.016776	1.5859e-06
1025	200	0.027695	2.9694e-07	0.027360	1.8047e-06	0.016774	3.5683e-07
2049	400	0.027695	1.1902e-08	0.027359	3.8010e-07	0.016774	3.1970e-09
4097	800	0.027695	2.9571e-09	0.027359	9.5037e-08	0.016774	7.5119e-10

and Hon [58] with quasi RBF method to validate their numerical scheme. In the Table 3.4, we have compared the proposed method with other existing RBF based method for strike price $E = 10$.

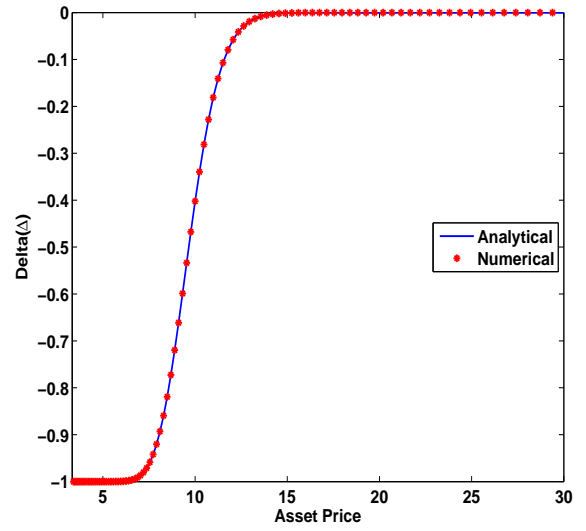
From the Table 3.4 we observe that proposed method have good agreement with analytical result and radial basis function based collocation method. In Figures 3.1a and 3.1b we plot

Table 3.4: Comparison of European put option for wide range of asset price for example 3.3.1.

S	Analytical	Gotoet et al.[53]	Hon [58]	Present	Error
2	7.75310	7.75310	7.7531	7.753099	4.1539e-08
4	5.75310	5.57310	5.7531	5.753099	4.0501e-08
6	3.75318	3.75318	3.7532	3.753181	8.4826e-08
8	1.79871	1.79823	1.7988	1.798715	6.7947e-08
10	0.44197	0.44055	0.4420	0.441970	2.2996e-06
12	0.04834	0.04780	0.0483	0.048344	5.6871e-05
14	0.00277	0.00271	0.0028	0.002775	8.0308e-08
16	0.00010	0.00010	0.0001	0.000103	2.2361e-08



(a)



(b)

Figure 3.1: Analytical and numerical approximation of the delta (Δ) and gamma (Γ) respectively.

the analytical and numerical value of Delta and the Gamma. These Figures show that the Greeks are very stable and no spurious oscillation occur at or around the strike price. These Figure show that Greeks are efficiently evaluated using proposed methods.

Example 3.3.2. *Two asset European put option with parameters: $r = 0.1$, $\sigma_1 = 0.2$,*

3.3.1. Numerical results for European options

$\sigma_2 = 0.3$, $\alpha_1 = 0.6$, $\alpha_2 = 0.4$, $q_1 = 0.05$, $q_2 = 0.01$, $E = 1$, $T = 1$.

Now we, present a numerical solution of the European basket put option with the payoff $\max(E - \alpha_1 s_1 - \alpha_2 s_2)$, which does not have analytical solution. The numerical simulation was carried out in truncated domain $x_{1,\max} = x_{2,\max} = 1.5$ and $x_{1,\min} = x_{2,\min} = -1.5$.

Table 3.5: Option value for the two asset European put option at different assets prices.

	V(0.9,1.0)	V(1.0,0.9)	V(1.0,1.0)	V(1.1,1.0)	V(1.0,1.1)	cpu(s)
11×11	0.101680	0.086247	0.063021	0.048665	0.051884	0.235
21×21	0.098306	0.084816	0.065042	0.043989	0.050711	0.842
41×41	0.096912	0.084179	0.064965	0.042094	0.049783	3.505
81×81	0.096369	0.083874	0.064820	0.041640	0.049472	15.400

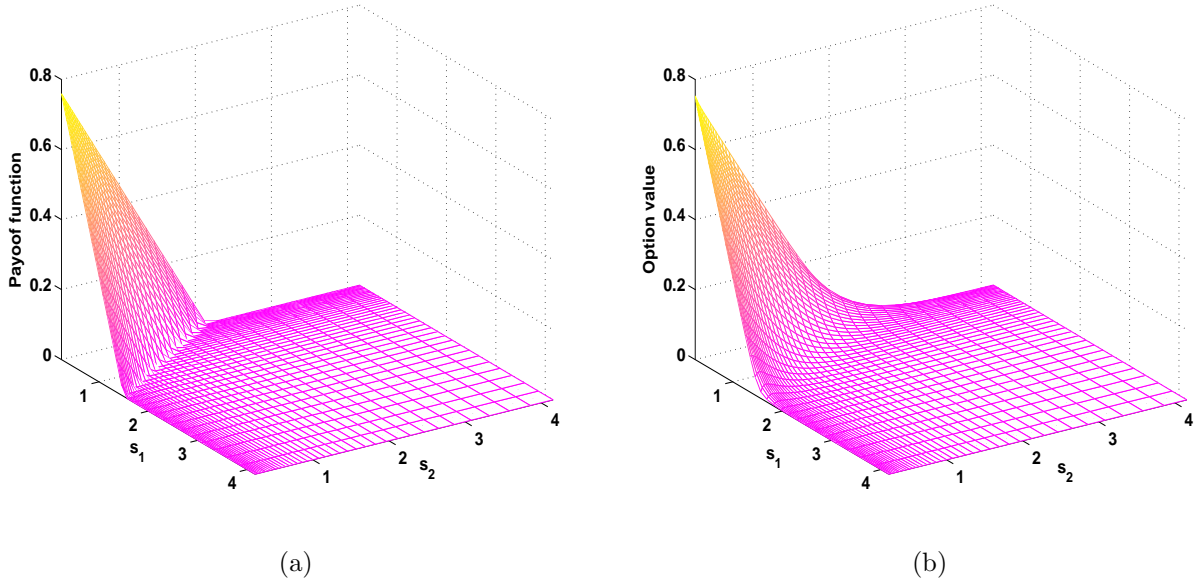


Figure 3.2: The payoff function (left) and the approximate solution of the two-asset European put option (right) at $T=1$.

The value of option at different assets price are reported in Table 3.5, with $\delta t = 0.002$, shape parameter $\epsilon = 1.5$. Finally in Figure 3.2 the option value and payoff function are plotted.

3.3.2 Numerical results for American options

The efficiency of the RBF-FD method has been demonstrated for European options. The pricing of American options is, however, usually more difficult due to the early exercise feature. The American option can be exercised at any time up to the maturity date and can be formulated as the linear complementarity problem.

Example 3.3.3. *American put option; the interest rate r has been fixed at 0.08, the volatility σ has the value 0.2, dividend $q = 0.04$ & 0.08, strike price $E = 100$, and the exercise time used was 3.0 year.*

The above parameter is considered by Ju [67] and Chung et al. [23]. The comparison of proposed method with existing ones for American option at different asset price, numerical experiment with the truncated domain as $x_{\min} = -1.5$ and $x_{\max} = 1.5$ with $M = 2000$ and $N = 500$ is carried out and reported in Table 3.6. For comparison purpose data are taken from the [67]. From the Table, we can observe that proposed method has nice agreement with previous one. The numerical values of option delta are reported in Table 3.7. It is clear from the result presented in the table that the numerical value of option delta lie between -1 to 0 which is in nice agreement with what is mentioned in Hull [61].

Figure 3.3a shows the comparison of European and American option value where as Figure 3.3b shows the optimal exercise curve for American option for parameter given in example 3.3.3 with $q = 0.04$.

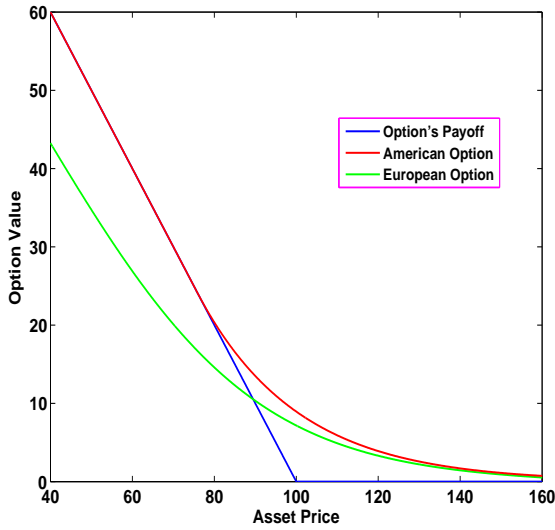
Example 3.3.4. *American put option; the interest rate r has been fixed at 0.1, the volatility σ has the value 0.3, dividend $q = 0$, strike price $E = 100$, and the exercise time used was 1.0 year.*

The above parameter are adopted from Hon [58] with truncated domain $x_{\min} = -5.0$ and $x_{\max} = 7.0$. To satisfy this early optimal exercise for the valuation of the American put options, he simply update, at each time step t_n , in the valuation of the European option. In his computation he has considered 2000 spatial and 500 temporal points and

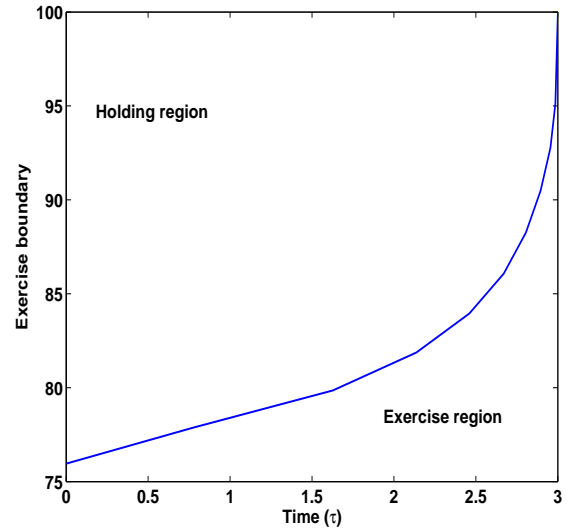
3.3.2. Numerical results for American options

Table 3.6: Price of American put option at different asset price with parameter given in example 3.3.3.

(S, q)	Binomial	LUBA[13]	MGJ [14]	HSY4[60]	HSY6[60]	EXP3[67]	RBF-FD
(80,0.04)	20.3500	20.3335	20.0000	20.5225	20.3932	20.3511	20.350395
(90,0.04)	13.4968	13.4982	14.0246	13.3784	13.4602	13.5000	13.496851
(100,0.04)	8.9438	8.9424	9.1086	8.8038	8.9891	8.9474	8.943894
(110,0.04)	5.9119	5.9122	5.9310	5.9186	5.9269	5.9146	5.911670
(120,0.04)	3.8975	3.8980	3.8823	3.9778	3.8834	3.8997	3.897207
(80,0.08)	22.2050	22.1985	22.7106	22.2445	22.1493	22.2084	22.205090
(90,0.08)	16.2071	16.1986	16.5305	16.1340	16.2578	16.2106	16.207026
(100,0.08)	11.7037	11.6988	11.8106	11.7175	11.7237	11.7066	11.703729
(110,0.08)	8.3671	8.3630	8.4072	8.4355	8.3563	8.3695	8.366811
(120,0.08)	5.9299	5.9261	5.9310	5.9881	5.9323	5.9323	5.929564



(a)



(b)

Figure 3.3: American and European put option value, and optimal early exercise boundary.

apply the quasi-RBFs method with the implicit time integration scheme to compute the American put option values. In Table 3.8, we compared the proposed numerical method with Analytical(Binomial Tree Solution), Global RBF collocation method and quasi-RBFs

3.3.2. Numerical results for American options

Table 3.7: Values of options delta (Δ) of American put option at different asset price with parameter given in example 3.3.3.

(S, q)	Binomial	LUBA[13]	MGJ [14]	HSY4[60]	HSY6[60]	EXP3[67]	RBF-FD
(80,0.04)	-0.8374	-1.0000	-0.8570	-0.8500	-0.8338	-0.8372	-0.837458
(90,0.04)	-0.5541	-0.5939	-0.5754	-0.5472	-0.5547	-0.5540	-0.554144
(100,0.04)	-0.3691	-0.3853	-0.3568	-0.3664	-0.3689	-0.3691	-0.369077
(110,0.04)	-0.2456	-0.2571	-0.2328	-0.2508	-0.2455	-0.2456	-0.245587
(120,0.04)	-0.1628	-0.1645	-0.1606	-0.1630	-0.1628	-0.1628	-0.162825
(80,0.08)	-0.6878	-0.3540	-0.7164	-0.6788	-0.6887	-0.6877	-0.687854
(90,0.08)	-0.5189	-0.5439	-0.5152	-0.5150	-0.5168	-0.5190	-0.518926
(100,0.08)	-0.3871	-0.4043	-0.3779	-0.3929	-0.3869	-0.3872	-0.387133
(110,0.08)	-0.2847	-0.2897	-0.2831	-0.2847	-0.2846	-0.2847	-0.284679
(120,0.08)	-0.2064	-0.2092	-0.2091	-0.2048	-0.2064	-0.2064	-0.206417

Table 3.8: Comparison of American put option for wide range of asset price for example 3.3.4.

S	Analytical	Global RBF	Hon [58]	Present	Error
80	20.268862	20.2777	20.2655	20.268951	8.8798e-05
90	13.120783	13.1142	13.1185	13.120770	1.2970e-05
100	8.337577	8.3338	8.3363	8.337778	2.0099e-04
110	5.208741	5.2092	5.2079	5.208825	8.3069e-05
120	3.207809	3.2108	3.2072	3.207774	3.5771e-05

method with same number of spatial and temporal node for shape parameter $\epsilon = 1.5$. From the Table we observe the proposed method provide much accurate approximation of option than other RBF based numerical method.

Example 3.3.5. *Two asset American put option with parameters: $r = 0.1$, $\sigma_1 = 0.2$, $\sigma_2 = 0.3$, $\alpha_1 = 0.6$, $\alpha_2 = 0.4$, $q_1 = 0.05$, $q_2 = 0.01$, $E = 1$, $T = 1$.*

These parameters are adopted from Fasshauer et al. [35] and numerical simulation are done in computation domain $x_{1,\max} = x_{2,\max} = 1.5$ and $x_{1,\min} = x_{2,\min} = -1.5$. Approximate values of the two assets American put option with uncorrelated assets at different

asset prices for different numbers of node points are displayed in Table 3.9. The parameter for numerical simulation are $\delta t = 0.002$, shape parameter $\epsilon = 1.5$. The option value and the payoff function of two asset American put option are plotted in the Figure 3.4.

Table 3.9: Option value for the two asset American put option at different assets prices.

	V(0.9,1.0)	V(1.0,0.9)	V(1.0,1.0)	V(1.1,1.0)	V(1.0,1.1)	cpu(s)
11×11	0.103421	0.087293	0.063635	0.049124	0.052369	0.293
21×21	0.099706	0.085870	0.065701	0.044370	0.051165	1.308
41×41	0.098302	0.085266	0.065657	0.042445	0.050234	3.873
81×81	0.097765	0.084982	0.065533	0.041997	0.049934	18.677

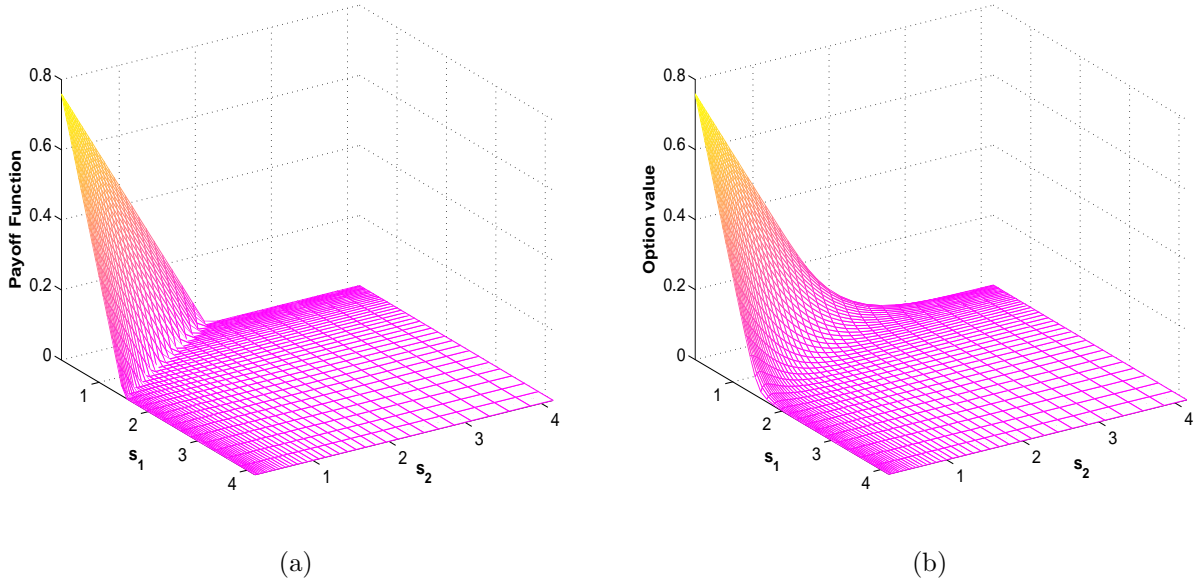


Figure 3.4: The payoff function (left) and the approximate solution of the two-asset American put option (right) at $T=1$.

3.4 Conclusion

In this chapter, a local radial basis function based operator splitting method for numerical solution of multi-dimension American option pricing problem is developed. Numerical

studies for both one and two dimensional problems for European and American put option have been carried out. To compare the method with other existing method, uniform distribution of nodal points has been chosen, though the method can be used on any scattered nodal distribution. It was observed that numerical results are in good agreement with those obtained by other numerical and analytical methods in literature. It has been shown that method is second order accurate in space.

In the next chapter we explore the use of radial basis function based method to solve an European Asian call option problem.

A RBF based finite difference method for Asian option

The purpose of this chapter is to design and describe the valuation of Asian option by radial basis function approximation. A one state variable partial differential equation which characterizes the price of European type Asian call option is discussed. The governing equation is discretized by the θ -method and the option price is approximated by radial basis function based finite difference method. Numerical experiments are performed with European option and Asian option and results are compared with theoretical and numerical results available in the literature. Moreover stability of the scheme is also discussed.

4.1 Introduction

Asian option is an option with the special feature that its payoff depends on arithmetic average of underlying asset price over its lifetime. Since no closed form solution is available to price Asian option, various strategies have been developed to examine it. To cite a few, Thompson [126], gave very constrict bounds, Geman and Yor [47] evaluated the Laplace transformation of Asian option but it was examined that for low volatility and short ma-

turity its numerical inversion created difficulties as shown by Fu et al. [46]. Monte-Carlo simulation methods [10, 73] work well for option pricing, but it is computationally expensive.

Another track to look at Asian option is through solving partial differential equations in two space dimensions, which is prone to oscillatory solution. Ingersoll [63] showed that two dimensional floating strike Asian option can be transformed to one dimensional PDE. Rogers and Shi [108] provided a new transformation to model floating as well as fixed strike Asian option in one dimensional framework, and investigate new bound for it. Chen and Lyuu [19] successfully extended the concept of Rogers and Shi for general maturity. Several independent efforts have been made to price Asian option in recent years, see e.g. Zvan et al. [149], Vecer [66], Benhamou et al. [8]. Zhang [141, 142], Patidar [96] and references therein.

In the present work, equation governing Asian option, derived by Alziary et al. [3] is discretized by using the well known θ -method on time interval and the option price is discretized by using radial basis function based scheme.

We will now describe the outline of the chapter more precisely. In section 4.2, we present the partial differential equation characterizing Asian option problem. The development of the scheme to solve the resulting equation is given in sections 4.3. We study stability of the scheme in section 4.4. Numerical results are presented in section 4.5. Finally, we conclude this chapter in section 4.6.

4.2 The model formulation for Asian option

The pricing of Asian call options with arithmetically averaged strike price can be shown to satisfy a parabolic equation. It can be shown [132] that the two dimensional partial differential equation governing arithmetic Asian call option is given by

$$\frac{\partial V}{\partial \tau} + \frac{1}{2}\sigma^2 S^2 \frac{\partial^2 V}{\partial S^2} + rS \frac{\partial V}{\partial S} + S \frac{\partial V}{\partial I} - rV = 0 \quad (4.2.1)$$

$$V(S, I, T) = \max\left(\frac{I}{T} - E, 0\right). \quad (4.2.2)$$

Here $S = S(\tau)$ denote the price of underlying asset, σ the volatility of underlying asset, r -the risk free interest rate, which is fixed through out the time period of interest, E is the exercise price of the option, T the time of expiry and $I := I(\tau) = \int_0^\tau S(\varphi)d\varphi$ denotes the average price of the underlying asset in some time interval.

The value of Asian put option can easily be deduced from the Put-Call parity. Now taking advantage of Put-Call parity [3, 132], if the known part of average value is greater than strike price, i.e. $(E - \frac{1}{T} \int_0^\tau S(\varphi)d\varphi) \leq 0$, then Geman et al.[47] gave the approximation of call option as

$$V = \frac{S}{Tr} (1 - e^{-r(T-\tau)}) - e^{-r(T-\tau)} \left(E - \frac{1}{T} \int_0^\tau S(\varphi)d\varphi \right). \quad (4.2.3)$$

It is important to point out that the above problem is a two-dimensional PDE which is computationally expensive to solve. Thus taking advantage of homogeneous nature of $V(S, I, T)$ with respect to S and I , several attempts were made to reduce dimensional problem to make it easier from computational point of view. Rogers and Shi[108], Alziary et al.[3] have systematized new one dimensional partial differential equation for Asian option. By introducing new state variable,

$$\begin{cases} V = Su(y, \tau), \\ y = \frac{E - \frac{1}{T} \int_0^\tau S(\varphi)d\varphi}{S}, \end{cases} \quad (4.2.4)$$

the two dimensional PDE (4.2.1-4.2.2) can be reduced to one dimensional PDE as

$$\begin{aligned} \frac{\partial u}{\partial \tau} + \frac{1}{2}\sigma^2 y^2 \frac{\partial^2 u}{\partial y^2} + \left(-\frac{1}{T} - ry\right) \frac{\partial u}{\partial y} &= 0 \\ u(y, T) &= \max(-y, 0). \end{aligned} \quad (4.2.5)$$

Now taking into account of the fact that value of option is known in the case $I \geq ET$ (i.e. $y \leq 0$) and given by expression (4.2.3), by making the change of variables as in (4.2.4) we obtain

$$u = \frac{1}{Tr} (1 - e^{-r(T-\tau)}) - e^{-r(T-\tau)} y. \quad (4.2.6)$$

Hence we are required to solve above PDE (4.2.5) only for $y \geq 0$ using (4.2.6) for the boundary condition at $y = 0$. Therefore, we have the following PDE

$$\frac{\partial u}{\partial \tau} + \frac{1}{2}\sigma^2 y^2 \frac{\partial^2 u}{\partial y^2} + \left(-\frac{1}{T} - ry\right) \frac{\partial u}{\partial y} = 0 \quad (y, \tau) \in (0, \infty) \times [0, T) \quad (4.2.7)$$

with terminal and boundary conditions

$$\begin{aligned} u(y, T) &= \max(-y, 0), \quad y \in (0, \infty) \\ u(0, \tau) &= \frac{1}{Tr} (1 - e^{-r(T-\tau)}), \quad \tau \in [0, T] \\ \lim_{y \rightarrow \infty} u(y, \tau) &= 0, \quad \tau \in [0, T]. \end{aligned} \quad (4.2.8)$$

The boundary condition at infinity comes evidently from the definition of Asian call option, i.e. if strike become very large the option becomes worthless.

The resulting PDE given by (4.2.7) is backward in time and defined on positive real axis, so by introducing new state variable $x = e^{-y}$ and $t = T - \tau$, we get the final problem as follows:

$$\frac{\partial u}{\partial t} = \frac{1}{2} \sigma^2 x^2 (\ln x)^2 \frac{\partial^2 u}{\partial x^2} + \left[\left(\frac{1}{T} - r \ln x \right) x + \frac{\sigma^2}{2} x (\ln x)^2 \right] \frac{\partial u}{\partial x}, \quad (x, t) \in (0, 1) \times (0, T] \quad (4.2.9)$$

with initial and boundary conditions

$$\begin{aligned} u(x, 0) &= 0, \quad x \in (0, 1) \\ u(0, t) &= 0, \quad t \in [0, T] \\ u(1, t) &= \frac{1}{Tr} (1 - e^{-rt}), \quad t \in [0, T]. \end{aligned} \quad (4.2.10)$$

We solve the resulting initial boundary value problem by using RBF based technique discussed in the next section. Once the solution $u(y, \tau)$ is obtained the price of the Asian option is determined by $V(S, I, \tau) = Su(y, \tau)$.

4.3 RBF approximation and time stepping

In order to make this chapter self contained, a brief description of radial basis function based finite difference method is presented.

4.3.1 RBF-FD approximation of space operator

To derive local RBF-FD approximation of any linear differential operator $\mathcal{L} := \frac{d^k}{dx^k}$ of order k at a specific node point x_i , in the discretized domain $\Omega := \{x_1, x_2, \dots, x_n\}$ containing n

number of nodes, consider any subset Ω_i containing $n_i (<< n)$ nodes in the neighborhood of x_i . In RBF-FD approach we are required to compute weights w_j such that;

$$\mathcal{L}u(x_i) = \sum_{j=1}^{n_i} w_j u(x_j). \quad (4.3.1)$$

For each node $x_i \in \Omega$ we compute the weights w_j on each local support Ω_i . In traditional methods, generally these nodes are equidistant and the weights are computed using classical polynomial interpolation. At the same time in radial basis function interpolation, randomly distributed nodes are used.

Let $s(x)$ be a radial basis function interpolant that interpolates function $u(x)$ at the interpolation points contained in Ω_i . Then $s(x)$ can be represented by

$$s(x) = \sum_{j=1}^{n_i} \lambda_j \phi(\|x - x_j\|) + \sum_{j=1}^l \gamma_j p_j(x) \quad (4.3.2)$$

where $\|\cdot\|$ is the Euclidian norm and $\{p_j(x)\}_{j=1}^l$ denote basis of \prod_{m-1}^d , which is space of d -variate polynomials of total degree $\leq m-1$, where m is order of ϕ . The coefficients λ_j and γ_j are evaluated by imposing the following conditions

$$s(x_i) = u(x_i), \quad 1 \leq i \leq n_i \quad (4.3.3)$$

$$\sum_{j=1}^{n_i} \lambda_j p_k(x_j) = 0, \quad 1 \leq k \leq l. \quad (4.3.4)$$

Imposing conditions (4.3.3-4.3.4) on $s(x)$ gives a linear system

$$\begin{pmatrix} \Phi & P \\ P^t & O \end{pmatrix} \begin{pmatrix} \lambda \\ \gamma \end{pmatrix} = \begin{pmatrix} u|_{\Omega_i} \\ O \end{pmatrix} \quad (4.3.5)$$

where $\Phi := (\phi(\|x_i - x_j\|))_{1 \leq i, j \leq n_i} \in \mathbb{R}^{n_i \times n_i}$, $P := (p_j(x_i))_{1 \leq i \leq n_i, 1 \leq j \leq l} \in \mathbb{R}^{n_i \times l}$.

Suppose ϕ is conditionally positive definite function of order m on \mathbb{R}^d and the points $\Omega_i := \{x_i \in \mathbb{R}^d; i = 1, 2, \dots, n_i\}$ form $(m-1)$ unisolvent set of centers. Then the system (4.3.5) is uniquely solvable. We will refer coefficient matrix in (4.3.5) by ‘ A ’ for future reference.

To derive RBF-FD approximation the interpolant is represented in Lagrangian form as

$$s(x) = \sum_{j=1}^{n_i} \psi_j(x) u(x_j) \quad (4.3.6)$$

where $\psi_j(x)$ are Lagrange functions that satisfy the cardinal conditions,

$$\psi_j(x_k) = \delta_{jk}, \quad j, k = 1, 2, \dots, n_i. \quad (4.3.7)$$

A closed form expression for each $\psi_j(x)$ can be obtained in terms of corresponding radial basis functions by modeling another set of RBF interpolation problems and is given as: [39];

$$\psi_j(x) = \frac{|A_j(x)|}{|A|}, \quad j = 1, 2, \dots, n_i \quad (4.3.8)$$

where matrix ' $A_j(x)$ ' can be obtained from matrix ' A ', by replacing j^{th} row vector by

$$B(x) = [\phi(\|x - x_1\|) \ \phi(\|x - x_2\|) \ \dots \ \phi(\|x - x_{n_i}\|) \ | \ p_1(x) \ p_2(x) \ \dots \ p_l(x)]. \quad (4.3.9)$$

Now application of operator \mathcal{L} on the interpolant in (4.3.6) gives

$$\mathcal{L}u(x_i) \approx \mathcal{L}s(x_i) = \sum_{j=1}^{n_i} \mathcal{L}\psi_j(x_i)u(x_j). \quad (4.3.10)$$

From equations (4.3.1) and (4.3.10), the weights w_j can be written as,

$$w_j = \mathcal{L}\psi_j(x_i) = \mathcal{L} \frac{|A_j(x)|}{|A|} \Big|_{x=x_i}, \quad j = 1, 2, \dots, n_i. \quad (4.3.11)$$

After some applications of Cramer's rule to (4.3.10), and taking advantage of the nature of interpolation matrix, the weights are given by

$$\begin{pmatrix} \Phi & P \\ P^t & O \end{pmatrix} \begin{pmatrix} w \\ \xi \end{pmatrix} = (\mathcal{L}B(x))^T \Big|_{x=x_i} \quad (4.3.12)$$

where $B(x)$ is the vector defined by (4.3.9) ξ is a dummy vector corresponding to the vector γ in (4.3.2). It was shown by Wright et al.[133] that in the case of uniform points distribution, weights of RBF-FD formula converge to the weights of corresponding classical finite difference formula.

It is obvious from the linear system(4.3.12) that its size is only $n_i + l$, which is much smaller than the size $n + l$ of global RBF collocation. Thus the proposed method provides more stable system for a wide class of shape parameter ϵ .

4.3.2 Temporal approximation

The numerical solution of Asian option, using any implicit technique, requires the generation of a modified PDE operator through a finite difference approximation of time derivative, we will do this using weighted θ -method.

Consider the following initial-boundary value problem

$$\begin{aligned}\frac{\partial u(x, t)}{\partial t} &= \mathcal{L}u(x, t), \quad x \in \Omega, 0 \leq t \leq T \\ u(x, 0) &= u_0 \\ u(x, t) &= g(x, t), \quad x \in \partial\Omega,\end{aligned}\tag{4.3.13}$$

where $\mathcal{L}u = \frac{1}{2}\sigma^2 x^2 (\ln x)^2 \frac{\partial^2 u}{\partial x^2} + \left[\left(\frac{1}{T} - r \ln x \right) x + \frac{\sigma^2}{2} x (\ln x)^2 \right] \frac{\partial u}{\partial x}$, $u_0 = 0$, $g(0, t) = 0$ and $g(1, t) = \frac{1}{Tr} (1 - e^{-rt})$. A finite difference approximation made for the time derivative with notation $u^n(x)$ that approximate the exact solution $u(x, t)$ at t^n and $t^n = t^{n-1} + \delta t$, we obtain

$$\frac{u^{n+1} - u^n}{\delta t} = \theta \mathcal{L}u^{n+1} + (1 - \theta) \mathcal{L}u^n.\tag{4.3.14}$$

For each fixed time level t_n , above is linear system of ODEs. Now using radial basis function based finite difference method discussed through (4.3.1) to (4.3.12) for spacial discretization of operator $\mathcal{L}u$ leads to

$$[I - \theta \delta t L] U^{n+1} = [I + (1 - \theta) \delta t L] U^n\tag{4.3.15}$$

where L is the discretization matrix for the RBF based space discretization of linear differential operator $\mathcal{L}u$ and I is the identity matrix.

4.4 Stability Analysis

In this section, we present an analysis of the stability of the radial basis function based finite difference method using the matrix method. A small perturbation at n^{th} time level $e^n = U^n - \tilde{U}^n$ is introduced in the equation (4.3.15), where U^n is exact and \tilde{U}^n is numerical solution. The equation for the error e^{n+1} can be written as $e^{n+1} = G e^n$, where the amplification matrix $G = [I - \theta \delta t L]^{-1} [I + (1 - \theta) \delta t L]$. The numerical scheme will be stable if

as $n \rightarrow \infty$, the error $e^n \rightarrow 0$. This can be ensured provided $\rho(G) < 1$, where $\rho(G)$ denote the spectral radius of G .

It can be seen that the stability is assured if all eigenvalues of the matrix $[I - \theta\delta t L]^{-1}[I + (1 - \theta)\delta t L]$ satisfies the following condition

$$\left| \frac{1 + (1 - \theta)\delta t \lambda}{1 - \theta\delta t \lambda} \right| \leq 1 \quad (4.4.1)$$

where λ is an eigenvalue of the matrix L . For the case of the Crank-Nicolson scheme ($\theta = 0.5$) the inequality (4.4.1) is always satisfied provided $Re(\lambda) \leq 0$. This show that scheme is unconditionally stable if $Re(\lambda) \leq 0$. The eigenvalues of matrix L is highly dependent on the mesh spacing parameter ' h ' (' h ' is defined to be the minimal distance between any two points in the domain) and the shape parameter ' ϵ '. In the case of global collocation, it is found that condition number of the collocation matrix becomes very large and the system leads to ill-conditioning, when ' ϵ ' and ' h ' become very very small. The present local RBF approximation is free from these complexities. Since it is not possible to find explicit relationship among the eigenvalue of matrix L , number of nodes and the shape parameter ' ϵ ', we investigate this dependence numerically and is given in Figure 4.1.

Figure 4.1a shows how maximum eigenvalue $Re(\lambda)$ of matrix L varies as a function of shape parameter ϵ , when mesh spacing parameter ' h ' is constant. Figure 4.1b shows that effect of mesh length ' h ' for eigenvalue of matrix L , when the shape parameter ' ϵ ' is constant. It can be seen that in both cases, the scheme satisfies the stability condition for wide range of these parameters.

4.5 Numerical simulation and discussion

Using the RBF approach, the resulting problems for European call and Asian call option are solved via Crank-Nicolson's method. The computational domain (x_{\min}, x_{\max}) are partitioned with M equispaced spatial nodes x_i with mesh length $h = 1/(M - 1)$. The temporal domain is divided into N equispace points with $T/(N - 1)$. In all numerical experiments equispaced grid with $n_i = 3$ are used, although there is no restriction on choice of grid points.

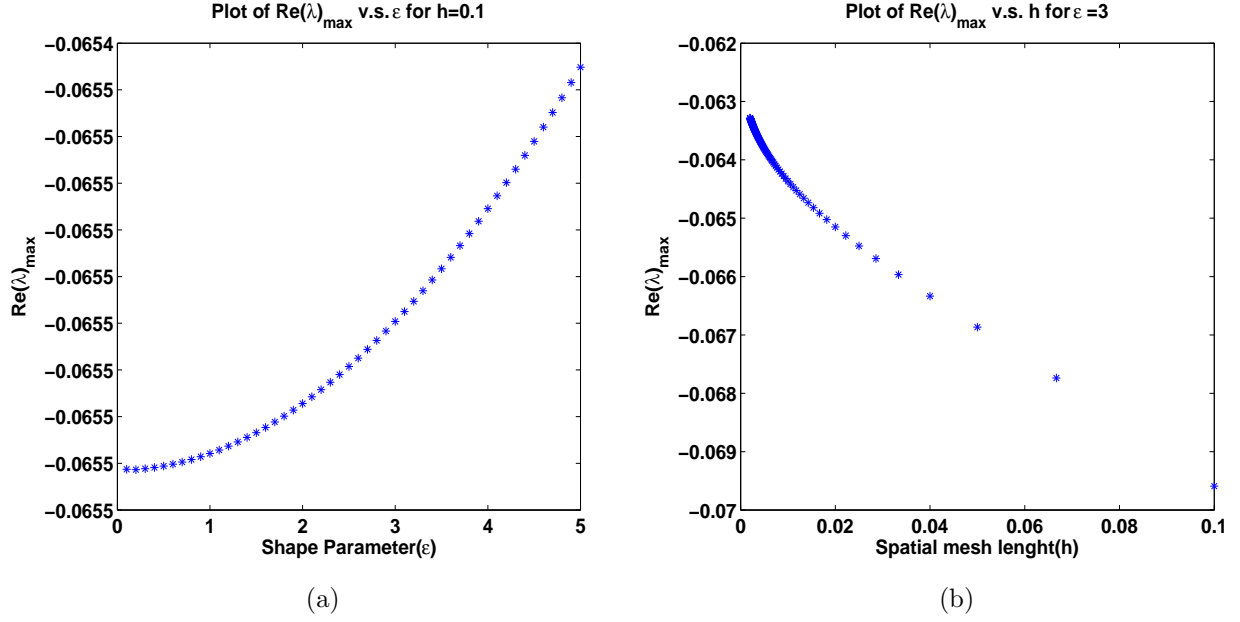


Figure 4.1: A stability plot for RBF-FD method

4.5.1 European call option

The European call option can be modeled by Black-Scholes PDE

$$\frac{\partial V}{\partial \tau} + \frac{1}{2}\sigma^2 S^2 \frac{\partial^2 V}{\partial S^2} + rS \frac{\partial V}{\partial S} - rV = 0, \quad (S, \tau) \in (0, \infty) \times [0, T] \quad (4.5.1)$$

with the payoff function given as

$$V(S, T) = \max(S - E, 0). \quad (4.5.2)$$

The boundary conditions are given as

$$V(S, \tau) = \begin{cases} 0 & \text{for } S = 0, \\ S - Ee^{-r(T-\tau)} & \text{for } S \rightarrow \infty. \end{cases} \quad (4.5.3)$$

The analytical solution for the European call option is

$$V(S, \tau) = S\mathcal{N}(d_1(S, \tau)) - Ee^{-r(T-\tau)}\mathcal{N}(d_2(S, \tau)) \quad (4.5.4)$$

where $\mathcal{N}(\cdot)$ is the cumulative distribution function of the standard normal distribution with:

$$\begin{aligned} d_1(S, \tau) &= \frac{\ln(\frac{S}{E}) + (r + \frac{1}{2}\sigma^2)(T - \tau)}{\sigma\sqrt{T - \tau}} \\ d_2(S, \tau) &= \frac{\ln(\frac{S}{E}) + (r - \frac{1}{2}\sigma^2)(T - \tau)}{\sigma\sqrt{T - \tau}}. \end{aligned}$$

A simple transformation $x = \ln(\frac{S}{E})$ and $t = T - \tau$ changes equation (4.5.1) and condition(4.5.2) and (4.5.3) to

$$\frac{\partial u}{\partial t} + \frac{1}{2}\sigma^2 \frac{\partial^2 u}{\partial x^2} + (r - \frac{1}{2}\sigma^2) \frac{\partial u}{\partial x} - ru = 0, \quad (x, \tau) \in (-\infty, \infty) \times (0, T] \quad (4.5.5)$$

with initial and boundary conditions;

$$u(x, 0) = \max(Ee^x - E, 0) \quad (4.5.6)$$

$$u(x, t) = \begin{cases} 0 & \text{for } x \rightarrow -\infty, \\ Ee^x - Ee^{-rt} & \text{for } x \rightarrow \infty. \end{cases} \quad (4.5.7)$$

To illustrate accuracy of proposed method, numerical simulation was done for European call option with the parameter $x_{\min} = -2$, $x_{\max} = 2$, $r = 0.05$, $\sigma = 0.2$, $T = 0.5$ year and $E = 10$. Table 4.1 show the convergence trends of the present method, with $n_i = 3$, $N = M$ where M and N are number of points in spatial and temporal domain. From the tabular results one can observe that the Crank-Nicholson's method converges to the true solution.

4.5.2 Asian option

We now demonstrate the accuracy of the method for Asian option by extensive numerical experiments. It is important that accuracy of RBF method highly depends upon the value of shape parameter ϵ . In order to compute optimal value of shape parameter, extensive numerical experiments were carried out for fixed strike price $E = 100$, taking true solution as given by Zhang[141]. Figures 4.2a-4.3d show the effect of shape parameter ϵ on the error in the option price at asset price $S = 100$.

Table 4.1: Absolute error and rate of convergence for European call option with uniform points and different values of ϵ

M	$\epsilon = 0.7$		$\epsilon = 1.5$		$\epsilon = 3.0$	
	E_∞	<i>rate</i>	E_∞	<i>rate</i>	E_∞	<i>rate</i>
41	3.624805e-02		2.798608e-02		8.502729e-02	
81	8.056097e-03	2.17	6.620065e-03	2.08	2.433330e-02	1.80
161	1.973117e-03	2.03	1.682036e-03	2.00	6.328063e-03	1.94
321	4.909534e-04	2.00	4.217498e-04	2.00	1.596444e-03	1.98
641	1.229137e-04	2.00	1.055320e-04	2.00	4.000567e-04	2.00

In the sequel, we first perform numerical experiments with parameter, interest rate $r = 0.09$, spot price $S = 100$, maturity time $T = 1$ for wide range of volatilities σ and strike price E . Table 4.2 presents option value by proposed method and its comparison with Zhang [141, 142], and Chen-Lyuu [19]. From the table we observe that our results are never more than 0.33% away from the method of Zhang[141]. These errors are observed at small value of volatility ($\sigma = 0.05$) due to convection dominant nature of the problem. Table 4.3 compares the proposed method with approximation method of Ju [68], the PDE method of Zhang [141], and method of Chen-Lyuu [19] for long maturity time $T = 3$ years. Our results are not more than 0.036% away from Zhang [141], and 0.046% away from Chen-Lyuu[19] algorithm, which is treated as accurate result for long maturity.

In Table 4.4 we compared the present method with Zhang [141], and Chen-Lyuu[19] and tight bounds produced by Rogers and Shi [108] for different value of interest rate r and volatility σ , it shows that our results are not away more than 0.657% for $\sigma = 0.05$, 0.114% for $\sigma = 0.1$, 0.0064% for $\sigma = 0.20$, and 0.0042% for $\sigma = 0.30$ of Zhang [141].

Finally our method for fixed strike Asian option approximate option value very well and from tabulated data we observe that results obtained by the proposed method are in nice agreement with result available in literature.

Table 4.2: Comparison of numerical solution of Asian option with $S = 100$, $r = 0.09$, and $T = 1$ for a wide range of volatilities.

E	σ	Zhang[141]	Zhang-AA2[142]	Zhang-AA3[142]	Chen-Lyuu[19]	Present method
95	0.05	8.8088392	8.80884	8.80884	8.808839	8.808746
100		4.3082350	4.30823	4.30823	4.308231	4.293767
105		0.9583841	0.95838	0.95838	0.958331	0.961122
95	0.1	8.9118509	8.91171	8.91184	8.911836	8.909864
100		4.9151167	4.91514	4.91512	4.915075	4.911250
105		2.0700634	2.07006	2.07006	2.069930	2.070191
95	0.2	9.9956567	9.99597	9.99569	9.995362	9.995095
100		6.7773481	6.77758	6.77738	6.776999	6.776948
105		4.2965626	4.29643	4.29649	4.295941	4.296579
95	0.3	11.6558858	11.65747	11.65618	11.654758	11.655882
100		8.8287588	8.82942	8.82900	8.827548	8.828822
105		6.5177905	6.51763	6.51802	6.516355	6.517978
95	0.4	13.5107083	13.51426	13.51182	13.507892	13.510673
100		10.9237708	10.92507	10.92474	10.920891	10.923771
105		8.7299362	8.72936	8.73089	8.726804	8.729990
95	0.5	15.4427163	15.44890	15.44587	15.437069	15.442694
100		13.0281555	13.03015	13.03107	13.022532	13.028158
105		10.9296247	10.92800	10.93253	10.923750	10.929655

4.6 Conclusion

This chapter describes the application of local radial basis function based grid free method for numerical solution of Asian option. The governing equation is discretized by Crank-Nicolson method on time interval and option price is approximated by RBF based method. Numerical study with European call option and Asian option is carried out that are in good agreement with those obtained by other numerical and analytical methods in literature. It has been shown that method is second order accurate in space.

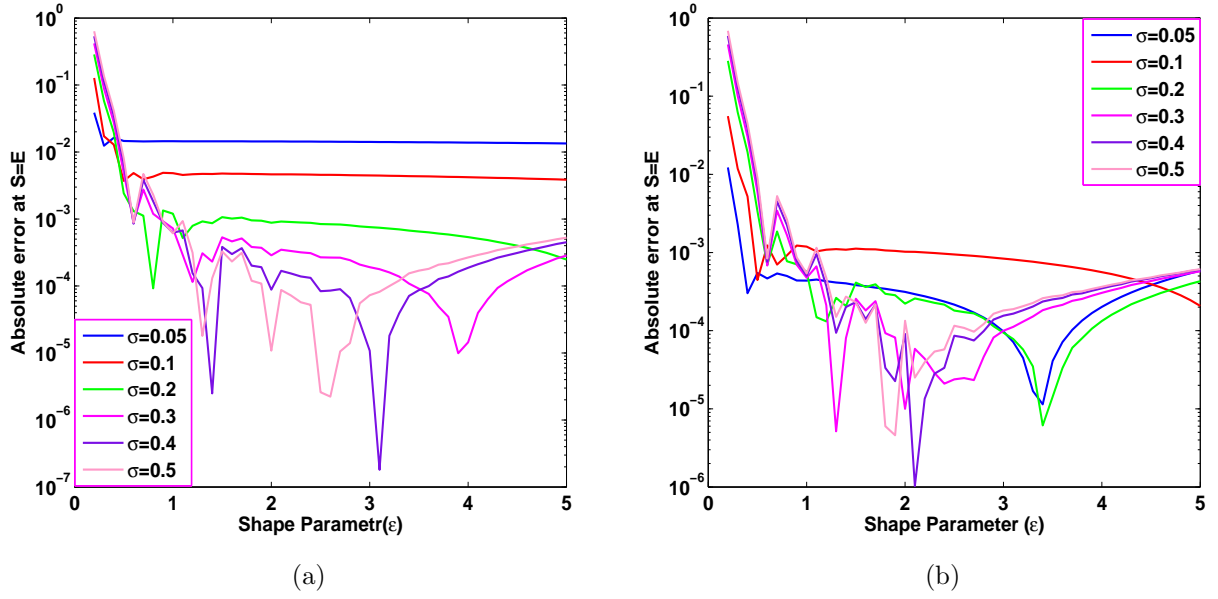
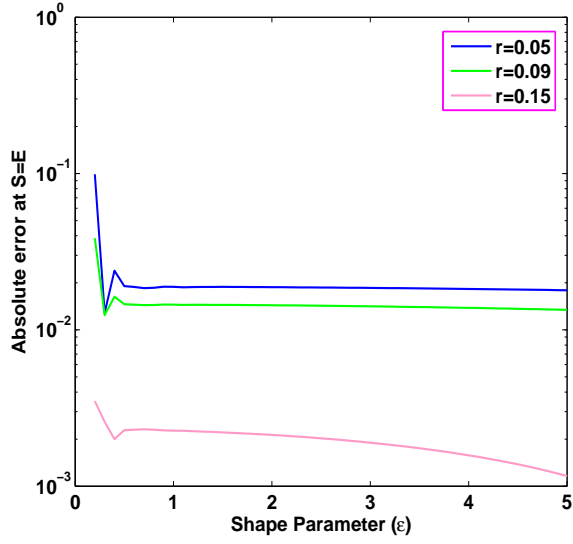
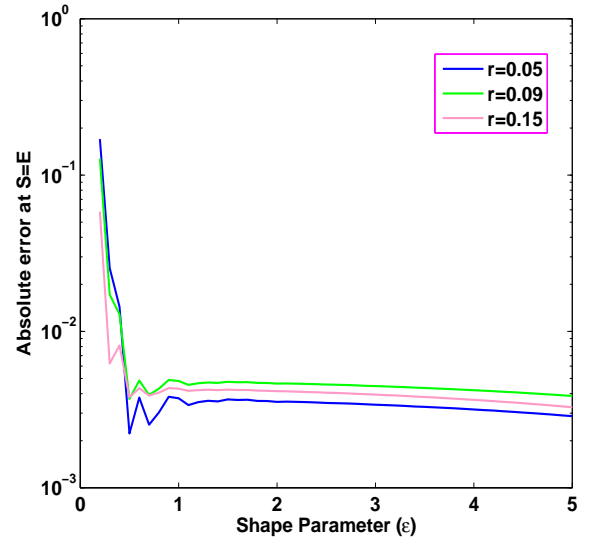


Figure 4.2: Error plot for Asian option for parameters $E = 100$, $r = 0.09$ with maturity year $T = 1$ and $T = 3$.

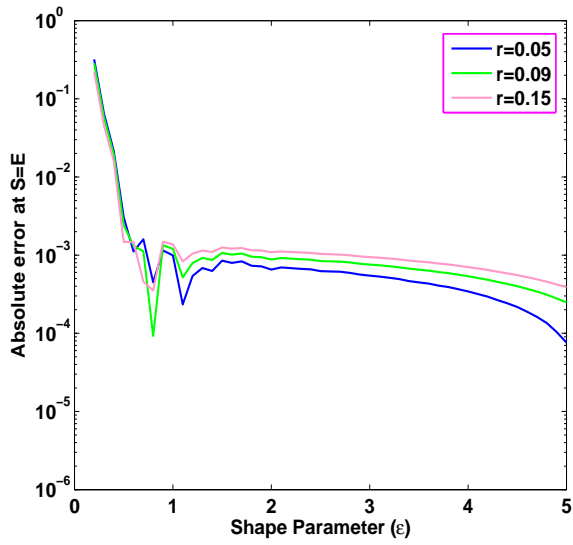
In next chapter, we discuss the application of the proposed approach to solve American style Bond option.



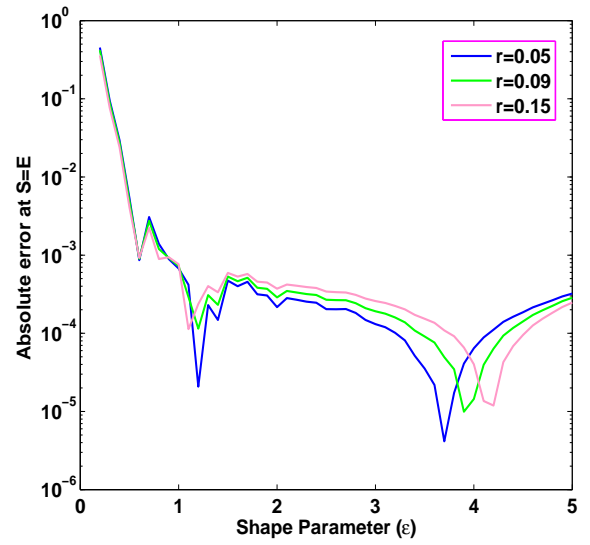
(a)



(b)



(c)



(d)

Figure 4.3: Error plot for Asian option for parameter $E = 100$, $T = 1$ with volatility $\sigma = 0.05$, $\sigma = 0.1$, $\sigma = 0.2$ and $\sigma = 0.3$ respectively.

Table 4.3: Comparison of numerical solution of Asian option with $S = 100$, $r = 0.09$, and $T = 3$ for a wide range of volatilities.

E	σ	Zhang[141]	N. Ju [68]	Chen-Lyu[19]	Present Method
95	0.05	15.1162646	15.11626	15.116264	15.116784
100		11.3036080	11.30360	11.303605	11.303619
105		7.5533233	7.55335	7.553278	7.550559
95	0.1	15.2138005	15.21396	15.213761	15.214139
100		11.6376573	11.63798	11.637525	11.637450
105		8.3912219	8.39140	8.390833	8.390679
95	0.2	6.6372081	16.63942	16.636109	16.637222
100		13.7669267	13.76770	13.765476	13.766921
105		11.2198706	11.21879	11.217842	11.219881
95	0.3	19.0231619	19.02652	19.018567	19.023123
100		16.5861236	16.58509	16.581024	16.586118
105		14.3929780	14.38751	14.387081	14.392999
95	0.4	21.7409242	21.74461	21.729124	21.740921
100		19.5882516	19.58355	19.575938	19.588251
105		17.6254416	17.61269	17.612310	17.625444
95	0.5	24.5718705	24.57740	24.547903	24.571875
100		22.6307858	22.62276	22.606509	22.630790
105		20.8431853	20.82213	20.818216	20.843189

4.6. Conclusion

Table 4.4: Comparison of numerical solution of Asian call option with $S = 100$, $T = 1$ and different value of E , σ and r .

E	σ	r	Zhang[141]	Chen-Lyu[19]	LB[108]	UB[108]	Present Method
95	0.05	0.05	7.1777275	7.177726	7.178	7.183	7.175765
100			2.7161745	2.716168	2.716	2.722	2.698446
105			0.3372614	0.337231	0.337	0.343	0.352965
95	0.09	0.09	8.8088392	8.808839	8.809	8.821	8.808758
100			4.3082350	4.308231	4.308	4.318	4.283546
105			0.9583841	0.958331	0.958	0.968	0.954690
95	0.15	0.15	11.0940944	11.094094	11.094	11.114	11.09415
100			6.7943550	6.794354	6.794	6.810	6.792121
105			2.7444531	2.744406	2.744	2.761	2.726415
90	0.10	0.05	11.9510927	11.951076	11.951	11.973	11.953215
100			3.6413864	3.641344	3.641	3.663	3.637219
110			0.3312030	0.331074	0.331	0.353	0.337345
90	0.09	0.09	13.3851974	13.385190	13.385	13.410	13.388299
100			4.9151167	4.915075	4.915	4.942	4.909945
110			0.6302713	0.630064	0.630	0.657	0.6362398
90	0.15	0.15	15.3987687	15.398767	15.399	15.445	15.402474
100			7.0277081	7.027678	7.028	7.066	7.024155
110			1.4136149	1.413286	1.413	1.451	1.416265
90	0.20	0.05	12.5959916	12.595602	12.595	12.687	12.597362
100			5.7630881	5.762708	5.762	5.854	5.763635
110			1.9898945	1.989242	1.989	2.080	1.991436
90	0.09	0.09	13.8314996	13.831220	13.831	13.927	13.833212
100			6.7773481	6.776999	6.777	6.872	6.777822
110			2.5462209	2.545459	2.545	2.641	2.547564
90	0.15	0.15	15.6417575	15.641598	15.641	15.748	15.643980
100			8.4088330	8.408519	8.408	8.515	8.409378
110			3.5556100	3.554687	3.554	3.661	3.556587
90	0.30	0.05	13.9538233	13.952421	13.952	14.161	13.954513
100			7.9456288	7.944357	7.944	8.153	7.946030
110			4.0717942	4.070115	4.070	4.279	4.072374
90	0.09	0.09	14.9839595	14.982782	14.983	15.194	14.984747
100			8.8287588	8.827548	8.827	9.039	8.829161
110			4.6967089	4.694902	4.695	4.906	4.697238
90	0.15	0.15	16.5129113	16.512024	16.512	16.732	16.513864
100			10.2098305	10.208724	10.208	10.429	10.210269
110			5.7301225	5.728161	5.728	5.948	5.730579

A RBF based operator splitting method for pricing American option on zero coupon bond

In this chapter, we present a numerical method to price an American put option on zero-coupon bond. Using the concept that American option can be formalized in form of linear complementarity problems, we proposed a radial basis function based operator splitting method. The time semi discretization is done by an implicit method and operator splitting method to treat the American constraints and space discretization of underlying equation is done by using RBF based finite difference method. In numerical experiment, the prices of zero-coupon bond, European bond option and American put option are given and the optimal early interest rate is also provided.

5.1 Introduction

In the recent days pricing of interest rate derivatives, like bond options, interest rate caps and swaps have been getting much attention by both mathematicians and financial engi-

neers. The dynamics of interest rates play an important role in the decisions related to an investment, its risk management and also the transactions based on lending and borrowing. Interest rate models are typically used in the pricing of the interest rate derivatives. Pricing and hedging interest rate derivatives have greater challenges than stock derivatives. For example, in Bond option, the Bond as its underlying derivative and price of Bond depend both on interest rate and time. Hence, their study has gained importance in the developing economics literature.

In this chapter we analyze the pricing of zero coupon bond and bond option when the short term interest rate $r = r(\tau)$ can be nested in the Chan-Karolyi-Longstaff-Sanders (CKLS) model [17] and defined by

$$dr = \kappa(\theta - r)d\tau + \sigma r^\gamma dW, \quad (5.1.1)$$

where κ is the speed of mean reversion, θ is long term interest rate, σ is volatility of diffusion, W denote the standard Brownian motion and γ is the parameter used for nesting the different models. This specification (5.1.1) includes the Vasicek model which correspond to the choice $\gamma = 0$ and the Cox-Ingersoll-Ross (CIR) model for which $\gamma = 1/2$, in which the explicit solution for zero coupon bond and bond price exist. In the pioneering paper of Chan et al. [17], it is claimed that model which allow $\gamma \geq 1$ have a greater ability to capture the dynamics of the short term interest rate better than $\gamma < 1$. For these values of the γ in the model (5.1.1), numerical approach is required for valuation of zero coupon bond and bond price.

In the recent work of Choi and Wirjanto [22], an approximated analytical formula was suggested for zero coupon bond price. Its derivation are basically based on approximation of the integral term in the probabilistic representation of the solution. However using the exact solution for the CIR zero coupon bond price, we can observe that the given formula is only accurate for small value of volatility. Hence a more accurate numerical method is required. In [125], Tangman et al. provided a new time integration scheme called exponential time integration for pricing zero coupon bond and bond option price under CKLS model.

It is well known that the American options on zero-coupon bond can be formulated in the form of linear complementarity problem (LCP). Due to early exercise feature of these problems, do not admit the analytical solution. Hence, numerical methods are normally used for pricing American bond options. Various approximation techniques have been developed for the solution of American bond option pricing problem. To cite a few, in [1], Allegretto et al. used both finite element and finite difference method to price the option. Zhang and Song [144] used fitted finite volume method. In [147], Zhou et al. presented a new scheme to solve LCP and they also compared their result with Brennan-Schwartz algorithm. In [118], ShuJin et al. provided characteristic nature of option value and early exercise curve for different value of strike price for American put option.

The chapter is organized as follows. In section 5.2, we introduce the mathematical model for pricing American options on a bond which is a partial differential complementarity problem. Section 5.3 deals with the construction of three time level implicit scheme to discretize the model. The time semi discrete equation is coupled with radial basis function based finite difference method for spatial discretization. We also provide extension of proposed method for pricing American option by utilizing concept of operator splitting method. In section 5.4, we give some numerical results for bond value and option value for both American and European options. Finally the chapter ends with some conclusive remarks in section 5.5.

5.2 The pricing model of zero coupon bond and option

Under the assumption of interest rate model (5.1.1), one can derive the pricing equation of zero coupon bond and European call (similarly put) option on the bond using no arbitrage assumption. In fact the pricing equation is same in both financial product. Let us consider the price of zero coupon bond with face value K and maturity T^* . Then the bond price $B(r, \tau)$, satisfies the following equation:

$$\frac{\partial B}{\partial \tau} + \frac{1}{2}\sigma^2 r^{2\gamma} \frac{\partial^2 B}{\partial r^2} + \kappa(\theta - r) \frac{\partial B}{\partial r} - rB = 0, \quad (5.2.1)$$

$$B(r, T^*) = K. \quad (5.2.2)$$

Furthermore, let $V(r, \tau)$ represent the value of European call/put option on the above bond with maturity $T(< T^*)$ and exercise price E . Although the underlying asset is the bond, the independent variable in the governing equation is the stochastic interest rate. However bond price is used in the final and boundary conditions. Then the pricing equation is given by

$$\frac{\partial V}{\partial \tau} + \frac{1}{2}\sigma^2 r^{2\gamma} \frac{\partial^2 V}{\partial r^2} + \kappa(\theta - r) \frac{\partial V}{\partial r} - rV = 0, \quad (5.2.3)$$

together with final condition [26]

$$V(r, T) = \begin{cases} \max(B(r, T^* - T) - E, 0) & \text{for call option} \\ \max(E - B(r, T^* - T), 0) & \text{for put option.} \end{cases} \quad (5.2.4)$$

In order to solve the option price problems (5.2.3) and (5.2.4), we need to solve the (5.2.1) and (5.2.2) for bond price first. In Sorwar [121] the asymptotic boundary conditions $B(\infty, t) = V(\infty, t) = 0$ are used. However to compute the bond value numerically, in [121] the dynamic boundary condition at $r = 0$ and the Dirichlet boundary condition at $r = R$ are used, where short term interest rate r lie in computational domain $[0, R]$, for sufficiently large R . However in our case we use one side approximation of first and second derivatives in place of any boundary conditions.

Now similar to the American put option on stocks, there is optimal interest rate $r^*(\tau)$, known as early interest rate for American put option on bonds. It is the smallest value of the interest rate at which the exercise of the put becomes optimal. The American put option value satisfies the following linear complementarity problem [144]:

$$\begin{cases} \frac{\partial V}{\partial \tau} + \mathcal{L}V \leq 0, \\ V(r, \tau) - g(r, \tau) \geq 0, \\ (\frac{\partial V}{\partial \tau} + \mathcal{L}V)(V(r, \tau) - g(r, \tau)) = 0, \end{cases} \quad (5.2.5)$$

for $(r, \tau) \in (0, R) \times (0, T]$ together with initial condition

$$V(r, T) = g(r, T) \quad (5.2.6)$$

and boundary conditions

$$\begin{cases} V(r, \tau) = g(r, \tau), & r = 0 \\ V(r, \tau) = g(r, \tau), & r = R, \end{cases} \quad (5.2.7)$$

where $g(r, \tau) = \max(E - B(r, \tau, T^*), 0)$ and $\mathcal{L} = \frac{1}{2}\sigma^2 r^{2\gamma} \frac{\partial^2}{\partial r^2} + \kappa(\theta - r) \frac{\partial}{\partial r} - r$.

It is worth to be noted that E should be strictly less than $B(0, \tau, T^*)$, otherwise exercise the option would never be optimal.

5.3 Numerical scheme

Introducing a time-reverse transformation $t = T - \tau$ and $\mathcal{G}(r, t) = g(r, T - \tau)$, with the notation $u(r, t)$ represent either Bond value or Bond option value, the option pricing problem can be formulated as the following parabolic partial differential equation on truncated domain $\Omega \times [0, T)$.

$$\frac{\partial u(r, t)}{\partial t} = \mathcal{L}u(r, t), \quad (r, t) \in \Omega \times [0, T) \quad (5.3.1)$$

$$u(r, 0) = \mathcal{G}(r, 0), \quad x \in \bar{\Omega} \quad (5.3.2)$$

Let $\{0 = t_0 < t_1 < \dots < t_N = T; t_n - t_{n-1} = \delta t, 1 \leq n \leq N\}$ be a partition of the interval $[0, T]$. Let us use the notation $u^n := u(x, t_n)$ then equation (5.3.1) will be discretized by following implicit scheme,

$$\frac{1}{\delta t} \left(\frac{3}{2}u^{n+1} - 2u^n + \frac{1}{2}u^{n-1} \right) = \mathcal{L}u^{n+1}, \quad n \geq 1. \quad (5.3.3)$$

The above discretization method of the operator $\mathcal{L}u$ is called implicit backward difference method. In order to use the proposed method we need two initial values on the zeroth and first time level. The value u^0 at the zeroth time level is given by initial condition on the model problem, and the value u^1 can be obtained by applying the implicit backward difference method of order one,

$$\frac{u^{n+1} - u^n}{\delta t} = \mathcal{L}u^{n+1}. \quad (5.3.4)$$

We solve the resulting time semi discrete scheme by using radial basis function based finite difference method discussed in previous chapters.

Algorithm to evaluate an European option

The approximated value of the solution $u_m^n = u(r_m, t_n)$ denoted by U_m^n can be obtained by following time stepping problem;

```

for  $n = 0 : N - 1$ 
  if  $n = 0$ 
     $\frac{U_m^{n+1} - U_m^n}{\delta t} = \mathcal{L}_\Delta U_m^{n+1}$ 
  else
     $\frac{1}{\delta t} \left( \frac{3}{2} U_m^{n+1} - 2U_m^n + \frac{1}{2} U_m^{n-1} \right) = \mathcal{L}_\Delta U_m^{n+1}$ 
  end
end

```

Where $\mathcal{L}_\Delta U$ is local RBF based space discretization of differential operator $\mathcal{L}u$ obtained by using procedure described above. Since the option price problem has non smooth payoff function, there is possibility to have an oscillation on the final time level. To overcome this problem, the solutions on two time levels are calculated by the implicit Euler method.

5.3.1 Operator splitting method

The discussed time discretization for the European option can be combined with the operator splitting method to solve the linear complementarity problem (LCM) (5.2.5) for the American option. The basic idea behind the operator splitting method is the formulation with the auxiliary variable ψ such that $\psi = u_t - \mathcal{L}u$. Now the reformulated LCP (5.2.5) for American put option is

$$\left\{ \begin{array}{l} \frac{\partial u}{\partial t} - \mathcal{L}u = \psi, \\ (u(r, t) - \mathcal{G}(r, t)) \cdot \psi = 0, \\ u(r, t) - \mathcal{G}(r, t) \geq 0, \\ \psi \geq 0. \end{array} \right. \quad (5.3.5)$$

Now consider the operator splitting method that split the governing equation $u_t - \mathcal{L}u = \psi$ on the $(n + 1)^{th}$ time level into two discrete equations as

$$\frac{1}{\delta t} \left(\frac{3}{2} \tilde{U}_m^{n+1} - 2U_m^n + \frac{1}{2} U_m^{n-1} \right) - \mathcal{L}_\Delta \tilde{U}_m^{n+1} = \Psi_m^n, \quad (5.3.6)$$

$$\frac{1}{\delta t} \left(\frac{3}{2} U_m^{n+1} - 2U_m^n + \frac{1}{2} U_m^{n-1} \right) - \mathcal{L}_\Delta \tilde{U}_m^{n+1} = \Psi_m^{n+1}. \quad (5.3.7)$$

Now the discrete problem for LCM (5.3.5) is to look for the pair $(U_m^{n+1}, \Psi_m^{n+1})$, which satisfy the discrete equations (5.3.6)-(5.3.7) and the constraints

$$\begin{cases} U_m^{n+1} \geq \mathcal{G}_m^{n+1} \\ \Psi_m^{n+1} \geq 0, \\ \Psi_m^{n+1}(U_m^{n+1} - \mathcal{G}_m^{n+1}) = 0, \end{cases} \quad (5.3.8)$$

respectively.

Now the second step of the operator splitting method is to derive a relationship in (5.3.7) between U_m^{n+1} and Ψ_m^{n+1} . To do this rewrite the equation (5.3.7) using equation (5.3.6) together with the constraints in (5.3.8) as a problem to find the pair $(U_m^{n+1}, \Psi_m^{n+1})$, such that

$$\begin{cases} \frac{3}{2} \frac{U_m^{n+1} - \tilde{U}_m^{n+1}}{\delta t} = \Psi_m^{n+1} - \Psi_m^n, \\ \Psi_m^{n+1}(U_m^{n+1} - \mathcal{G}_m^{n+1}) = 0, \end{cases} \quad (5.3.9)$$

with the constraints

$$U_m^{n+1} \geq \mathcal{G}_m^{n+1} \quad \text{and} \quad \Psi_m^{n+1} \geq 0. \quad (5.3.10)$$

Now by solving the problems (5.3.9)-(5.3.10), we get

$$(U_m^{n+1}, \Psi_m^{n+1}) = \begin{cases} (\mathcal{G}_m^{n+1}, \Psi_m^n + \frac{3}{2} \frac{\mathcal{G}_m^{n+1} - \tilde{U}_m^{n+1}}{\delta t}) & \text{if } \tilde{U}_m^{n+1} - \frac{2\delta t}{3} \Psi_m^n \leq \mathcal{G}_m^{n+1}, \\ (\tilde{U}_m^{n+1} - \frac{2\delta t}{3} \Psi_m^n, 0) & \text{otherwise.} \end{cases} \quad (5.3.11)$$

Thus, one can do the second step by solving discrete equation (5.3.7) with the updating formula (5.3.11). Proposed implicit method with three time levels requires the value on previous two time levels. The pair (U_m^0, Ψ_m^0) on zeroth time level can be obtained by using initial condition and assign value $\Psi_m^0 = 0$. To find the pair (U_m^1, Ψ_m^1) at first level, the first step is to compute the intermediate value \tilde{U}_m^1 as follow:

$$\frac{\tilde{U}_m^1 - U_m^0}{\delta t} - \mathcal{L}_\Delta \tilde{U}_m^1 = \Psi_m^0. \quad (5.3.12)$$

The second step is to find the pair (U_m^1, Ψ_m^1) such that

$$(U_m^1, \Psi_m^1) = \begin{cases} (\mathcal{G}_m^1, \Psi_m^0 + \frac{\mathcal{G}_m^1 - \tilde{U}_m^1}{\delta t}) & \text{if } \tilde{U}_m^1 - \delta t \Psi_m^0 \leq \mathcal{G}_m^1, \\ (\tilde{U}_m^1 - \delta t \Psi_m^0, 0) & \text{otherwise.} \end{cases} \quad (5.3.13)$$

Algorithm to evaluate an American put option

```

for  $n = 0 : N - 1$ 
  if  $n = 0$ 
     $\frac{\tilde{U}_m^{n+1} - U_m^n}{\delta t} - \mathcal{L}_\Delta \tilde{U}_m^{n+1} = \Psi_m^n$ 
     $U_m^{n+1} = \max(\tilde{U}_m^{n+1} - \delta t \Psi_m^n, \mathcal{G}_m^{n+1})$ 
     $\Psi_m^{n+1} = \Psi_m^n + \frac{U_m^{n+1} - \tilde{U}_m^{n+1}}{\delta t}$ 
  else
     $\frac{1}{\delta t} \left( \frac{3}{2} \tilde{U}_m^{n+1} - 2U_m^n + \frac{1}{2} U_m^{n-1} \right) - \mathcal{L}_\Delta \tilde{U}_m^{n+1} = \Psi_m^n$ 
     $U_m^{n+1} = \max(\tilde{U}_m^{n+1} - \frac{2\delta t}{3} \Psi_m^n, \mathcal{G}_m^{n+1})$ 
     $\Psi_m^{n+1} = \Psi_m^n + \frac{3}{2} \frac{U_m^{n+1} - \tilde{U}_m^{n+1}}{\delta t}$ 
  end
end
end

```

Since the option price function have non smooth payoff, hence to overcome this problem, the initial few steps are computed using implicit Euler method.

5.4 Numerical simulation and discussion

We present some numerical experiments to illustrate the efficiency of the proposed method. Numerical results are presented using multi quadric radial basis functions. In all numerical experiments equispaced grid with $n_i = 3$ is used.

Consider European call option with parameter $\kappa = 0.5$, $\theta = 0.08$, $\sigma = 0.1$ and $\gamma = 0.5$. Table 5.1 gives bond price and option price and respective errors with parameters $T^* = 15$, $T = 10$, $r_0 = 0.05$ and $E = 35$ with $\delta t = 0.001$ for face value $K = 100$ in computation domain $R = 0.5$. From the table we observe that the proposed scheme is convergent with second order accuracy in both cases.

Table 5.2 provides the results for option values for wide range of maturity for different values of interest rate. From the table we observe that the proposed method is accurate up to four digits after decimal points. Further for the CIR model, the mispricing in the bond value using the proposed method can be observed in Table 5.3 for long maturities.

Table 5.1: Bond price and bond option prices and respective errors with present method for $T^* = 15$, $T = 10$, $r_0 = 0.05$ and $E = 35$.

M	Value B	Error B	ratio	Value V	Error V	ratio	cpu(s)
101	32.54140	2.7805e-03	-	15.68524	1.2897e-03	-	0.7921
201	32.54348	7.0677e-04	3.9340	15.68620	3.2894e-04	3.9207	0.9622
401	32.54401	1.7676e-04	3.9984	15.68645	8.1940e-05	4.0144	1.5183
801	32.54414	4.3906e-05	4.0258	15.68651	2.0015e-05	4.0939	2.5702
1601	32.54417	1.0520e-05	4.1735	15.68652	4.4159e-06	4.5324	4.6830

 Table 5.2: Bond option prices calculate using CIR exact formula and the present method for $T^* = 10$.

	T	5	4	3	2	1
$r_0 = 0.05$	CIR	23.30145	21.34565	19.29010	17.17497	15.08175
	RBF-FD	23.30142	21.34562	19.29007	17.17493	15.08172
$r_0 = 0.08$	CIR	21.88019	19.95086	17.85851	15.58605	13.11523
	RBF-FD	21.88019	19.95086	17.85851	15.58631	13.11523
$r_0 = 0.11$	CIR	20.54484	18.64443	16.52343	14.11063	11.28633
	RBF-FD	20.54487	18.64447	16.52347	14.11067	11.28635

Table 5.3: Percentage relative mispricings in the zero coupon bond with different maturity.

T^*	5	10	15	20	25	30
$r_0 = 0.05$	3.3617e-06	2.1036e-05	4.2838e-05	5.4419e-05	5.9502e-05	6.6349e-05
$r_0 = 0.08$	3.8116e-05	4.1001e-05	4.3326e-05	4.4115e-05	4.4040e-05	3.9921e-05
$r_0 = 0.11$	7.9864e-05	1.0302e-04	1.2948e-04	1.4265e-04	1.4758e-04	1.4619e-04

We observe that the absolute error relative to exact price is less than 0.00014% for all T^* .

For other different value of CKLS parameter γ for which no closed form solution is known, numerical results are given in Table 5.4. To get error in Table 5.4, we computed the successive price changes of the option value for each value of γ . From the table we observe that solution generally converges with second order accuracy.

Now consider the American put option with parameter $\kappa = 0.1$, $\theta = 0.08$, $\sigma = 0.1$, $\gamma = 0.5$, $E = 60$ which matures at $T = 1$ year on the zero coupon bond with maturity $T^* = 5$ and face value $K = 100$. The reference value is calculated on very fine mesh. For example, some evaluated values are 0.001957 at $r = 0.05$, 0.088704 at $r = 0.08$ and 1.098981 at

Table 5.4: Bond option prices and respective errors under CKLS with present method for $T^* = 10$, $T = 5$, $r_0 = 0.08$ and $E = 35$.

M	$\gamma = 0.4$		$\gamma = 0.6$		$\gamma = 0.8$	
	Value	Error	Value	Error	Value	Error
101	22.135991	-	21.721855	-	21.563903	-
201	22.135365	6.2669e-04	21.721599	2.5670e-04	21.563814	8.8720e-05
401	22.135195	1.6987e-04	21.721533	6.5146e-05	21.563790	2.4511e-05
801	22.135152	4.2805e-05	21.721517	1.6299e-05	21.563784	6.1331e-06
1601	22.135141	1.0539e-05	21.721513	4.0083e-06	21.563782	1.5084e-06

$r = 0.11$.

From Table 5.5, we observe that the proposed method converges with second order

Table 5.5: American put option value and error at different values of interest rate under CIR model.

M	N	$r = 0.05$		$r = 0.08$		$r = 0.11$	
		Value	Error	Value	Error	Value	Error
51	100	0.002908	9.5039e-04	0.095048	6.3429e-03	1.103792	4.8104e-03
101	200	0.002194	2.3700e-04	0.090313	1.6083e-03	1.099678	6.9657e-04
201	400	0.002019	6.1489e-05	0.089144	4.3894e-04	1.099093	1.1119e-04
401	800	0.001970	1.3290e-05	0.088792	8.7499e-05	1.098947	3.4618e-05
801	1600	0.001959	2.2685e-06	0.088720	1.5045e-05	1.098969	1.2511e-05

accuracy. In Figure 5.1a, we plotted surface plot of American put option. From the figure we observe that the option value is an increasing function of interest rate r . The reason is that the value of the zero coupon bond is a decreasing function of the state variable r .

Figure 5.1b plots the optimal exercise boundary of American put option. The above curve divide the domain between two regions called exercise region and holding region. We observe that the American option should not be exercised before the 0.12 year when the interest rate is below 0.13.

In Figure 5.2a, we plot the American put option on zero coupon bond for different value of strike price. We observe that the larger the strike price of the option is, the higher the value of American put option written on the zero coupon bond. Same phenomena also

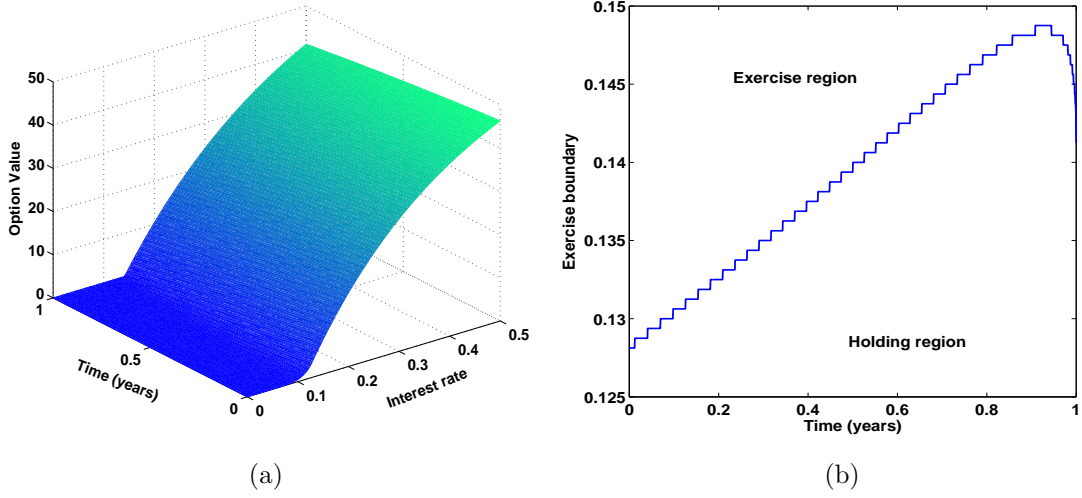


Figure 5.1: American put option value, and early exercise boundary for strike price $K = 60$.

occur with American put option on stock.

In Figures 5.2b and 5.2c we plot the curve of optimal early exercise interest rate versus the strike price of American put options. By coupling with Figure 5.1b we observe that the early interest rate is arising when the the strike price decreases. This corresponds to the fact that the holding region is increasing. The above phenomena indicate that the smaller strike price is, the less probability the put option is exercised.

5.5 Conclusion

In this chapter, RBF based method has been extended for valuation of European and American option on zero coupon bond under CKLS model. After time semi discretization of governing equation, the resulting linear differential equation is solved using RBF based finite difference method. The operator splitting method is presented to solve the linear complementarity problem. Numerical results show that the proposed method has second order convergence rate. We present the plots of the early exercise boundary for American put option. We observe that the holding region is increasing when strike price decreases. This phenomena show that probability of exercising the option is decreased.

5.5. Conclusion

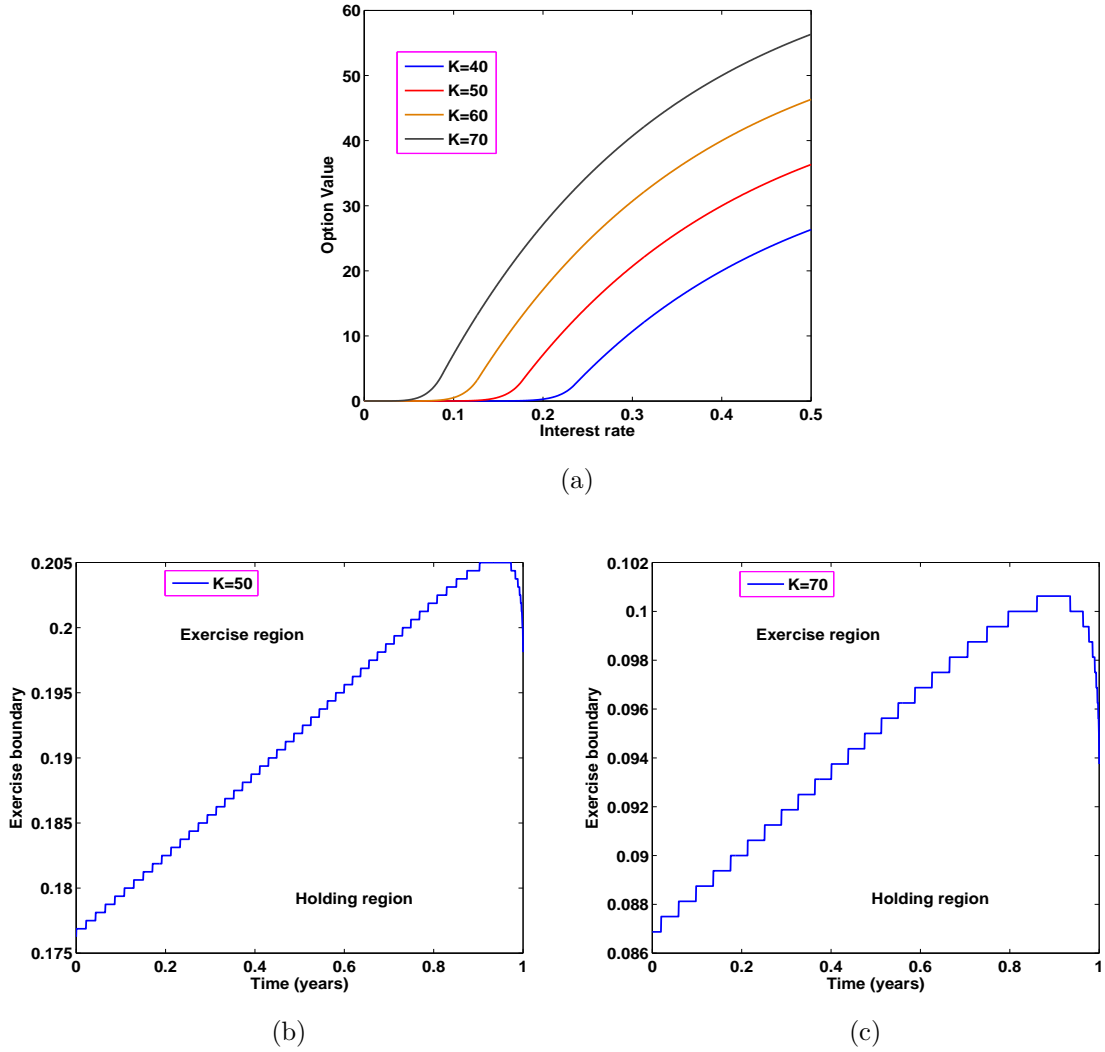


Figure 5.2: American put option and early exercise curve for different value of strike price.

In next chapter, we discuss the application of the proposed approach to solve European and American option under Merton's and Kou jump-diffusion model.

A RBF based IMEX method for pricing options under jump-diffusion model

In this chapter, we present a radial basis function based implicit explicit numerical method to solve the partial integro-differential equation which describe the nature of the option price under jump diffusion model. The governing equation is time semi discretized by using the IMEX-BDF2 followed by radial basis function based finite difference (RBF-FD) method. The numerical scheme derived for European option is extended for American option by using operator splitting method. Numerical results for put and call option under Merton and Kou models are given to illustrate the efficiency and accuracy of the present method. The stability of time semi discretized scheme is also proved.

6.1 Introduction

There is evidence to suggest that the Black Scholes model for stock price behavior does not always model real stock behavior. Jumps can appear at a random time and these jumps

can not be captured by the log normal distribution characteristic of the stock price in the Black Scholes model. These phenomena is also referred as the volatility skew or smiles and exist in all option markets. To overcome the above shortcoming, several models have been proposed in the literature. Among these, the jump diffusion model introduced by Merton[92] and Kou [81] is most used models. Merton proposed a log-normally distributed process for the jump-amplitudes, while Kou suggested log-double-exponentially distributed process.

The valuation of option under jump diffusion process requires to solve a partial integro differential equation containing a non local integral term. There are several numerical methods available in the literature to approximate the above equation. In [2] Almendral and Osterlee presented an implicit second order accurate time discretization with finite difference and finite element spatial discretization on uniform grid. Andersen et al. [4] proposed an unconditionally stable alternate direct implicit method for its solution. Song Wang et al. [143] developed a fitted finite volume method for jump diffusion process. Their method is based on fitted finite volume method spatial discretization and Crank Nicolson scheme for temporal discretization. More recently, Patidar et al. [98] developed an efficient method for pricing Merton jump diffusion option, combining the spectral domain decomposition method and the Laplace transform method. The scheme proposed by d'Halluin et al. [30] required to use an iterative procedure to solve discrete equations. The main difficulty with implicit scheme is due to the non local integral term in governing equation, which leads to a dense discretization matrix where as fully explicit scheme imposes stability restriction on it. An approach based on implicit-explicit schemes in which integral term is treated explicitly has been proposed by YongHoon Kwon et al. [83] and Briani et al. [12]. More recently Tangman et al. [123] introduced a new scheme called exponential time integration (ETI) scheme to solve the PIDE. In ETI scheme, the time direction of PIDE is directly tackled by a 'one step' formula, which means temporal discretization is not required. Tangman et al. [123] used the central difference approach with ETI to provide very efficient and second order accurate result.

Golbabai et al. [52], developed an algorithm based on radial basis function collocation

for jump diffusion process. Bhuruth et al. [109] proposed a radial basis function based differential quadrature rule for spatial discretization with exponential time integration to solve jump diffusion model. In more recent work, Chan et al. [18] used new RBF called cubic spline as basis function to solve PIDE, and show that their scheme is second order accurate. In the present chapter, we have extended the RBF based method to solve jump diffusion models. The governing equations are discretized by a three level implicit and explicit time scheme followed by RBF based finite difference method.

The chapter is organized as follow. In section 6.2, mathematical models for pricing option with jump diffusion process are given in terms of partial integro-differential equations and provide a brief review of both the Merton and Kou jump diffusion models. Section 6.3 deals with the construction of three time level implicit explicit scheme to discretize the jump diffusion model. The stability of the proposed method is also discussed in the respective section. Section 6.3, provide extension of proposed method for pricing American option by utilizing concept of operator splitting method. In section 6.5, we give some numerical results for Merton and Kou model and a comparison of the accuracy of our solution with finite difference and finite element method. Finally the chapter ends with some conclusion in section 6.6.

6.2 The mathematical model

In this section, we give brief discussion about the mathematical model for option with jump diffusion process. Consider an asset with the asset price S , then the movement of stock price is modeled by the following stochastic differential equation

$$\frac{dS}{S} = (\nu - \kappa\lambda)d\tau + \sigma dZ + (\eta - 1)dq \quad (6.2.1)$$

where, ν is drift rate, σ represent the constant volatility, dZ is an increment of standard Gauss-Wiener process. The term λ is the intensity of the independent Poisson process dq with

$$dq = \begin{cases} 0 & \text{with probability } 1 - \lambda d\tau, \\ 1 & \text{with probability } \lambda d\tau. \end{cases}$$

The expected relative jump size $\mathbb{E}(\eta - 1)$ is denoted by κ , where $\mathbb{E}[\cdot]$ is the expectation operator and $\eta - 1$ is an impulse function producing jump from S to $S\eta$.

Let $V(S, \tau)$ represent the value of a contingent claim that depend on the underlying asset price S with current time τ . Then $V(S, \tau)$ satisfies following backward partial integro differential equation

$$\frac{\partial V}{\partial \tau} + \frac{1}{2}\sigma^2 S^2 \frac{\partial^2 V}{\partial S^2} + (r - \lambda\kappa)S \frac{\partial V}{\partial S} - (r + \lambda)V + \lambda \int_0^\infty V(S\eta)g(\eta)d\eta = 0, \quad (6.2.2)$$

for $(S, \tau) \in (0, \infty) \times (0, T]$, where, r is risk free interest rate and $g(\eta)$ is probability density function of the jump with amplitude η with properties that $\forall \eta, g(\eta) \geq 0$ and $\int_0^\infty g(\eta)d\eta = 1$.

The value of V at the expiry date is given by,

$$V(S, T) = \mathcal{G}(S), \quad S \in (0, \infty), \quad (6.2.3)$$

where $\mathcal{G}(S)$ is the pay-off function for the option contract. Under Merton's model $g(\eta)$ is given by the log-normal density

$$g(\eta) := \frac{1}{\sqrt{2\pi}\sigma_J\eta} e^{-\frac{(\ln \eta - \mu_J)^2}{2\sigma_J^2}}. \quad (6.2.4)$$

In this case $\kappa := \mathbb{E}(\eta - 1) = \exp(\mu_J + \frac{\sigma_J^2}{2}) - 1$, where μ_J and σ_J^2 are the mean and the variance of jump in return. Under a modified version of Kou's jump-diffusion model $g(\eta)$ is the following log-double-exponential density

$$g(\eta) := \frac{1}{\eta} \left(p\eta_1 e^{-\eta_1 \ln(\eta)} \mathcal{H}(\ln(\eta)) + q\eta_2 e^{\eta_2 \ln(\eta)} \mathcal{H}(-\ln(\eta)) \right), \quad (6.2.5)$$

where $\eta_1 > 1$, $\eta_2 > 0$, $p > 0$, $q = 1 - p$, and $\mathcal{H}(\cdot)$ is the Heaviside function. We can show that $\kappa : \frac{p\eta_1}{\eta_1 - 1} + \frac{q\eta_2}{\eta_1 + 1} - 1$.

By using change of variable $x = \ln(\frac{S}{E})$, $y = \ln(\eta)$, where E is strike price and letting $t = T - \tau$, computation of the option value requires solving the PIDE

$$\frac{\partial u}{\partial t} = \frac{1}{2}\sigma^2 \frac{\partial^2 u}{\partial x^2} + \left(r - \frac{\sigma^2}{2} - \lambda\kappa\right) \frac{\partial u}{\partial x} - (r + \lambda)u + \lambda \int_{-\infty}^\infty u(y, t) f(y - x) dy, \quad (6.2.6)$$

where $u(x, t) := V(Ee^x, T - t)$ and $f(y) = g(e^y)e^y$. Under the above transformation the function $f(y)$ can be written as;

$$f(y) := \begin{cases} \frac{1}{\sqrt{2\pi}\sigma_J} e^{-\frac{(y-\mu_J)^2}{2\sigma_J^2}} & \text{Merton's model,} \\ (p\eta_1 e^{-\eta_1 y} \mathcal{H}(y) + q\eta_2 e^{\eta_2 y} \mathcal{H}(-y)) & \text{Kou's model.} \end{cases} \quad (6.2.7)$$

The initial condition and asymptotic behavior of the price of a European put option is described by

$$u(x, 0) = \max(E - Ee^x, 0) \quad (6.2.8)$$

$$u(x, t) = \begin{cases} Ee^{-rt} - Ee^x & x \rightarrow -\infty, \\ 0 & x \rightarrow \infty. \end{cases} \quad (6.2.9)$$

Other types of initial and boundary conditions can be suitably defined for different type options.

In contrast, the American option can be exercised at any time up to the maturity date and can be formulated as the linear complementarity problem(LCP) of the form

$$\begin{cases} \frac{\partial u}{\partial t} - \mathcal{L}u \geq 0, \\ u(x, t) - \mathcal{G}(x) \geq 0, \\ (\frac{\partial u}{\partial t} - \mathcal{L}u)(u(x, t) - \mathcal{G}(x)) = 0, \end{cases} \quad (6.2.10)$$

for $(x, t) \in (0, \infty) \times [0, T)$ together with the boundary conditions

$$u(x, t) = \begin{cases} E - Ee^x & x \rightarrow -\infty, \\ 0 & x \rightarrow \infty, \end{cases} \quad (6.2.11)$$

where \mathcal{L} is the partial integro differential operator on the right side of (6.2.6).

6.3 Time semi discretizations

In this section we shall construct an implicit explicit time semi discretization called IMEX-BDF2 scheme for following PIDE on truncated domain $\Omega \times [0, T)$,

$$\frac{\partial u(x, t)}{\partial t} = \mathcal{L}u(x, t), \quad (x, t) \in \Omega \times (0, T] \quad (6.3.1)$$

$$u(x, 0) = \mathcal{G}(x), \quad x \in \bar{\Omega} \quad (6.3.2)$$

where \mathcal{L} is the partial integro differential operator on the right side of (6.2.6).

We split the PIDE operator \mathcal{L} into two parts as follows:

$$\frac{\partial u(x, t)}{\partial t} = \mathcal{D}u(x, t) + \lambda \mathcal{I}u(x, t), \quad (6.3.3)$$

where \mathcal{D} is differential operator and \mathcal{I} is integral operator of \mathcal{L} such that

$$\mathcal{D}u(x, t) = \frac{1}{2}\sigma^2 \frac{\partial^2 u}{\partial x^2} + (r - \frac{\sigma^2}{2} - \lambda\kappa) \frac{\partial u}{\partial x} - (r + \lambda)u, \quad (6.3.4)$$

$$\mathcal{I}u(x, t) = \int_{-\infty}^{\infty} u(y, t) f(y - x) dy. \quad (6.3.5)$$

In order to approximate the integral operator $\mathcal{I}u$ in (6.3.5) numerically, we first divide the integral into two parts on Ω and on $\Omega^c := \mathbb{R} \setminus \Omega$. Now the the integral operator can be split as

$$\mathcal{I}u(x, t) = \int_{\Omega} u(y, t) f(y - x) dy + R(t, x). \quad (6.3.6)$$

By using asymptotic behavior of the option the integral over Ω^c is given by

$$R(t, x) := \int_{\Omega^c} (Ee^{-rt} - Ee^y) f(y - x) dy. \quad (6.3.7)$$

In Merton model, the above integral can be written as,

$$\begin{aligned} R(t, x) &= \int_{-\infty}^{x_{\min}} (Ee^{-rt} - Ee^y) \frac{1}{\sqrt{2\pi}\sigma_J} e^{-\frac{(y-x-\mu_J)^2}{2\sigma_J^2}} dy \\ &= Ee^{-rt} \int_{-\infty}^{x_{\min}} \frac{1}{\sqrt{2\pi}\sigma_J} e^{-\frac{(y-x-\mu_J)^2}{2\sigma_J^2}} dy - E \int_{-\infty}^{x_{\min}} e^y \frac{1}{\sqrt{2\pi}\sigma_J} e^{-\frac{(y-x-\mu_J)^2}{2\sigma_J^2}} dy \\ &= \frac{Ee^{-rt}}{\sqrt{2\pi}} \int_{-\infty}^{\frac{x_{\min}-x-\mu_J}{\sigma_J}} e^{-\frac{w^2}{2}} dw - \frac{E}{\sqrt{2\pi}} \int_{-\infty}^{\frac{x_{\min}-x-\mu_J}{\sigma_J}} e^{w\sigma_J+x+\mu_J} e^{-\frac{w^2}{2}} dw \\ &= \frac{Ee^{-rt}}{\sqrt{2\pi}} \int_{-\infty}^{\frac{x_{\min}-x-\mu_J}{\sigma_J}} e^{-\frac{w^2}{2}} dw - \frac{Ee^{x+\mu_J}}{\sqrt{2\pi}} \int_{-\infty}^{\frac{x_{\min}-x-\mu_J}{\sigma_J}} e^{w\sigma_J} e^{-\frac{w^2}{2}} dw \\ &= \frac{Ee^{-rt}}{\sqrt{2\pi}} \int_{-\infty}^{\frac{x_{\min}-x-\mu_J}{\sigma_J}} e^{-\frac{w^2}{2}} dw - \frac{Ee^{x+\mu_J+\frac{\sigma_J^2}{2}}}{\sqrt{2\pi}} \int_{-\infty}^{\frac{x_{\min}-x-\mu_J}{\sigma_J}} e^{-\frac{1}{2}(w-\sigma_J)^2} dw \\ &= \frac{Ee^{-rt}}{\sqrt{2\pi}} \int_{-\infty}^{\frac{x_{\min}-x-\mu_J}{\sigma_J}} e^{-\frac{w^2}{2}} dw - \frac{Ee^{x+\mu_J+\frac{\sigma_J^2}{2}}}{\sqrt{2\pi}} \int_{-\infty}^{\frac{x_{\min}-x-\mu_J-\sigma_J^2}{\sigma_J}} e^{-\frac{z^2}{2}} dz. \end{aligned}$$

where $\mathcal{N}(\cdot)$ is the cumulative normal distribution.

In the case of the Kou model,

$$\begin{aligned} R(t, x) &= \int_{-\infty}^{x_{\min}} (Ee^{-rt} - Ee^y) q \eta_2 e^{\eta_2(y-x)} \\ &= Ee^{-rt} q e^{-\eta_2 x} \int_{-\infty}^{x_{\min}} \eta_2 e^{\eta_2 y} - E q e^{-\eta_2 x} \int_{-\infty}^{x_{\min}} \eta_2 e^{(\eta_2+1)y} \\ &= E q e^{-rt+\eta_2(x_{\min}-x)} - E q \frac{\eta_2}{\eta_2+1} e^{-\eta_2 x + (\eta_2+1)x_{\min}}. \end{aligned}$$

For the European put option the expression $R(t, x)$ is given as;

$$R(t, x) := \begin{cases} Ee^{-rt} \mathcal{N}\left(\frac{x_{\min}-x-\mu_J}{\sigma_J}\right) - Ee^{x+\mu_J+\frac{\sigma_J^2}{2}} \mathcal{N}\left(\frac{x_{\min}-x-\mu_J-\sigma_J^2}{\sigma_J}\right) & \text{Merton's ,} \\ E(1-p)e^{-rt+\eta_2(x_{\min}-x)} - E(1-p)\frac{\eta_2}{\eta_2+1} e^{-\eta_2 x + (\eta_2+1)x_{\min}} & \text{Kou's .} \end{cases} \quad (6.3.8)$$

In the case of American put option above expression can be reformulated as;

$$R(t, x) := \begin{cases} E \mathcal{N}\left(\frac{x_{\min}-x-\mu_J}{\sigma_J}\right) - Ee^{x+\mu_J+\frac{\sigma_J^2}{2}} \mathcal{N}\left(\frac{x_{\min}-x-\mu_J-\sigma_J^2}{\sigma_J}\right) & \text{Merton's,} \\ E(1-p)e^{\eta_2(x_{\min}-x)} - E(1-p)\frac{\eta_2}{\eta_2+1} e^{-\eta_2 x + (\eta_2+1)x_{\min}} & \text{Kou's.} \end{cases} \quad (6.3.9)$$

We use composite trapezoidal rule to approximate the integral term on truncated domain Ω .

Let $\{0 = t_0 < t_1 < \dots < t_N = T; t_n - t_{n-1} = \delta t, 1 \leq n \leq N\}$ be a partition of the interval $[0, T]$. Let us use the notation $u^n := u(x, t_n)$ then equation (6.3.1) will be discretized by following implicit explicit scheme,

$$\frac{1}{\delta t} \left(\frac{3}{2} u^{n+1} - 2u^n + \frac{1}{2} u^{n-1} \right) = \mathcal{D}u^{n+1} + \lambda \mathcal{I}(Eu^n), \quad n \geq 1, \quad (6.3.10)$$

where $Eu^n = 2u^n - u^{n-1}$.

The above discretization method of the operator $\mathcal{L}u$ is called IMEX-BDF2 method with three time levels. In order to use the proposed method we need two initial values on the zeroth and first time level. The value u^0 at the zeroth time level is given by initial condition of the model problem, and the value u^1 can be obtained by applying the implicit explicit backward difference method of order one,

$$\frac{u^{n+1} - u^n}{\delta t} = \mathcal{D}u^{n+1} + \lambda \mathcal{I}u^n. \quad (6.3.11)$$

6.3.1 Stability Analysis

Now we prove the stability of the time discrete scheme (6.3.10).

It can be easily shown that for all $u(\cdot, t) \in L^2(\Omega)$, $t \in (0, T)$ such that

$$\bar{u}(x, t) = \begin{cases} u(x, t) & : (x, t) \in \Omega \times [0, T], \\ 0 & : (x, t) \in \Omega^c \times [0, T], \end{cases}$$

the integral operator satisfies the condition

$$\|\mathcal{I}\bar{u}(\cdot, t)\| \leq C_I \|u(\cdot, t)\|, \quad (6.3.12)$$

for some constant C_I independent of t , where $\|v\| := (\int_{\Omega} |v(x)|^2 dx)^{1/2}$.

Let us suppose that u^n be exact solution of the equation (6.3.10) and \tilde{u}^n be approximate solution of perturbed equation

$$\frac{1}{\delta t} \left(\frac{3}{2} \tilde{u}^{n+1} - 2\tilde{u}^n + \frac{1}{2} \tilde{u}^{n-1} \right) = \mathcal{D}\tilde{u}^{n+1} + \lambda \mathcal{I}(E\tilde{u}^n) + \delta^{n+1}, \quad n \geq 1, \quad (6.3.13)$$

with error $e^n = \tilde{u}^n - u^n$, then we have the following stability result.

Theorem 6.3.1. (*L^2 -stability*) For sufficiently small δt such that $\delta t < \frac{1}{(2+4\alpha+2\lambda C_I)}$, we have

$$\|e^m\|^2 \leq C(\|e^0\|^2 + \|e^1\|^2 + \delta t \sum_{j=2}^m \|\delta^j\|^2), \quad \forall 2 \leq m \leq \frac{T}{\delta t}, \quad (6.3.14)$$

where $\alpha = \left| \frac{(r - \frac{\sigma^2}{2} - \lambda\kappa)^2 - 2(r+\lambda)\sigma^2}{2\sigma^2} \right|$ and C is generic constant depending on the parameter C_I , r , σ , λ , and T .

Proof. The error will be of the following form;

$$\frac{(3e^{n+1} - 4e^n + e^{n-1}))}{2\delta t} = \mathcal{D}e^{n+1} + \lambda \mathcal{I}(Ee^n) + \delta^{n+1}, \quad (6.3.15)$$

Taking the inner product of the equation (6.3.15) with e^{n+1} , we obtain;

$$\left(\frac{(3e^{n+1} - 4e^n + e^{n-1}))}{2\delta t}, e^{n+1} \right) = (\mathcal{D}e^{n+1}, e^{n+1}) + \lambda (\mathcal{I}(Ee^n), e^{n+1}) + (\delta^{n+1}, e^{n+1}),$$

$$\begin{aligned}
 &= -\frac{\sigma^2}{2}\|e_x^{n+1}\|^2 + \left(r - \frac{\sigma^2}{2} - \lambda\kappa\right)(e_x^{n+1}, e^{n+1}) - (r + \lambda)\|e^{n+1}\|^2 \\
 &\quad + \lambda(\mathcal{I}(Ee^n), e^{n+1}) + (\delta^{n+1}, e^{n+1})
 \end{aligned} \tag{6.3.16}$$

by simplification of the above relation we have

$$\begin{aligned}
 \left(\frac{(3e^{n+1} - 4e^n + e^{n-1})}{2\delta t}, e^{n+1}\right) &= -\frac{\sigma^2}{2}\left(\|e_x^{n+1} - \frac{(r - \frac{\sigma^2}{2} - \lambda\kappa)}{\sigma^2}e^{n+1}\|^2\right) \\
 &\quad + \frac{(r - \frac{\sigma^2}{2} - \lambda\kappa)^2 - 2(r + \lambda)\sigma^2}{2\sigma^2}\|e^{n+1}\|^2 + \lambda(\mathcal{I}(Ee^n), e^{n+1}) \\
 &\quad + (\delta^{n+1}, e^{n+1}) \\
 &\leq \alpha\|e^{n+1}\|^2 + \lambda(\mathcal{I}(Ee^n), e^{n+1}) + (\delta^{n+1}, e^{n+1})
 \end{aligned} \tag{6.3.17}$$

where $\alpha = \left| \frac{(r - \frac{\sigma^2}{2} - \lambda\kappa)^2 - 2(r + \lambda)\sigma^2}{2\sigma^2} \right|$.

Now by using the relation $2(3a - 4b + c, a) = \|a\|^2 - \|b\|^2 + \|2a - b\|^2 - \|2b - c\|^2 + \|a - 2b + c\|^2$, we have

$$\begin{aligned}
 \frac{1}{4\delta t} [\|e^{n+1}\|^2 - \|e^n\|^2 + \|2e^{n+1} - e^n\|^2 - \|2e^n - e^{n-1}\|^2] &\leq \alpha\|e^{n+1}\|^2 + \lambda(\mathcal{I}(Ee^n), e^{n+1}) \\
 &\quad + (\delta^{n+1}, e^{n+1})
 \end{aligned}$$

$$\begin{aligned}
 \frac{1}{4\delta t} [\|e^{n+1}\|^2 - \|e^n\|^2 + \|2e^{n+1} - e^n\|^2 - \|2e^n - e^{n-1}\|^2] &\leq \alpha\|e^{n+1}\|^2 + \lambda C_I \|Ee^n\| \|e^{n+1}\| \\
 &\quad + \|\delta^{n+1}\| \|e^{n+1}\|
 \end{aligned}$$

$$\begin{aligned}
 \frac{1}{4\delta t} [\|e^{n+1}\|^2 - \|e^n\|^2 + \|2e^{n+1} - e^n\|^2 - \|2e^n - e^{n-1}\|^2] &\leq \left(\alpha + \frac{1}{2} + \frac{\lambda C_I}{2}\right)\|e^{n+1}\|^2 \\
 &\quad + \frac{\lambda C_I}{2}\|Ee^n\|^2 + \frac{1}{2}\|\delta^{n+1}\|^2
 \end{aligned}$$

$$\begin{aligned}
 \frac{1}{4\delta t} [\|e^{n+1}\|^2 - \|e^n\|^2 + \|2e^{n+1} - e^n\|^2 - \|2e^n - e^{n-1}\|^2] &\leq \left(\alpha + \frac{1}{2} + \frac{\lambda C_I}{2}\right)\|e^{n+1}\|^2 \\
 &\quad + \lambda C_I(4\|e^n\|^2 + \|e^{n-1}\|^2) \\
 &\quad + \frac{1}{2}\|\delta^{n+1}\|^2
 \end{aligned}$$

$$\|e^{n+1}\|^2 - \|e^n\|^2 + \|2e^{n+1} - e^n\|^2 - \|2e^n - e^{n-1}\|^2 \leq \delta t[(2 + 4\alpha + 2\lambda C_I)\|e^{n+1}\|^2 + 2\|\delta^{n+1}\|^2]$$

$$+16\lambda C_I \|e^n\|^2 + 4\lambda C_I \|e^{n-1}\|^2]$$

After summing up for n between 1 to $m-1$, we get

$$\begin{aligned} \|e^m\|^2 - \|e^2\|^2 - \|2e^2 - e^1\|^2 &\leq \delta t [4\lambda C_I \|e^1\|^2 + 20\lambda C_I \|e^2\|^2 + 2 \sum_{j=2}^m \|\delta^j\|^2 \\ &\quad + (2 + 4\alpha + 22\lambda C_I) \sum_{j=2}^{m-1} \|e^j\|^2 + (2 + 4\alpha + 2\lambda C_I) \|e^m\|^2]. \end{aligned}$$

Now consider the δt sufficiently small such that $1 - \delta t(2 + 4\alpha + 2\lambda C_I) > 0$ that is $\delta t < \frac{1}{(2+4\alpha+2\lambda C_I)}$, then above relation imply that

$$\|e^m\|^2 \leq C(\|e^0\|^2 + \|e^1\|^2 + \delta t \sum_{j=2}^m \|\delta^j\|^2 + \delta t \sum_{j=2}^{m-1} \|e^j\|^2) \quad (6.3.18)$$

where C is a positive constant which is independent of mesh length. Now by applying the discrete Gronwall's inequality, we get the result. \square

We solve the resulting time semi discrete scheme by using radial basis function based finite difference method discussed in the previous chapter.

Algorithm to evaluate an European option

We descretize the domain Ω into M equispaced spatial nodes $x_i = x_{\min} + (i-1)h$ for $i = 1, 2, \dots, M$ with $h = (x_{\max} - x_{\min})/(M-1)$. Then the approximated value of the solution $u_m^n = u(x_m, t_n)$ denoted by U_m^n can be obtained by following time stepping problem:

```

for  $n = 0 : N - 1$ 
  if  $n = 0$ 
     $\frac{U_m^{n+1} - U_m^n}{\delta t} = \mathcal{D}_\Delta U_m^{n+1} + \lambda \mathcal{I}_\Delta U_m^n$ 
  else
     $\frac{1}{\delta t} \left( \frac{3}{2} U_m^{n+1} - 2U_m^n + \frac{1}{2} U_m^{n-1} \right) = \mathcal{D}_\Delta U_m^{n+1} + \lambda \mathcal{I}_\Delta (EU_m^n)$ 
  end
end
    
```

Where $\mathcal{D}_\Delta U$ is local RBF based space discretization of differential operator $\mathcal{D}u$, obtained by using procedure described above and \mathcal{I}_Δ is numerical approximation of integral operator defined by equation (6.3.6). Since the option price problems have non smooth payoff function, there is possibility to have oscillation on the final time level. To overcome this problem, the solution on two time levels is calculated by implicit Euler method.

6.4 American Options

The RBF based IMEX method discussed in previous section can be extend to solve LCP (6.2.10) for American option problem coupled with operator splitting method. The operator splitting method was introduced by Ikonen and Toivanen [62] to evaluate the American put option. The basic idea behind the operator splitting method is the formulation with the auxiliary variable ψ such that $\psi = u_t - \mathcal{L}u$. Now the reformulated LCP (6.2.10) is

$$\left\{ \begin{array}{l} \frac{\partial u}{\partial t} - \mathcal{L}u = \psi, \\ (u(x, t) - \mathcal{G}(x)) \cdot \psi = 0, \\ u(x, t) - \mathcal{G}(x) \geq 0, \\ \psi \geq 0, \end{array} \right. \quad (6.4.1)$$

in the region $\Omega \times [0, T)$.

Let us split the governing equation $u_t - \mathcal{L}u = \psi$ on the $(n+1)^{th}$ time level into two discrete equations as

$$\frac{1}{\delta t} \left(\frac{3}{2} \tilde{U}_m^{n+1} - 2U_m^n + \frac{1}{2} U_m^{n-1} \right) - \left\{ \mathcal{D}_\Delta \tilde{U}_m^{n+1} + \lambda \mathcal{I}_\Delta (EU_m^n) \right\} = \Psi_m^n, \quad (6.4.2)$$

$$\frac{1}{\delta t} \left(\frac{3}{2} U_m^{n+1} - 2U_m^n + \frac{1}{2} U_m^{n-1} \right) - \left\{ \mathcal{D}_\Delta \tilde{U}_m^{n+1} + \lambda \mathcal{I}_\Delta (EU_m^n) \right\} = \Psi_m^{n+1}. \quad (6.4.3)$$

Now the discrete problem for LCM (6.4.1) is to look for the pair $(U_m^{n+1}, \Psi_m^{n+1})$, which satisfy the discrete equations (6.4.2) and (6.4.3) and the constraints

$$\left\{ \begin{array}{l} U_m^{n+1} \geq \mathcal{G}(x_m), \\ \Psi_m^{n+1} \geq 0, \\ \Psi_m^{n+1} (U_m^{n+1} - \mathcal{G}(x_m)) = 0. \end{array} \right. \quad (6.4.4)$$

The first step is to compute the intermediate approximation \tilde{U}_m^{n+1} by solving the equations (6.4.2) with known auxiliary term Ψ_m^n .

Now the second step of the operator splitting method is to derive a relationship in (6.4.3) between U_m^{n+1} and Ψ_m^{n+1} . To do this rewrite the equation (6.4.3) using equation (6.4.2) together with the constraints in (6.4.4) as a problem to find the pair $(U_m^{n+1}, \Psi_m^{n+1})$, such that

$$\begin{cases} \frac{3}{2} \frac{U_m^{n+1} - \tilde{U}_m^{n+1}}{\delta t} = \Psi_m^{n+1} - \Psi_m^n, \\ \Psi_m^{n+1}(U_m^{n+1} - \mathcal{G}(x_m)) = 0, \end{cases} \quad (6.4.5)$$

with the constraints

$$U_m^{n+1} \geq \mathcal{G}(x_m) \quad \text{and} \quad \Psi_m^{n+1} \geq 0. \quad (6.4.6)$$

Now by solving the problems (6.4.5) and (6.4.6), we get

$$(U_m^{n+1}, \Psi_m^{n+1}) = \begin{cases} (\mathcal{G}(x_m), \Psi_m^n + \frac{3}{2} \frac{\mathcal{G}(x_m) - \tilde{U}_m^{n+1}}{\delta t}) & \text{if } \tilde{U}_m^{n+1} - \frac{2\delta t}{3} \Psi_m^n \leq \mathcal{G}(x_m), \\ (\tilde{U}_m^{n+1} - \frac{2\delta t}{3} \Psi_m^n, 0) & \text{otherwise.} \end{cases} \quad (6.4.7)$$

Thus, one can do the second step by solving discrete equation (6.4.2) with the updating formula (6.4.7). The above implicit method with three time levels requires the value on previous two time levels. The pair (U_m^0, Ψ_m^0) on zeroth time level can be obtained by using initial condition and assign value $\Psi_m^0 = 0$ or one can use the algorithm discussed in [82]. To find the pair (U_m^1, Ψ_m^1) at first level, the first step is to compute the intermediate value \tilde{U}_m^1 as follows:

$$\frac{\tilde{U}_m^1 - U_m^0}{\delta t} - \left\{ \mathcal{D}_\Delta \tilde{U}_m^1 + \lambda \mathcal{I}_\Delta U_m^0 \right\} = \Psi_m^0. \quad (6.4.8)$$

The second step is to find the pair (U^1, Ψ^1) such that

$$(U_m^1, \Psi_m^1) = \begin{cases} (\mathcal{G}(x_m), \Psi_m^0 + \frac{\mathcal{G}(x_m) - \tilde{U}_m^1}{\delta t}) & \text{if } \tilde{U}_m^1 - \delta t \Psi_m^0 \leq \mathcal{G}(x_m), \\ (\tilde{U}_m^1 - \delta t \Psi_m^0, 0) & \text{otherwise.} \end{cases} \quad (6.4.9)$$

Algorithm to evaluate an American option

for $n = 0 : N - 1$

if $n = 0$

$$\frac{\tilde{U}_m^{n+1} - U_m^n}{\delta t} = \mathcal{D}_\Delta \tilde{U}_m^{n+1} + \lambda \mathcal{I}_\Delta U_m^n + \Psi_m^n$$

```


$$U_m^{n+1} = \max(\tilde{U}_m^{n+1} - \delta t \Psi_m^n, \mathcal{G}(x_m))$$


$$\Psi_m^{n+1} = \Psi_m^n + \frac{U_m^{n+1} - \tilde{U}_m^{n+1}}{\delta t}$$

else

$$\frac{1}{\delta t} \left( \frac{3}{2} \tilde{U}_m^{n+1} - 2U_m^n + \frac{1}{2} U_m^{n-1} \right) = \mathcal{D}_\Delta \tilde{U}_m^{n+1} + \lambda \mathcal{I}_\Delta(EU_m^n) + \Psi_m^n$$


$$U_m^{n+1} = \max(\tilde{U}_m^{n+1} - \frac{2\delta t}{3} \Psi_m^n, \mathcal{G}(x_m))$$


$$\Psi_m^{n+1} = \Psi_m^n + \frac{3}{2} \frac{U_m^{n+1} - \tilde{U}_m^{n+1}}{\delta t}$$

end
end
    
```

6.5 Numerical simulation and discussion

In this section, we present several numerical experiments to illustrate the efficiency and accuracy of proposed method. We used the FFT algorithm to compute the product of a dense matrix and a column vector in the discrete integral operator in expression (6.3.6). Thus the implicit-explicit method with three time levels requires totally $O(MN \log_2(M))$ operations, where N is the number of time steps and M is the number of spatial steps. Numerical results are presented for both call option and put option under Merton and Kou model using multi quadric radial basis functions. By keeping the shape parameter ϵ fixed, the computational error produced by the numerical schemes was measured against the value of analytical solution or reference solution at specific asset price. In all numerical experiments equispaced grid with $n_i = 3$ is used.

6.5.1 Numerical results for European options

We consider numerical solution of European option under Merton and Kou model using proposed method.

Example 6.5.1. *European option under Merton model with parameters $\sigma = 0.15$, $r = 0.05$, $\sigma_J = 0.45$, $\mu_J = -0.90$, $\lambda = 0.10$, $T = 0.25$, $E = 100$.*

These parameters are also used by YongHoon Kwon and Younhee Lee [83] for Pricing European put option with truncated domain $x_{\min} = -1.5$ and $x_{\max} = 1.5$, and by Y.

6.5.1. Numerical results for European options

Table 6.1: Numerical results for European put options under the Merton model at different asset price with parameters as given in Example 6.5.1.

M	N	$S = 90$		$S = 100$		$S = 110$	
		Value	Error	Value	Error	Value	Error
129	25	9.283266	2.1520e-03	3.120808	2.8218e-02	1.396156	5.0297e-03
257	50	9.284893	5.2475e-04	3.142100	6.9262e-03	1.399881	1.3053e-03
513	100	9.285282	1.3655e-04	3.147302	1.7240e-03	1.400852	3.3346e-04
1025	200	9.285384	3.4508e-05	3.148595	4.3054e-04	1.401101	8.5126e-05
2049	400	9.285409	8.7377e-06	3.148918	1.0776e-04	1.401165	2.1274e-05
4097	800	9.285416	2.5525e-06	3.148998	2.7723e-05	1.401180	5.5654e-06

d'Halluin, P. A. Forsythy, and K. R. Vetzal [30] for European call option. The analytical solution is obtained by using infinite series solution of Merton [92]. The reference values for European put option are 9.285418 at $S = 90$, 3.149026 at $S = 100$, and 1.401186 at $S = 110$ and for European call option are 0.527638 at $S = 90$, 4.391246 at $S = 100$, and 12.643406 at $S = 110$.

The numerical results for put option and call option are listed in Tables 6.1 and 6.2

Table 6.2: Numerical results for European call options under the Merton model at different asset price with parameters as given in Example 6.5.1.

M	N	$S = 90$		$S = 100$		$S = 110$	
		Value	Error	Value	Error	Value	Error
129	25	0.525486	2.1520e-03	4.363028	2.8218e-02	12.638376	5.0297e-03
257	50	0.527113	5.2475e-04	4.384320	6.9262e-03	12.642101	1.3053e-03
513	100	0.527501	1.3655e-04	4.389522	1.7240e-03	12.643072	3.3346e-04
1025	200	0.527604	3.4508e-05	4.390815	4.3054e-04	12.643321	8.5126e-05
2049	400	0.527629	8.7377e-06	4.391138	1.0776e-04	12.643385	2.1274e-05
4097	800	0.527635	2.5525e-06	4.391218	2.7723e-05	12.643400	5.5654e-06

respectively. The option value and absolute error are given at different asset prices. From these tables, we can observe that the discretization scheme is convergent with quadratic rate, since the ratio in respective error is approximately four.

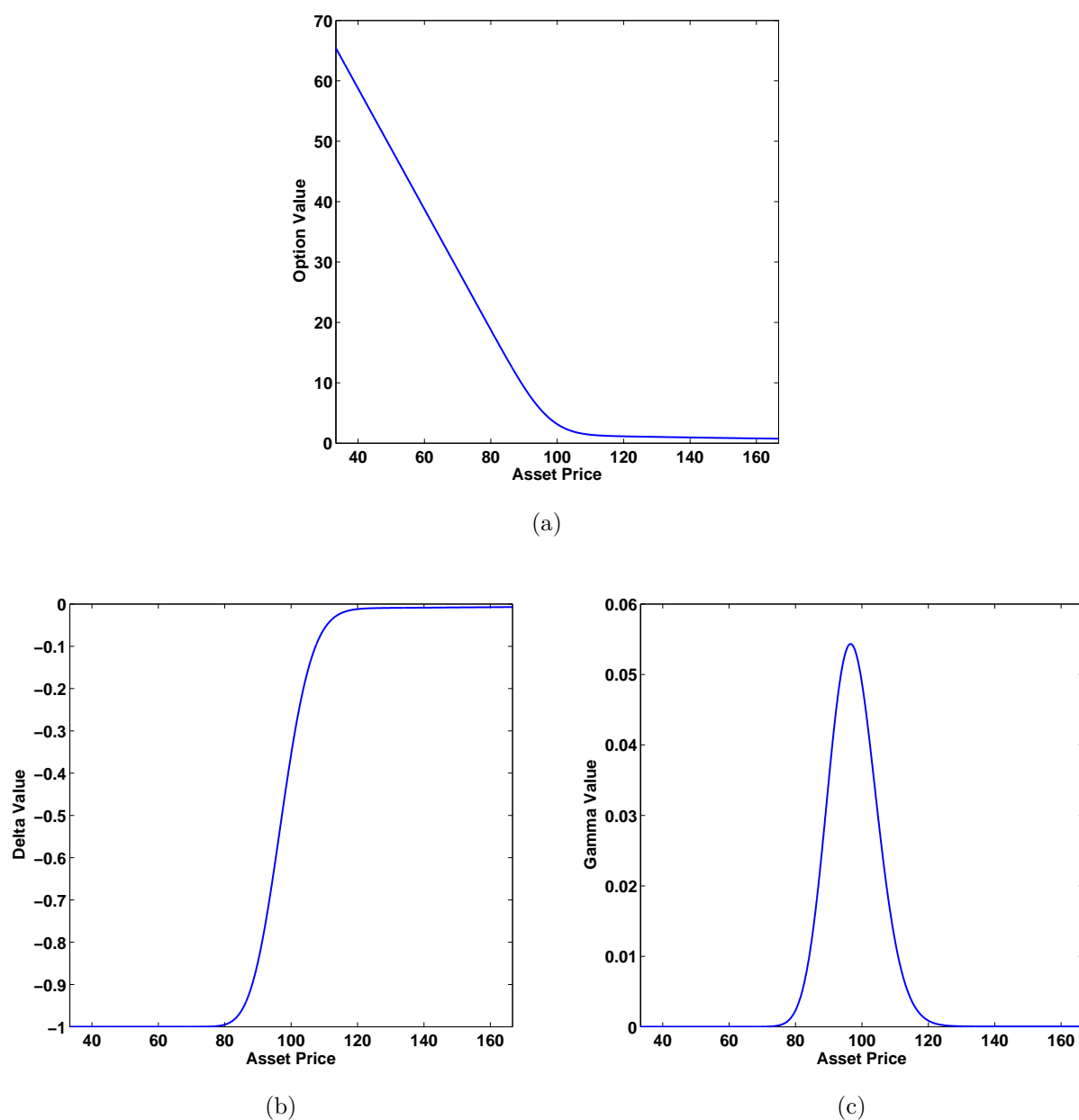


Figure 6.1: European put option value, Delta and Gamma under the Merton model with parameters as provided in the Example 6.5.1.

The Greeks help to provide important measurements of an option position's risks. Greeks are the quantities representing the sensitivity of the price of derivatives. Delta measures the rate of change of option value with respect to changes in the underlying asset's price,

where as Gamma represents the rate of change in the delta with respect to changes in the underlying price. For European put option the reference values of Delta are -0.84671538 at $S = 90$, -0.35566306 at $S = 100$, and -0.05810123 at $S = 110$, and the values of Gamma are 0.03486014 at $S = 90$, 0.04882567 at $S = 100$, and 0.01212941 at $S = 110$. Since radial basis functions are sufficiently smooth it helps us to compute some Greeks like Delta and Gamma.

Using the same parameter values which is employed for results in Table 6.1, we computed two Greeks viz Delta and Gamma at different asset prices and results obtained are reported in Table 6.3 and 6.4. From these tables we can observe that convergence rate of the proposed scheme is quadratic for computing Greeks as well. In Figure 6.1 we plot the option values, the Delta and the Gamma. The plot shows that the option values and Greeks are very stable and no spurious oscillation occur at or around the strike price. These figures show that Greeks are efficiently evaluated using proposed method.

Table 6.3: Numerical result for Delta of European put options under the Merton model at different asset price with parameters as given in Example 6.5.1.

M	N	$S = 90$		$S = 100$		$S = 110$	
		Value	Error	Value	Error	Value	Error
129	25	-0.847817	1.1019e-03	-0.358125	2.4621e-03	-0.059047	9.4544e-04
257	50	-0.847023	3.0807e-04	-0.356279	6.1556e-04	-0.058334	2.3319e-04
513	100	-0.846794	7.8244e-05	-0.355817	1.5392e-04	-0.058158	5.6766e-05
1025	200	-0.846735	1.9622e-05	-0.355702	3.8482e-05	-0.058115	1.3689e-05
2049	400	-0.846720	4.9210e-06	-0.355673	9.6151e-06	-0.058105	3.4368e-06
4097	800	-0.846717	1.3125e-06	-0.355665	2.3771e-06	-0.058102	8.1211e-07

Example 6.5.2. *European put option under Merton model with parameters $\sigma = 0.30$, $r = 0$, $\sigma_J = 0.50$, $\mu_J = 0$, $\lambda = 1.0$, $T = 0.50$, $E = 100$.*

These parameters are also used by N. Rambeerich et al. [105] and the option value is 15.03498881 at asset price $S = 100$. In their article first they used finite element approach

6.5.1. Numerical results for European options

Table 6.4: Numerical result for Gamma of European put options under the Merton model at different asset price with parameters as given in Example 6.5.1.

M	N	$S = 90$		$S = 100$		$S = 110$	
		Value	Error	Value	Error	Value	Error
129	25	0.034448	4.1186e-04	0.049816	9.9002e-04	0.012071	5.8559e-05
257	50	0.034758	1.0225e-04	0.049067	2.4124e-04	0.012117	1.2733e-05
513	100	0.034835	2.5208e-05	0.048886	5.9975e-05	0.012126	3.3105e-06
1025	200	0.034854	6.2791e-06	0.048841	1.4976e-05	0.012129	9.0800e-07
2049	400	0.034859	1.5713e-06	0.048829	3.7404e-06	0.012129	2.2477e-07
4097	800	0.034860	4.1016e-07	0.048827	9.2079e-07	0.012129	6.9091e-08

for spatial discretization and secondly, the use of exponential time integration(ETI) scheme for time marching. From Table 6.5, we observe that a second order rate is achieved for all three schemes. However, in terms of cpu time ETI scheme is approximately 7 time faster than the Crank-Nicolson scheme and the proposed implicit explicit scheme is much faster than ETI scheme. The cpu time and errors for both schemes ETI and Crank-Nicolson are adopted from N. Rambeerich et al. [105]. As suggested in [105] that the poor performance of Crank-Nicolson is because method is fully implicit and huge time required to take inverse of fully dense matrix resulting from discretisation of the convolution integral term.

Table 6.5: Comparison of different methods for European put options under the Merton model at strike price with parameters as given in Example 6.5.2.

M	N	Present Method		ETI[105]		Crank-Nicolson[105]	
		Error	cpu(s)	Error	cpu(s)	Error	cpu(s)
21	10	4.0167e-01	0.0197	3.6541e-01	0.008	3.6508e-01	0.026
41	20	4.9786e-02	0.0083	8.7613e-02	0.010	8.7540e-02	0.080
81	40	9.0855e-03	0.0111	2.1716e-02	0.027	2.1699e-02	0.317
161	80	2.0613e-03	0.0197	5.4188e-03	0.136	5.4169e-03	1.134
321	160	5.0327e-04	0.0463	1.3551e-03	0.964	1.3546e-03	7.874
641	320	1.2609e-04	0.1254	3.3980e-04	7.343	3.3968e-04	58.401
1281	640	3.2069e-05	0.4292	8.5980e-05	60.900	8.5992e-05	468.062

Example 6.5.3. *European call option under Merton model with parameters $\sigma = 0.20$, $r = 0$, $\sigma_J = 0.50$, $\mu_J = 0$, $\lambda = 0.10$, $T = 1.0$, $E = 1$.*

Table 6.6: Comparison of different methods for European call options under the Merton model at strike price with parameters as given in Example 6.5.3.

M	N	CM[16]		RBF-DQ[109]		Present Method	
		Value	Error	Value	Error	Value	Error
65	5	0.09102	4.01e-03	0.09182	2.32e-03	0.092339	1.7963e-03
129	10	0.09320	9.32e-04	0.93565	5.70e-04	0.093865	2.7096e-04
257	20	0.09413	2.72e-04	0.09399	1.38e-04	0.094076	5.9464e-05
513	40	0.09408	5.39e-05	0.09410	3.02e-05	0.094121	1.4369e-05

The above parameters are also considered by Bhuruth et al. [109] and Carry and Mayo [16]. In their article, Bhuruth et al. provided a new radial basis function based differential quadrature approach (RBF-DQ). They first used RBF-DQ approach for the spatial discretization followed by exponential time integration scheme for time discretization. Using Merton's closed form solution, the reference value 0.09413550 at strike price is calculated and the option value and absolute error at strike price are reported in Table 6.6. We observe that the results obtained with the present method have nice agreement with those given in [16, 109].

Example 6.5.4. *European option under Kou model with parameters $\sigma = 0.15$, $r = 0.05$, $\eta_1 = 3.0465$, $\eta_2 = 3.0775$, $\lambda = 0.10$, $p = 0.3445$, $T = 0.25$, $E = 100$.*

These parameters are adopted from [83, 30]. To perform the numerical simulations, we choose the truncated domain as $x_{\min} = -1.5$ and $x_{\max} = 1.5$. The analytical solution of the model can be found in Kou [81]. The value of European call option at different asset price are evaluated with six digit after the decimal points by d'Halluin et al [30]. The reference values for call option are 0.672677 at $S = 90$, 3.973479 at $S = 100$, and 11.794583 at $S = 110$. The reference price for put option is computed using put call parity. From Tables 6.7 and 6.8, we can observe that the point wise error at different asset price

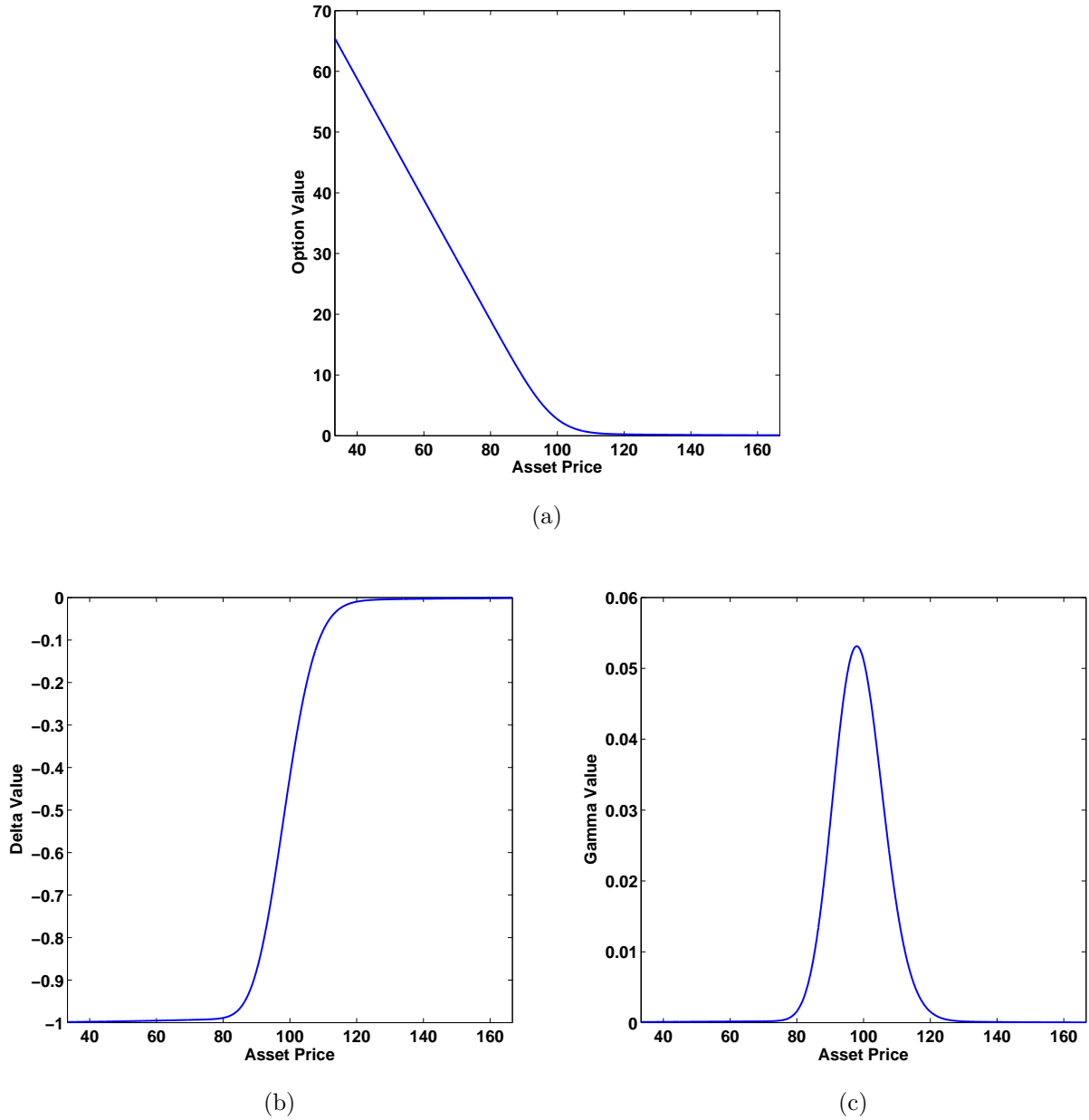


Figure 6.2: European put option value, Delta and Gamma under Kou's model at the last time step. The input parameters are provided in the caption of Table 6.7.

decrease, with convergence rate two. Finally in Figure 6.2, we plotted the option value and Greeks for put option. This shows that Greeks are efficiently evaluated under Kou model as well using proposed method.

6.5.2. Numerical results for American options

Table 6.7: Numerical results for European call options under the Kou model at different asset price with parameters as given in Example 6.5.4.

M	N	$S = 90$		$S = 100$		$S = 110$	
		Value	Error	Value	Error	Value	Error
129	25	0.670284	2.3932e-03	3.938910	3.4569e-02	11.787842	6.7414e-03
257	50	0.672105	5.7208e-04	3.964965	8.5136e-03	11.792817	1.7660e-03
513	100	0.672529	1.4783e-04	3.971358	2.1212e-03	11.794129	4.5366e-04
1025	200	0.672639	3.7620e-05	3.972948	5.3113e-04	11.794466	1.1692e-04
2049	400	0.672673	3.9368e-06	3.973363	1.1569e-04	11.794561	2.2399e-05
4097	800	0.672676	1.0867e-06	3.973450	2.9465e-05	11.794577	5.9222e-06

Table 6.8: Numerical results for European put options under the Kou model at different asset price with parameters as given in Example 6.5.4.

M	N	$S = 90$		$S = 100$		$S = 110$	
		Value	Error	Value	Error	Value	Error
129	26	9.428064	2.3932e-03	2.696690	3.4569e-02	0.545622	6.7413e-03
257	51	9.429885	5.7203e-04	2.722745	8.5135e-03	0.550597	1.7660e-03
513	101	9.430309	1.4778e-04	2.729138	2.1212e-03	0.551909	4.5361e-04
1025	201	9.430419	3.7571e-05	2.730728	5.3108e-04	0.552246	1.1687e-04
2049	401	9.430453	3.8874e-06	2.731143	1.1564e-04	0.552341	2.2349e-05
4097	801	9.430456	1.0373e-06	2.731230	2.9415e-05	0.552357	5.8728e-06

6.5.2 Numerical results for American options

The efficiency of the RBF-FD method with IMEX time-stepping has been demonstrated for European options. The pricing of American options is, however, usually more difficult due to the early exercise feature. The American option can be exercised at any time up to the maturity date and can be formulated as the linear complementarity problem.

Example 6.5.5. *American put option under the Merton model with parameters $\sigma = 0.15$, $r = 0.05$, $\sigma_J = 0.45$, $\mu_J = -0.90$, $\lambda = 0.10$, $T = 0.25$, $E = 100$.*

These parameters are consider by d'Halluin et al. [29] and by YongHoon Kwon et al.

[82] for Pricing American put option with truncated domain $x_{\min} = -1.5$ and $x_{\max} = 1.5$. In [29] authors have developed an implicit discretization coupled with penalty method for pricing such American options. The authors in [82] developed the three time level IMEX method coupled with operator splitting method to solve such problems. The option value and error at different asset price are reported in Table 6.9 with shape parameter $\epsilon = 3.0$. To obtain error at different asset price in Table 6.9, we have computed the successive changes in the option value at each asset price. From the above table, we observe that

Table 6.9: Numerical results for American put options under the Merton model at different asset price with parameters as given in Example 6.5.5.

M	N	$S = 90$		$S = 100$		$S = 110$	
		Value	Error	Value	Error	Value	Error
129	25	9.998080	-	3.207266	-	1.414138	-
257	50	10.000259	2.1789e-03	3.232387	2.5120e-02	1.418174	4.0361e-03
513	100	10.003020	2.7610e-03	3.238920	6.5333e-03	1.419327	1.1528e-03
1025	200	10.003934	9.1430e-04	3.240634	1.7132e-03	1.419660	3.3244e-04
2049	400	10.003835	9.9612e-05	3.241085	4.5131e-04	1.419759	9.9174e-05
4097	800	10.003866	3.1405e-05	3.241207	1.2209e-05	1.419790	3.0951e-05

pointwise errors generally converge with approximately second order accuracy, while near the optimal exercise boundary convergence is less accurate. The above phenomenon is also discussed in [29, 82].

In Figure 6.3, we provide the plot of both option values and the early exercise boundary for American put option under the Merton model.

Example 6.5.6. *American put option under the Kou model with parameters $\sigma = 0.15$, $r = 0.05$, $\eta_1 = 3.0465$, $\eta_2 = 3.0775$, $\lambda = 0.10$, $p = 0.3445$, $T = 0.25$, $E = 100$.*

These parameters are also adopted by YongHoon Kwon et al. [82] with same truncated domain and shape parameter. The reference values at different asset prices are given by Toivanen [127], are 10.005071 at $S = 90$, 2.807879 at $S = 100$, and 0.561876 at $S = 110$.

In Table 6.10, we get the same scenario as in the case of Merton model. We are getting

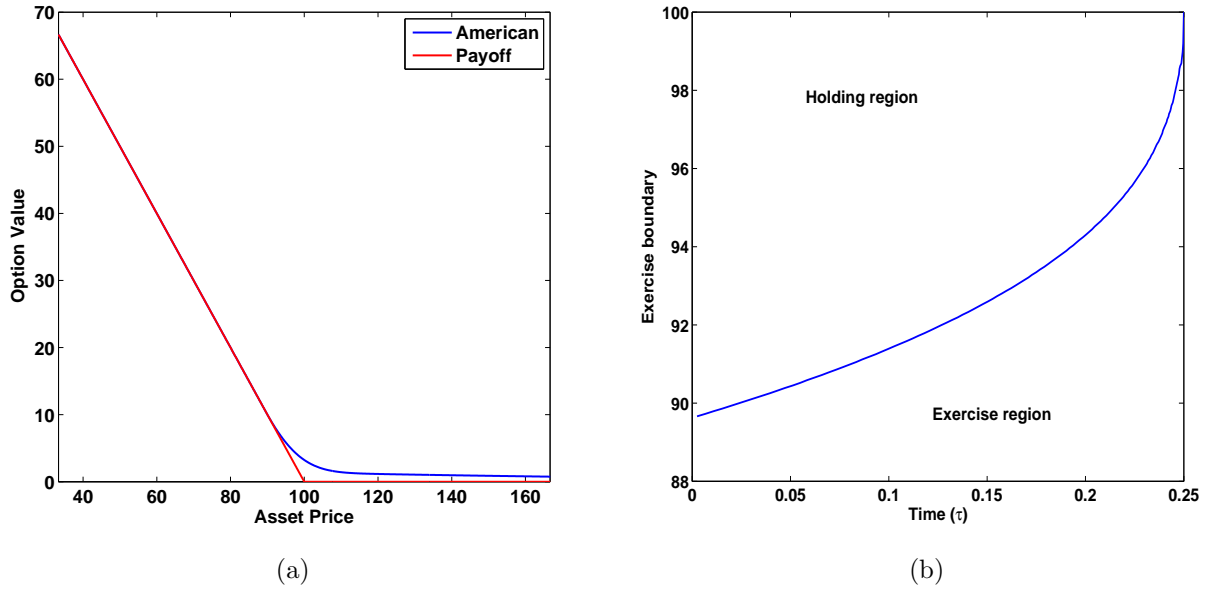


Figure 6.3: American put option value, and optimal early exercise boundary under the Merton model with parameters as provided in the Example 6.5.5.

Table 6.10: Numerical results for American put options under the Kou model at different asset price with parameters as given in Example 6.5.6.

M	N	$S = 90$		$S = 100$		$S = 110$	
		Value	Error	Value	Error	Value	Error
129	25	10.002131	-	2.777966	-	0.558356	-
257	50	10.000735	1.3951e-03	2.799956	2.1990e-02	0.560726	2.3706e-03
513	100	10.005015	4.2794e-03	2.805766	5.8098e-03	0.561502	7.7560e-04
1025	200	10.005055	3.9945e-05	2.807307	1.5414e-03	0.561750	2.4808e-04
2049	400	10.005088	3.3276e-05	2.807723	4.1541e-04	0.561834	8.3698e-05
4097	800	10.005098	9.4650e-06	2.807834	1.1140e-04	0.561861	2.7201e-05

approximately second order convergence rate, while we have less accuracy near by the early exercise boundary. Finally in Figure 6.4, we have plotted the option value and early exercise boundary for American put option under Kou model.

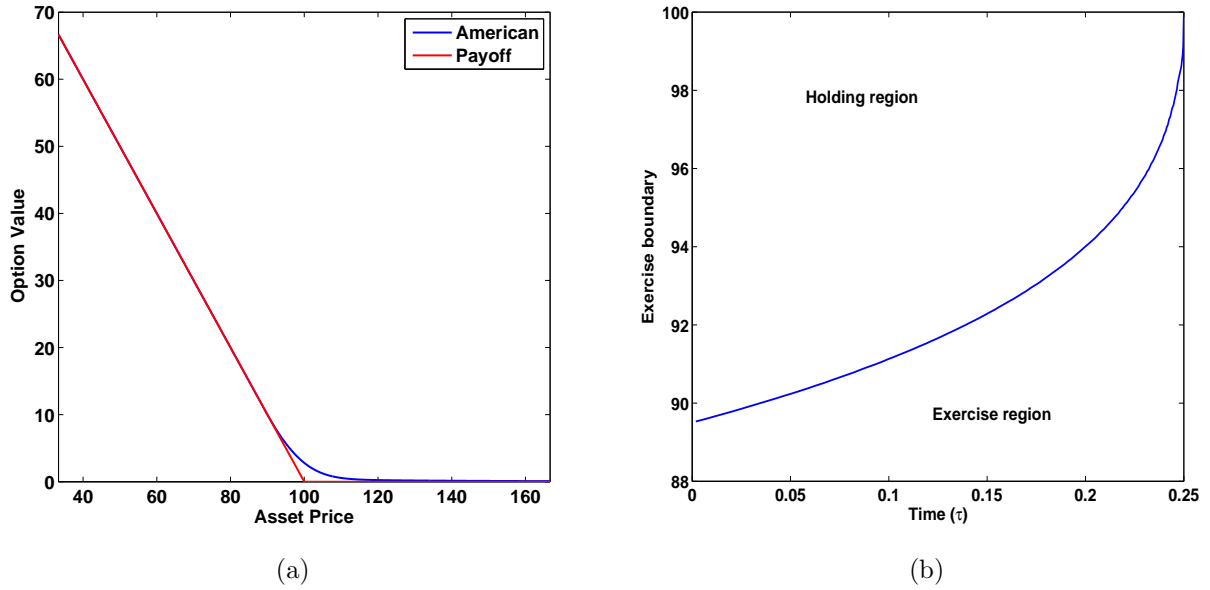


Figure 6.4: American put option value, and optimal early exercise boundary under the Kou model with parameters as provided in the Example 6.5.6.

6.6 Conclusions

In this chapter, we describe the valuation of European and American option under Merton's and Kou's jump diffusion model. After implicit explicit time semi discretization of governing equation, the resulting linear differential equations are solved using RBF based finite difference method, the integral term involve in PIDE is approximated with composite trapezoidal rule. The numerical simulation with European and American put and call option under Merton's and Kou's model is carried out. The results are compared against the FD, FEM, and RBF-DQ method available in literature and shown that the proposed method are more accurate and efficient. The proposed method approximate not only the option value but also some of its "Greeks" namely "Delta" and "Gamma" very efficiently.

In the next chapter we present a high order L-stable Padé time marching scheme for pricing exotic option

A RBF based L-stable Padé scheme for pricing exotic option

In this chapter, we extend the mesh free method which is developed in previous chapters to solve the problem for pricing several exotic option. The spatial discretization is done by radial basis function based local grid free method to achieve first order ordinary differential equation followed by fourth order L-stable method. Numerical study with one and two asset problems for digital option, butterfly spread and barrier option is carried out with highly accurate results that are in good agreement with those obtained by other numerical method in literature.

7.1 Introduction

Exotic options are one of the non standard options widely used in the field of finance. The features of these options are more complicated than European and American plain vanilla option. The exotic option is an option contract that can be exercised according to average value of the asset price during a specific period of time and their maximum and minimum prices. The most of the options are priced by mean of partial differential equations. The

numerical method for solution is more challenging due to the discontinuity of the pay off condition. The large error may appear into estimating the hedging parameters. The non smoothness in the data can lead to a serious problem in the convergence of numerical method. Explicit schemes are easy from the implementation point of view, but suffer from stability problem, some other implicit method like Crank-Nicolson method has spurious oscillation in numerical solution, unless the time step size is very small. We may use fully implicit Backward Euler method for numerical solution of Black-Scholes equation due to its strong stability property, but it has only first order accuracy in time. Khaliq et al. [79] developed a high order smoothing scheme utilizing a scheme developed by Ranacher. In [78], Khaliq et al. developed $(0, 4)$ Padé L-stable method with parallel implementation for exotic option. In this chapter we discuss the application of local radial basis function method for spatial discretization in conjunction with L-stable time stepping for pricing exotic option.

The rest of the chapter is organized as follows. In section 7.2 semidiscretization is done to dissociate spatial and temporal variable of differential operator. In section 7.3 we present high order L-stable Padé scheme for temporal discretization of resulting system followed by partial fraction form of fully discrete equation. Section 7.4 consists of computational results obtained by the present method which are compared with other numerical and analytical solutions available in literature. To conclude, we give some final remarks for the advantages of the presented radial basis function method in section 7.5.

7.2 Method of Lines semidiscretization

The method of lines is a well established numerical technique used for numerical solution of a wide class of PDEs that contains both spatial as well as time variable. The spatial discretization results in an approximating system of ODEs. For inhomogeneous linear PDE, the above method leads to inhomogeneous system of ODEs in time whose solution is obtained by a two-term recurrence relation involving the matrix exponential, where the matrix is determined by the form of spatial discretization. We use a local radial basis function based approximation for spatial discretization.

We consider the Black-Scholes PDE model

$$\frac{\partial V}{\partial \tau} + \mathcal{L}V(S, \tau) = 0 \quad \tau < T, \quad S \in \mathbb{R}_+^d \quad (7.2.1)$$

where

$$\mathcal{L}V(S, \tau) = \frac{1}{2} \sum_{i=1}^d \sum_{j=1}^d \rho_{ij} \sigma_i \sigma_j s_i s_j \frac{\partial^2 V}{\partial s_i \partial s_j} + \sum_{i=1}^d r s_i \frac{\partial V}{\partial s_i} - rV$$

with S represents the price of the underlying asset, serving as a space variable, r is the risk free interest rate and σ_i the volatility of i^{th} underlying asset, d denotes the number of underlying assets and thus the number of spatial dimension of the problem, and $V(S, \tau)$ is the value of the option before the expiry time T . Before solving the problem (7.2.1) numerically, we transform it from final value problem to initial value problem through transformation $t = T - \tau$ leading to

$$\frac{\partial V}{\partial t} - \mathcal{L}V(S, t) = 0. \quad (7.2.2)$$

Now the RBF's based finite difference method described in previous chapter to approximate $\mathcal{L}V$ at each node x_i , can be extended for semi-discretization in space to solve Black-Scholes equation. Let us leave temporal variable ' t ' continuous and discretize equation (7.2.2) in space using proposed local RBF scheme, which leads to following system of initial value problem;

$$\frac{dV}{dt} + \mathcal{A}V = f(t), \quad V(0) = g. \quad (7.2.3)$$

Where " \mathcal{A} " is the matrix containing weights for local RBF approximation of " $-\mathcal{L}V$ ", the vector " f " corresponding to boundary condition and the vector " g " of the transformed initial condition is the given payoff function, which depend on the option under consideration. The exact solution of the equation (7.2.3) satisfies the recurrence formula[139]

$$V(t_{m+1}) = e^{-\delta t \mathcal{A}} V(t_m) + \delta t \int_0^1 e^{-\delta t \mathcal{A}(1-\tau)} f(t_m + \tau \delta t) d\tau \quad (7.2.4)$$

where $0 < \delta t \leq \delta t_0$, for some δt_0 , is time step and $t_m = m\delta t$.

7.3 Time stepping scheme

Let $P_{n,m}(z)$ & $Q_{n,m}(z)$ be two polynomials of degree n and m respectively. Then the $(n+m)^{th}$ order rational Padé approximation of the exponential function e^{-z} can be written as

$$R_{n,m}(z) = \frac{P_{n,m}(z)}{Q_{n,m}(z)}$$

where

$$P_{n,m}(z) = \sum_{j=0}^n \frac{(m+n-j)!n!}{(m+n)!j!(n-j)!} (-z)^j$$

and

$$Q_{n,m}(z) = \sum_{j=0}^m \frac{(m+n-j)!m!}{(m+n)!j!(m-j)!} (z)^j.$$

The Padé approximation $R_{n,m}(z)$, to the exponential function e^{-z} is of the order $(n+m)$. The rational approximation $R_{n,m}(z)$ of e^{-z} is said to be A-stable if $|R_{n,m}(z)| < 1$ whenever $Re(z) < 0$ and L-stable if, in addition $|R_{n,m}(z)| \rightarrow 0$ as $Re(z) \rightarrow -\infty$. For practical purpose, we are particularly interested in following Padé approximation of e^{-z}

$$R_{22}(z) = \frac{1 - \frac{1}{2}z + \frac{1}{12}z^2}{1 + \frac{1}{2}z + \frac{1}{12}z^2}$$

and

$$R_{0,4}(z) = \frac{1}{1 + z + \frac{1}{2}z^2 + \frac{1}{6}z^3 + \frac{1}{24}z^4}.$$

Replacing the matrix exponential $e^{-\delta t \mathcal{A}}$ by (n, m) Padé approximation $R_{n,m}(\delta t \mathcal{A})$, the recurrence relation is approximated by [78];

$$V_{n+1} = R_{n,m}(\delta t \mathcal{A})V_n + \delta t \sum_{i=1}^s Q_{n,m}^{(i)}(\delta t \mathcal{A})f(t_n + \tau_i \delta t) \quad (7.3.1)$$

where $Q_{n,m}^{(i)}(z)$ are rational function, which have same denominator as those $R_{n,m}(z)$ and $\{\tau_i\}_{i=1}^s$ are the Gaussian points. The accuracy of corresponding scheme will be maintained provided

$$\sum_{i=1}^s \tau_i^l Q_{n,m}^{(i)}(z) = \frac{l!}{(-z)^{l+1}} \left(R_{n,m}(z) - \sum_{j=0}^l \frac{(-z)^j}{j!} \right), \quad l = 0, 1, 2, \dots, s-1 \quad (7.3.2)$$

which is linear system in $Q_{n,m}^{(i)}(z)$ and can be solved to determine $Q_{n,m}^{(i)}(z)$ corresponding to any choice of $R_{n,m}(z)$.

7.3.1 A fourth order L-stable method

Let us consider the fourth order L-stable Padé approximation $R_{0,4}(z)$ with $\tau_1 = \frac{3-\sqrt{3}}{2}$ and $\tau_2 = \frac{3+\sqrt{3}}{2}$, the Gaussian quadrature points of order two. Then system (7.3.2) reduces to

$$\begin{aligned} Q_{0,4}^{(1)}(z) + Q_{0,4}^{(2)}(z) &= -\frac{1}{z} (R_{0,4}(z) - 1) \\ \tau_1 Q_{0,4}^{(1)}(z) + \tau_2 Q_{0,4}^{(2)}(z) &= \frac{1}{z^2} (R_{0,4}(z) - 1 + z) \end{aligned}$$

solving the above system leads the following fourth order schemes

$$U_{n+1} = R_{0,4}(\delta t \mathcal{A}) U_n + \delta t Q_{0,4}^{(1)}(\delta t \mathcal{A}) f(t_n + \tau_1 \delta t) + \delta t Q_{0,4}^{(2)}(\delta t \mathcal{A}) f(t_n + \tau_2 \delta t) \quad (7.3.3)$$

where

$$\begin{aligned} Q_{0,4}^{(1)}(z) &= \frac{\frac{1}{2} + (\frac{3-\sqrt{3}}{12})z + (\frac{2-\sqrt{3}}{24})z^2 + (\frac{1-\sqrt{3}}{48})z^3}{1 + z + \frac{1}{2}z^2 + \frac{1}{6}z^3 + \frac{1}{24}z^4} \\ Q_{0,4}^{(2)}(z) &= \frac{\frac{1}{2} + (\frac{3+\sqrt{3}}{12})z + (\frac{2+\sqrt{3}}{24})z^2 + (\frac{1+\sqrt{3}}{48})z^3}{1 + z + \frac{1}{2}z^2 + \frac{1}{6}z^3 + \frac{1}{24}z^4}. \end{aligned}$$

7.3.2 Partial Fractional form of the schemes

Both schemes discussed above required to take inverse of higher order matrix polynomial which can cause computational difficulty due to higher power of matrix “ \mathcal{A} ”. For resolving this problem Khaliq (for more detail see [76, 78] and references therein) developed parallel version of these scheme.

If $n < m$, then we have

$$\begin{aligned} R_{n,m}(z) &= \sum_{j=1}^{q_1} \frac{w_j}{z - c_j} + 2 \sum_{j=q_1+1}^{q_1+q_2} \operatorname{Re} \left(\frac{w_j}{z - c_j} \right) \\ Q_{n,m}^{(i)}(z) &= \sum_{j=1}^{q_1} \frac{w_{ij}}{z - c_j} + 2 \sum_{j=q_1+1}^{q_1+q_2} \operatorname{Re} \left(\frac{w_{ij}}{z - c_j} \right), \quad i = 1, 2. \end{aligned} \quad (7.3.4)$$

And for the case $n = m$, the partial fraction form for $R_{m,m}(z)$ and $Q_{n,m}^{(i)}(z)$ is given by [78]

$$\begin{aligned} R_{m,m}(z) &= (-1)^m + \sum_{j=1}^{q_1} \frac{w_j}{z - c_j} + 2 \sum_{j=q_1+1}^{q_1+q_2} \operatorname{Re} \left(\frac{w_j}{z - c_j} \right) \\ Q_{n,m}^{(i)}(z) &= \sum_{j=1}^{q_1} \frac{w_{ij}}{z - c_j} + 2 \sum_{j=q_1+1}^{q_1+q_2} \operatorname{Re} \left(\frac{w_{ij}}{z - c_j} \right), \quad i = 1, 2 \end{aligned} \quad (7.3.5)$$

where $R_{n,m}(z)$ as well as $Q_{n,m}^{(i)}(z)$ have q_1 real and $2q_2$ complex pole c_j with $q_1 + 2q_2 = m$, and $w_j = \frac{P_{n,m}(c_j)}{Q'_{n,m}(c_j)}$ and $w_{ij} = \frac{\mathcal{N}_{n,m}^{(i)}(c_j)}{\mathcal{D}_{n,m}^{(i)}(c_j)}$. The polynomials $\mathcal{N}_{n,m}^{(i)}(z)$ and $\mathcal{D}_{n,m}^{(i)}(z)$ are the numerator and denominator of the function $Q_{n,m}^{(i)}(z)$.

The poles and weights for $R_{0,4}(z)$ and $Q_{0,4}(z)$ are: $q_1 = 0$, and $q_2 = 2$, and [78]

$$\begin{aligned} c_1 &= -0.270555768932292 + 2.50477590436244i, \\ c_2 &= -1.72944423106769 - 0.888974376121862i, \\ w_1 &= -0.541413348429154 + 0.248562520866115i, \\ w_2 &= 0.541413348429182 + 1.58885918222330i, \\ w_{11} &= 0.174204307471878 - 0.0234882684011149i, \\ w_{12} &= 0.508808394420347 + 0.00250791289107607i, \\ w_{21} &= -0.295373909958639 - 0.179575890979881i, \\ w_{22} &= 0.112361208066437 + 0.596907381204164i. \end{aligned}$$

The algorithm becomes;

$$V_{n+1} = 2\operatorname{Re}(y_1) + 2\operatorname{Re}(y_2) \quad (7.3.6)$$

where

$$\begin{aligned} (\delta t \mathcal{A} - c_1 I) y_1 &= w_1 V_n + \delta t w_{11} f(t_n + \tau_1 \delta t) + \delta t w_{21} f(t_n + \tau_2 \delta t) \\ (\delta t \mathcal{A} - c_2 I) y_2 &= w_2 V_n + \delta t w_{12} f(t_n + \tau_1 \delta t) + \delta t w_{22} f(t_n + \tau_2 \delta t) \end{aligned}$$

which can be solved in parallel on two machines for speed, or on a serial machine, to improve accuracy.

7.4 Numerical simulation and discussion

In this section, we discuss the performance of the algorithm on some important example from financial mathematics. Although the scheme works for all radial basis function but we will use multi-quadric($\sqrt{1 + (\epsilon r)^2}$) radial basis function on different experimental setup. Our first example is digital call option whose payoff has a jump discontinuity at the strike price. The second example is butterfly option, which has three strike prices, the payoff for this option has three corners at the strike price. The final example demonstrate the applicability of the scheme to double barrier option. Since radial basis function is infinitely differentiable, the value of derivative of the options is promptly available from the derivative of basis function, we also calculate value of delta(Δ) of an option which is the rate of change of the option value with respect to the asset price and gamma(Γ) of a portfolio of options on a underlying asset which is the rate of change of portfolio's delta with respect to the price of the underlying asset.

7.4.1 A digital call option

A digital call option, also known as cash or nothing call option, is an option with payoff zero before the strike price and any fixed amount after the strike price. This is modeled by Black-Scholes PDE

$$\frac{\partial V}{\partial \tau} + \frac{1}{2}\sigma^2 S^2 \frac{\partial^2 V}{\partial S^2} + rS \frac{\partial V}{\partial S} - rV = 0, \quad (S, \tau) \in (0, \infty) \times (0, T] \quad (7.4.1)$$

with the payoff function given as

$$V(S, T) = \begin{cases} 0 & \text{for } S < E, \\ 1 & \text{for } S > E. \end{cases}$$

Using the average of the payoff function

$$V(S, T) = \begin{cases} 0 & \text{for } S < E, \\ 0.5 & \text{for } S = E, \\ 1 & \text{for } S > E. \end{cases} \quad (7.4.2)$$

The boundary conditions are given as

$$V(S, \tau) = \begin{cases} 0 & \text{for } S = 0, \\ e^{-r(T-\tau)} & \text{for } S \rightarrow \infty. \end{cases} \quad (7.4.3)$$

The analytical solution for the digital option is

$$V(S, \tau) = e^{-r(T-\tau)} \mathcal{N}(d_2(S, \tau)) \quad (7.4.4)$$

where $\mathcal{N}(\cdot)$ is the cumulative distribution of the standard normal distribution function with:

$$d_2(S, \tau) = \frac{\ln(\frac{S}{E}) + (r - \frac{1}{2}\sigma^2)(T - \tau)}{\sigma\sqrt{T - \tau}}.$$

The behavior of delta of digital call at the expiry can be summarized as [78]

$$\lim_{\tau \rightarrow T} \frac{\partial V}{\partial S} = \begin{cases} 0 & \text{for } S < E, \\ \infty & \text{for } S = E, \\ 0 & \text{for } S > E. \end{cases} \quad (7.4.5)$$

To investigate performance of proposed method numerical simulation was done for digital call option at strike price $E = 0.5$ with the parameter $S_{\min} = 0$, $S_{\max} = 1$, $r = 0.05$, $\sigma = 0.2$, $T = 0.25$ taken from Khaliq et al.[78] with $h = 0.001$.

Table 7.1 show the convergence trends of the present method, the convergent order is

Table 7.1: Option value, error and rate of convergence for the digital call option at strike price E .

δt	Present method			Khaliq et al.[78]	
	Option value	Error	rate	Error	rate
0.125	0.05232980	1.221525e-05		1.222e-05	
0.0625	0.05233088	1.417290e-06	3.1075	1.417e-06	3.1081
0.03125	0.05233101	1.289255e-07	3.4585	1.283e-07	3.4653
0.015625	0.05233102	9.418614e-09	3.7749	8.722e-09	3.8784
0.0078125	0.05233102	1.120308e-10	6.3935	5.911e-10	3.8832

evaluated at the strike price E where the payoff function has a jump discontinuity. From the Table we can observe that our results are very close to those presented by Khaliq et al.[78]. The space time graph of option value with parameter $r = 0.1$, $\sigma = 0.5$, $E = 0.5$ and $T = 0.5$ are plotted in the Figure 7.1a and we also observe that the delta value of option at expiry given in (7.4.5) is consistent with Figure 7.1b.

7.4.2 Two-asset digital call option

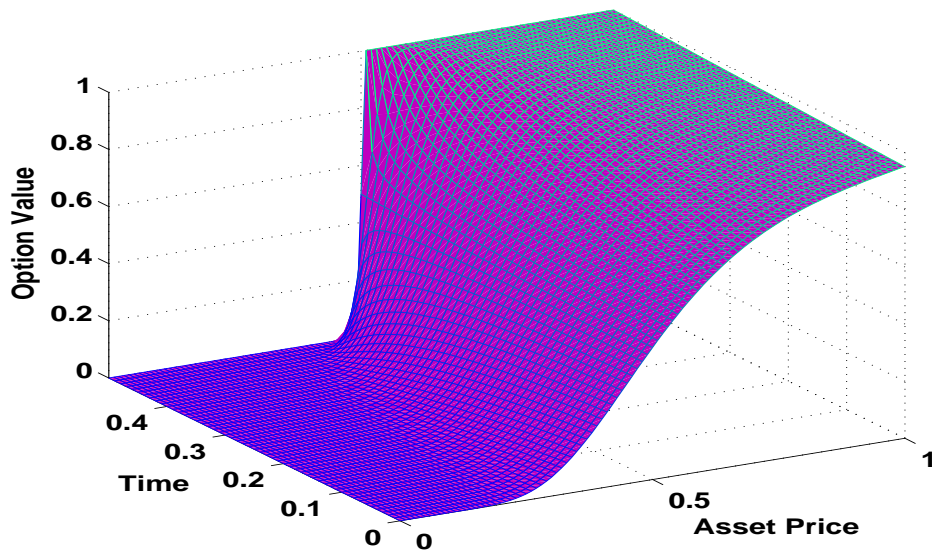
We consider two asset call option with the asset prices by s_1 and s_2 ;

$$\frac{\partial V}{\partial \tau} + \frac{1}{2}\sigma_1^2 s_1^2 \frac{\partial^2 V}{\partial s_1^2} + \frac{1}{2}\sigma_2^2 s_2^2 \frac{\partial^2 V}{\partial s_2^2} + \frac{1}{2}\rho\sigma_1\sigma_2 s_1 s_2 \frac{\partial^2 V}{\partial s_1 \partial s_2} + r s_1 \frac{\partial V}{\partial s_1} + r s_2 \frac{\partial V}{\partial s_2} - rV = 0 \quad (7.4.6)$$

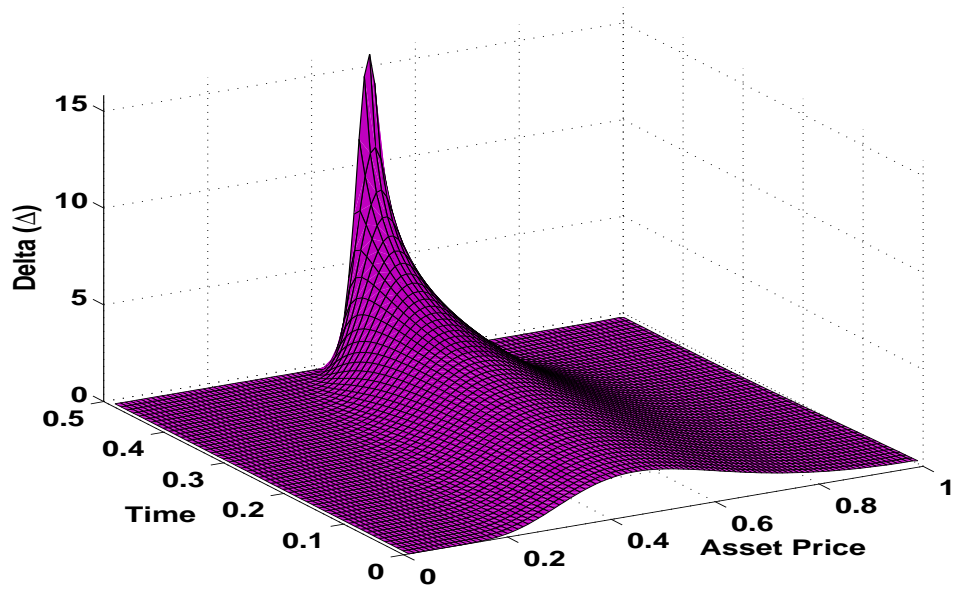
with non-smooth payoff for digital call option given by

$$V(S, T) = \begin{cases} 1 & \max\{s_1, s_2\} \geq E, \\ 0 & \text{otherwise.} \end{cases} \quad (7.4.7)$$

The proposed (0,4)-Padé scheme is implemented with parameter $\sigma_1 = 0.2$, $\sigma_2 = 0.2$, $\rho = 0.3$, $r = 0.05$, $T = 1$, $\delta t = 0.1$, $h = 0.1$ and strike price $E = 0.5$. The space time graph of payoff function and option value is given in Figures 7.2a, and 7.2b respectively. From the figure we can observe that proposed scheme provides accurate solution throughout the entire region of interest.

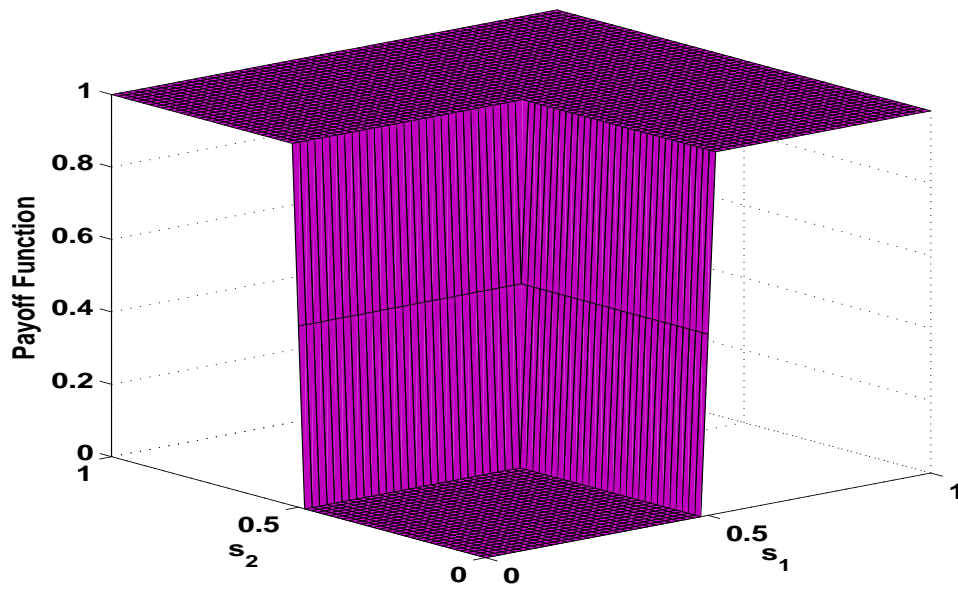


(a)

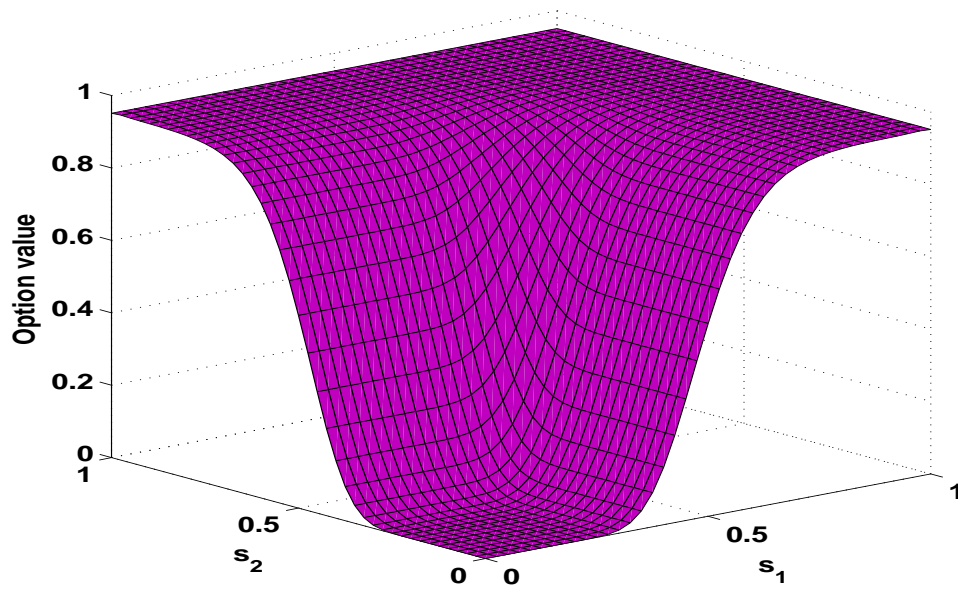


(b)

Figure 7.1: Space time graph of option value and delta for digital call option using (0,4) Padé scheme.



(a)



(b)

Figure 7.2: Space time graph of option payoff and option value for two asset digital call option using (0,4) Padé scheme.

7.4.3 A butterfly spread option

A Butterfly Spread option is a combination of three options with three strike prices, in which one contract is purchased with two outside strike prices and two contracts are sold at the middle strike price. The payoff function at expiry being

$$V(S, T) = \max(S - E_1, 0) - 2 \max(S - E_2, 0) + \max(S - E_3, 0) \quad (7.4.8)$$

where E_1 , E_2 , and E_3 are three strike prices with $E_1 < E_2 < E_3$ and $E_2 = \frac{E_1 + E_3}{2}$. This is homogeneous problem with corners in payoff functions, at E_1 , E_2 , E_3 and its delta have three jump discontinuities. The behavior of delta at the expiry can be summarized as [79]

$$\lim_{\tau \rightarrow T} \frac{\partial V}{\partial S} = \begin{cases} 0 & \text{for } 0 \leq S < E_1, \\ 1 & \text{for } E_1 \leq S < E_2, \\ -1 & \text{for } E_2 \leq S < E_3, \\ 0 & \text{for } S \geq E_3. \end{cases} \quad (7.4.9)$$

The numerical simulation was carried out with parameter $S_{\min} = 0$, $S_{\max} = 1$, $r = 0.1$, $\sigma = 0.5$, $T = 0.5$ taken from Khaliq et al.[79] and with $h = 0.001$. As the problem does not have analytical solution, the error is computed relative to the solution computed using backward Euler scheme on very fine mesh and the reference solution at the strike price $E_2 = 0.5$ is 0.02102705683555 [79]. The results obtained by the proposed method are reported in the Table 7.2 and compared with existing results. From the table we can observe that accuracy of the proposed method is superior. The space time graph of option value is plotted in the Figure 7.3a and we also observe that the delta value of option at expiry given in (7.4.9) is consistent with Figure 7.3b.

7.4.4 Two-asset butterfly spread option

We consider a two asset call option (7.4.6), with payoff at expiry given by

$$V(S, T) = \max(S_{\max} - E_1, 0) - 2 \max(S_{\max} - E_2, 0) + \max(S_{\max} - E_3, 0) \quad (7.4.10)$$

Table 7.2: Option value, error and rate of convergence for the butterfly spread option at strike price E_2 .

δt	Present method			Khaliq et al.[79]	
	Option value	Error	rate	Error	rate
0.25	0.02107993	5.287418e-05	-	1.987e-04	-
0.125	0.02103347	6.410909e-06	3.04396	2.124e-05	3.22565
0.0625	0.02102766	6.034304e-07	3.40927	1.789e-06	3.56937
0.03125	0.02102710	4.398879e-08	3.77798	1.325e-07	3.75493
0.015625	0.02102706	7.655368e-10	5.84452	8.707e-09	3.92811

where $S_{\max} = \max(s_1, s_2)$. The parameters for numerical implementation are $\sigma_1 = 0.65$, $\sigma_2 = 0.65$, $\rho = 0.5$, $r = 0.05$, $T = 2$, $\delta t = 0.1$, $h = 0.0125$ with three strike price $E_1 = 0.4$, $E_2 = 0.5$, $E_3 = 0.6$. The payoff function which has discontinuities at strike prices, is plotted in Figure 7.4a. Figure 7.4b shows the option value having no spurious oscillations.

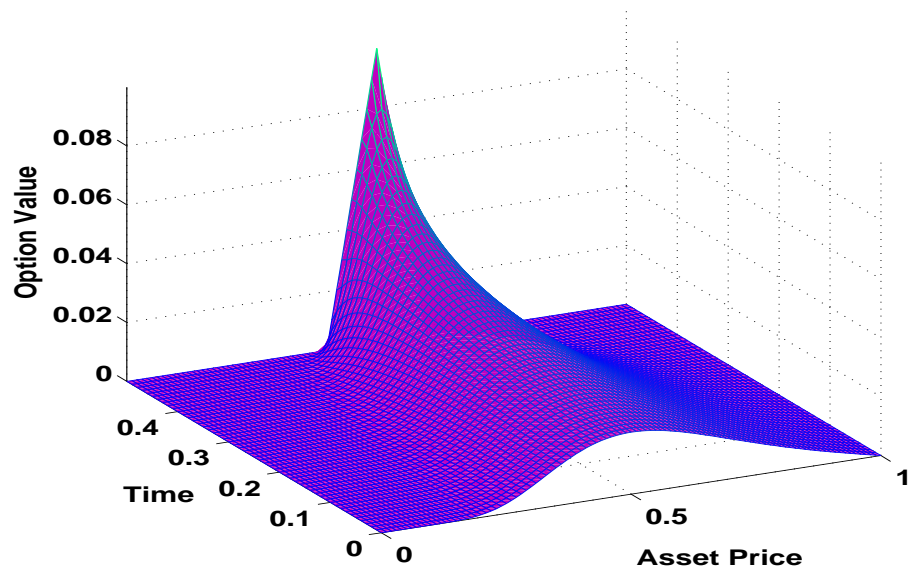
7.4.5 A double barrier option

A barrier option is an option where the payoff depends on whether the underlying asset price reaches a certain level during certain period of time. The payoff function at expiry is given by

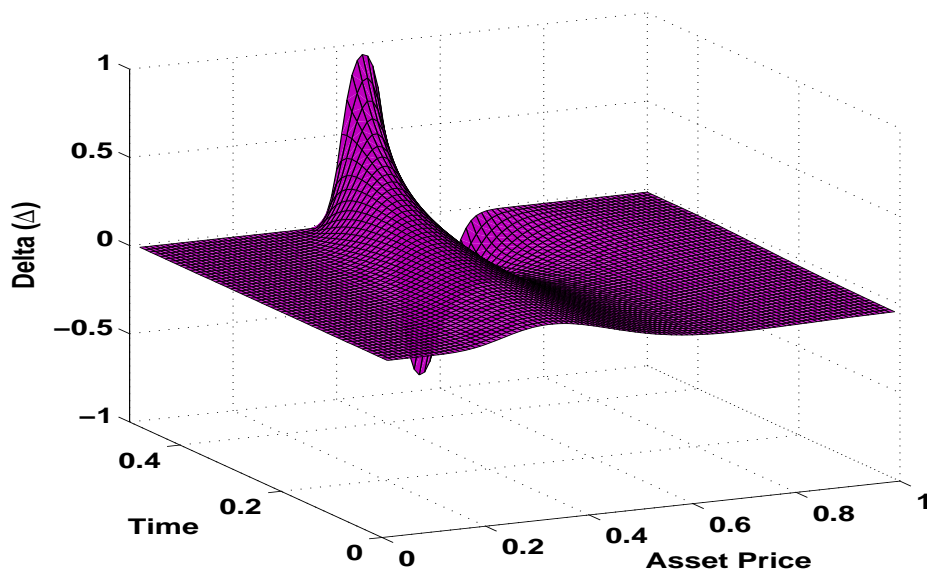
$$V(S, T) = \begin{cases} 0 & S \leq B_1, \\ \max(S - E, 0) & B_1 \leq S \leq B_2, \\ 0 & B_2 \leq S \end{cases} \quad (7.4.11)$$

and the barrier constraint

$$V(S, \tau) = \begin{cases} 0 & S \leq B_1 \text{ or } B_2 \leq S \text{ and } t \in \mathbb{B}, \\ V(S, \tau) & \text{otherwise.} \end{cases} \quad (7.4.12)$$

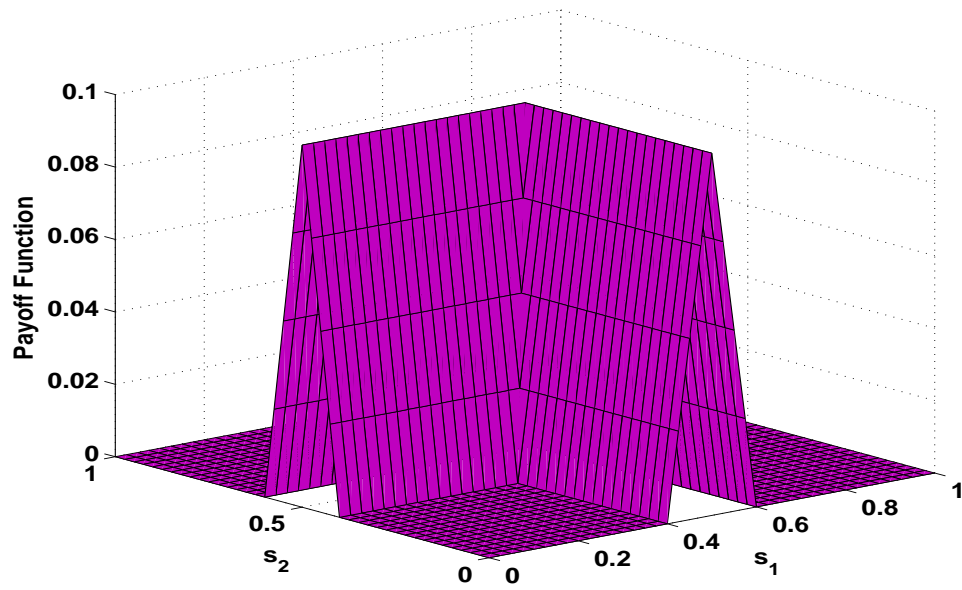


(a)

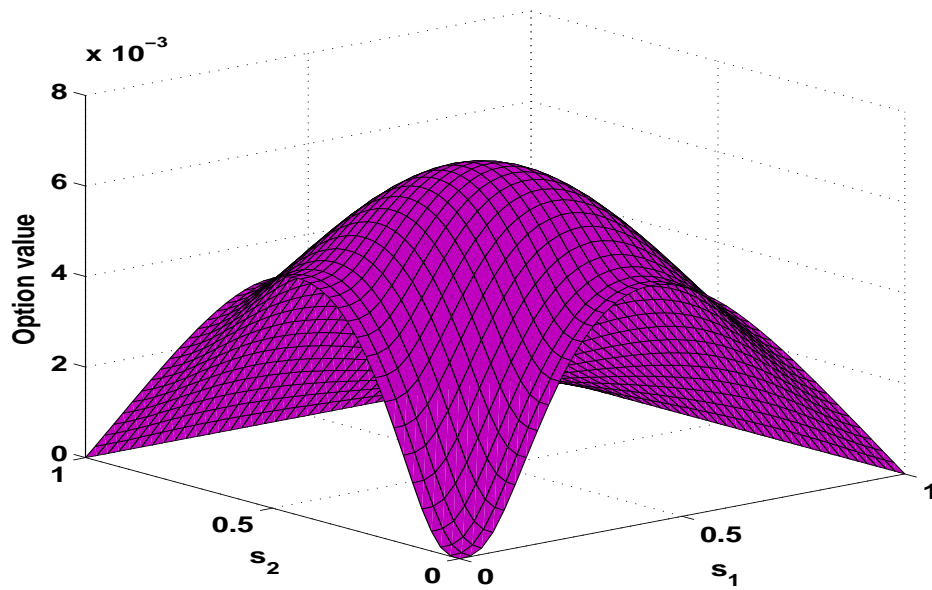


(b)

Figure 7.3: Space time graph of option value and delta for butterfly spread using (0,4) Padé scheme.



(a)



(b)

Figure 7.4: Space time graph of option payoff and option value for two asset butterfly spread using (0,4) Padé scheme.

Here, B_1 and B_2 are lower and upper barrier respectively, E is strike price. The set $\mathbb{B} = \{t_i | t_i \in [0, T]\}$ consists of all the times when barriers are applied. We assume that the barriers are applied discretely, like, daily or weekly, and the barrier time are distributed uniformly in the set \mathbb{B} . The numerical experiment was carried out for the asset price ranging from $S = 90$ to 115 , with parameter $r = 0.05$, $\sigma = 0.25$ and strike price $E = 100$ with $h = 0.0125$. The numerical experiment was done at two barriers $B_1 = 95$ and $B_2 = 110$ applied five times in the time domain $[0, T]$ where the expiry time T is 0.5 . Since the above problem does not have analytical solution, we used reference solution 0.09697960007895 at $B_1 = 95$ and 0.08148159339106 at $B_2 = 110$. The option value and error at barrier points

Table 7.3: Option value and error at B_1 & B_2 with various value of ϵ for double barrier option.

ϵ	Value at (B_1)	Error at (B_1)	Value at (B_2)	Error at (B_2)
0.05	0.09651039	5.570736e-04	0.08109755	4.538424e-04
0.1	0.09677250	2.949728e-04	0.08131382	2.375738e-04
0.2	0.09672588	3.415847e-04	0.08127534	2.760567e-04
0.3	0.09672448	3.429883e-04	0.08127414	2.772531e-04
0.4	0.09672123	3.462376e-04	0.08127141	2.799856e-04
0.5	0.09671669	3.507823e-04	0.08126759	2.838017e-04
1.0	0.09668007	3.873954e-04	0.08123683	3.145648e-04
2.0	0.09653367	5.337948e-04	0.08111383	4.375681e-04
3.0	0.09629065	7.768231e-04	0.08090964	6.417541e-04
4.0	0.09595243	1.115041e-03	0.08062549	9.259083e-04
5.0	0.09552101	1.546462e-03	0.08026304	1.288353e-03

B_1 and B_2 for different value of shape parameter ϵ are reported in Table 7.3.

We can observe that RBF based spatial discretization in conjunction with L-stable Padé scheme for temporal discretization can be implemented to solve multi-asset problem without increasing algebraic complexity of the algorithm. Thus, unlike finite difference, finite element method, pricing multi-asset option problems are significantly simpler.

7.5 Conclusion

In this chapter we have developed a L-stable method suitable for solving exotic options. We observe that the high order L-stable method is efficient for solving multi-asset exotic option as it can be implemented with the same computational complexity as the first order implicit Euler method. Numerical study with one and two dimension problems is carried out with highly accurate results that are in good agreement with those obtained by other numerical and analytical methods in literature.

Concluding remarks and scope for future research

8.1 Conclusions Based on the Thesis

A local radial basis function (RBF) based grid free scheme has been developed for solving option pricing problems, which poses many computational challenges, such as the unstable or slow convergent numerical solutions, multi-asset valuation, complexity of computation domain. An important concept, on which the scheme is based on, is the representation of the function in Lagrange (cardinal) form, i.e, as a linear combination of function values from the neighborhood of the center node with cardinal functions as basis functions. To obtain these cardinal functions in terms of RBFs, interpolation has been performed on the cardinal data using RBFs.

The developed scheme, is tested to solve some standard and non standard option.

In chapter 2 we developed a radial basis function based finite difference method to solve European and American option price problems in computational finance. The spatial discretization is performed by radial basis function based local grid free method to achieve

system of differential equation which are then solved by time integration method. The main difficulty in pricing the American option is due to the fact that these option are allowed to exercise at any time before expiry. We added a small penalty term into PDE to remove the free boundary. The numerical stability of the scheme is also analyzed. Numerical result describing the option value are presented and compared with existing result available in literature.

In chapter 3, we we present a RBF based operator splitting method to price American option in fixed domain.

In chapter 4, we extended the approach used in chapter 2 to solve problems of pricing Asian option.

In chapter 5, we presented a RBF based operator splitting method for pricing American bond option.

In chapter 6, we presented an implicit explicit numerical scheme to solve Jump Diffusion model.

Finally, in chapter 7, we extended this approach in conjunction with high order time integration viz $(0, 4)$ Padé scheme to solve some exotic option , namely European digital call option, a butterfly spread option and double barrier option. Finally we presented some numerical result with these method and shown its superiority with classical finite difference method.

Some advantage of proposed local RBF scheme is:

- The grid free nature of radial basis function made the present scheme grid independent and which provide more flexibility in the choice of local support, which is the main drawback of the grid based methods like finite difference, finite element or finite volume.
- Due to the localization nature, the scheme is able to reduce the ill-conditioning problem of the system, which is main drawback of global collocation method.
- The infinite smoothness of radial functions provide opportunity to approximate not

only option value but its successive derivatives called Greeks.

- The observation that the method converges to classical finite difference scheme (when uniform nodal distributions and the standard choice of supporting nodes as in FD are used) as the shape parameter $\epsilon \rightarrow 0$ makes the scheme a generalization of classical finite difference method.

8.2 Scope for the Future Work

Overall we found that the proposed method are very pleasing. However during the implementation of the scheme, we noticed some issues that require further investigation. Some of these points are:

- The main focus of the present study is on the numerical implementation of developed schemes, however, more investigation is needed on the stability aspects of the scheme.
- Choice of the support domain requires more attention, especially over non-uniform nodal distributions with nodal densities at some regions specially near the strike price.
- For small value of volatility σ the governing problem behave like convection dominated, so development of RBF based upwind finite difference method is another direction of extension.
- A further attention for other option price problems like European and American type Heston's model can be made.
- The present scheme can be modified by including Hermite RBF interpolation and be considered to further improve the accuracy with less number of supporting nodes.

Bibliography

- [1] Walter Allegretto, Yanping Lin, and Hongtao Yang. Numerical pricing of american put options on zero-coupon bonds. *Applied Numerical Mathematics*, 46(2):113–134, 2003.
- [2] Ariel Almendral and Cornelis W Oosterlee. Numerical valuation of options with jumps in the underlying. *Applied Numerical Mathematics*, 53(1):1–18, 2005.
- [3] Bénédicte Alziary, Jean-Paul Décamps, and Pierre-François Koehl. A pde approach to asian options: analytical and numerical evidence. *Journal of Banking & Finance*, 21(5):613–640, 1997.
- [4] Leif Andersen and Jesper Andreasen. Jump-diffusion processes: Volatility smile fitting and numerical methods for option pricing. *Review of Derivatives Research*, 4(3):231–262, 2000.
- [5] Armando Arciniega and Edward Allen. Extrapolation of difference methods in option valuation. *Applied Mathematics and Computation*, 153(1):165–186, 2004.
- [6] Giovanni Barone-Adesi. The saga of the american put. *Journal of Banking & Finance*, 29(11):2909–2918, 2005.
- [7] Victor Bayona, Miguel Moscoso, and Manuel Kindelan. Optimal variable shape parameter for multiquadric based rbf-fd method. *Journal of Computational Physics*, 231(6):2466–2481, 2012.

- [8] Eric Benhamou and Alexandre Duguet. Small dimension pde for discrete asian options. *Journal of Economic Dynamics and Control*, 27(11):2095–2114, 2003.
 - [9] G Bormetti, G Montagna, N Moreni, and O Nicosini. Pricing exotic options in a path integral approach. *Quantitative Finance*, 6(1):55–66, 2006.
 - [10] Phelim P Boyle. Options: A monte carlo approach. *Journal of financial economics*, 4(3):323–338, 1977.
 - [11] Michael J Brennan and Eduardo S Schwartz. Finite difference methods and jump processes arising in the pricing of contingent claims: A synthesis. *Journal of Financial and Quantitative Analysis*, 13(3):461–474, 1978.
 - [12] Maya Briani, Roberto Natalini, and Giovanni Russo. Implicit–explicit numerical schemes for jump–diffusion processes. *Calcolo*, 44(1):33–57, 2007.
 - [13] Mark Broadie and Jerome Detemple. American option valuation: new bounds, approximations, and a comparison of existing methods. *Review of Financial Studies*, 9(4):1211–1250, 1996.
 - [14] David S Bunch and Herb Johnson. A simple and numerically efficient valuation method for american puts using a modified geske-johnson approach. *The Journal of Finance*, 47(2):809–816, 1992.
 - [15] Ralph E Carlson and Thomas A Foley. The parameter r^2 in multiquadric interpolation. *Computers & Mathematics with Applications*, 21(9):29–42, 1991.
 - [16] Peter Carr and Anita Mayo. On the numerical evaluation of option prices in jump diffusion processes. *European Journal of Finance*, 13(4):353–372, 2007.
 - [17] Kalok C Chan, G Andrew Karolyi, Francis A Longstaff, and Anthony B Sanders. An empirical comparison of alternative models of the short-term interest rate. *The journal of finance*, 47(3):1209–1227, 1992.
-

- [18] Ron Tat Lung Chan and Simon Hubbert. Options pricing under the one-dimensional jump-diffusion model using the radial basis function interpolation scheme. *Review of Derivatives Research*, 17(2):161–189, 2014.
- [19] Kuan-Wen Chen and Yuh-Dauh Lyuu. Accurate pricing formulas for asian options. *Applied Mathematics and Computation*, 188(2):1711–1724, 2007.
- [20] Chung-Ki Cho, Sunbu Kang, Taekkeun Kim, and Yonghoon Kwon. Parameter estimation approach to the free boundary for the pricing of an american call option. *Computers & Mathematics with Applications*, 51(5):713–720, 2006.
- [21] S Choi and MD Marcozzi. The valuation of foreign currency options under stochastic interest rates. *Computers & Mathematics with Applications*, 46(5):741–749, 2003.
- [22] Youngsoo Choi and Tony S Wirjanto. An analytic approximation formula for pricing zero-coupon bonds. *Finance Research Letters*, 4(2):116–126, 2007.
- [23] San-Lin Chung, Mao-Wei Hung, and Jr-Yan Wang. Tight bounds on american option prices. *Journal of Banking & Finance*, 34(1):77–89, 2010.
- [24] Simon S Clift and Peter A Forsyth. Numerical solution of two asset jump diffusion models for option valuation. *Applied Numerical Mathematics*, 58(6):743–782, 2008.
- [25] Georges Courtadon. A more accurate finite difference approximation for the valuation of options. *Journal of Financial and Quantitative Analysis*, 17(5):697–703, 1982.
- [26] Georges Courtadon. The pricing of options on default-free bonds. *Journal of Financial and Quantitative Analysis*, 17(01):75–100, 1982.
- [27] Oleg Davydov and Dang Thi Oanh. On the optimal shape parameter for gaussian radial basis function finite difference approximation of the poisson equation. *Computers & Mathematics with Applications*, 62(5):2143–2161, 2011.

- [28] Oleg Davydov and Dang Thi Oanh. On the optimal shape parameter for gaussian radial basis function finite difference approximation of the poisson equation. *Computers & Mathematics with Applications*, 62(5):2143–2161, 2011.
 - [29] Yann dHalluin, Peter A Forsyth, and George Labahn. A penalty method for american options with jump diffusion processes. *Numerische Mathematik*, 97(2):321–352, 2004.
 - [30] Yann dHalluin, Peter A Forsyth, and Kenneth R Vetzal. Robust numerical methods for contingent claims under jump diffusion processes. *IMA Journal of Numerical Analysis*, 25(1):87–112, 2005.
 - [31] Tobin A Driscoll and Bengt Fornberg. Interpolation in the limit of increasingly flat radial basis functions. *Computers & Mathematics with Applications*, 43(3):413–422, 2002.
 - [32] Malin Engström and Lars Nordén. The early exercise premium in american put option prices. *Journal of Multinational Financial Management*, 10(3):461–479, 2000.
 - [33] Gregory E Fasshauer. Solving partial differential equations by collocation with radial basis functions. In *Proceedings of Chamonix*, volume 1997, pages 1–8. Citeseer, 1996.
 - [34] Gregory E Fasshauer. Hermite interpolation with radial basis functions on spheres. *Advances in Computational Mathematics*, 10(1):81–96, 1999.
 - [35] Gregory Eric Fasshauer, Abdul Qayyum Masud Khaliq, and David Albert Voss. Using meshfree approximation for multi-asset american options. *Journal of the Chinese Institute of Engineers*, 27(4):563–571, 2004.
 - [36] Michael S Floater and Armin Iske. Multistep scattered data interpolation using compactly supported radial basis functions. *Journal of Computational and Applied Mathematics*, 73(1):65–78, 1996.
-

- [37] Bengt Fornberg and Grady Wright. Stable computation of multiquadric interpolants for all values of the shape parameter. *Computers & Mathematics with Applications*, 48(5):853–867, 2004.
 - [38] Bengt Fornberg and Julia Zuev. The runge phenomenon and spatially variable shape parameters in rbf interpolation. *Computers & Mathematics with Applications*, 54(3):379–398, 2007.
 - [39] Bengt Fornberg, Grady Wright, and Elisabeth Larsson. Some observations regarding interpolants in the limit of flat radial basis functions. *Computers & mathematics with applications*, 47(1):37–55, 2004.
 - [40] Bengt Fornberg, Elisabeth Larsson, and Natasha Flyer. Stable computations with gaussian radial basis functions. *SIAM Journal on Scientific Computing*, 33(2):869–892, 2011.
 - [41] Bengt Fornberg, Erik Lehto, and Collin Powell. Stable calculation of gaussian-based rbf-fd stencils. *Computers & Mathematics with Applications*, 2012.
 - [42] PA Forsyth and KR Vetzal. Quadratic convergence for valuing american options using a penalty method. *SIAM Journal on Scientific Computing*, 23(6):2095–2122, 2002.
 - [43] Carsten Franke and Robert Schaback. Convergence order estimates of meshless collocation methods using radial basis functions. *Advances in Computational Mathematics*, 8(4):381–399, 1998.
 - [44] Carsten Franke and Robert Schaback. Solving partial differential equations by collocation using radial basis functions. *Applied Mathematics and Computation*, 93(1):73–82, 1998.
 - [45] Richard Franke. Scattered data interpolation: Tests of some methods. *Mathematics of computation*, 38(157):181–200, 1982.
-

- [46] Michael C Fu, Dilip B Madan, and Tong Wang. Pricing continuous asian options: a comparison of monte carlo and laplace transform inversion methods. *Journal of Computational Finance*, 2(2):49–74, 1999.
- [47] Halyette Geman and Marc Yor. Bessel processes, asian options, and perpetuities. *Mathematical Finance*, 3(4):349–375, 1993.
- [48] Robert Geske and Herb E Johnson. The american put option valued analytically. *The Journal of Finance*, 39(5):1511–1524, 1984.
- [49] Robert Geske and Kuldeep Shastri. Valuation by approximation: a comparison of alternative option valuation techniques. *Journal of Financial and Quantitative Analysis*, 20(1):45–71, 1985.
- [50] Robert Geske and Kuldeep Shastri. Valuation by approximation: a comparison of alternative option valuation techniques. *Journal of Financial and Quantitative Analysis*, 20(1):45–71, 1985.
- [51] Michael B Giles and Rebecca Carter. Convergence analysis of crank-nicolson and rannacher time-marching. *Journal of Computational Finance*, 9(2):89–112, 2006.
- [52] Ahmad Golbabai, Davood Ahmadian, and Mariyan Milev. Radial basis functions with application to finance: American put option under jump diffusion. *Mathematical and Computer Modelling*, 55(3):1354–1362, 2012.
- [53] Yumi Goto, Zhai Fei, Shen Kan, and Eisuke Kita. Options valuation by using radial basis function approximation. *Engineering analysis with boundary elements*, 31(10):836–843, 2007.
- [54] Houde Han and Xiaonan Wu. A fast numerical method for the black–scholes equation of american options. *SIAM Journal on Numerical Analysis*, 41(6):2081–2095, 2003.
- [55] Rolland L Hardy. Multiquadric equations of topography and other irregular surfaces. *Journal of geophysical research*, 76(8):1905–1915, 1971.

- [56] Steve Heston and Guofu Zhou. On the rate of convergence of discrete-time contingent claims. *Mathematical Finance*, 10(1):53–75, 2000.
- [57] YC Hon and Robert Schaback. On unsymmetric collocation by radial basis functions. *Applied Mathematics and Computation*, 119(2):177–186, 2001.
- [58] Yiu-Chung Hon. A quasi-radial basis functions method for american options pricing. *Computers & Mathematics with Applications*, 43(3):513–524, 2002.
- [59] Yiu-Chung Hon and Xian-Zhong Mao. A radial basis function method for solving options pricing models. *Journal of Financial Engineering*, 8:31–50, 1999.
- [60] Jing-zhi Huang, Marti G Subrahmanyam, and G George Yu. Pricing and hedging american options: a recursive investigation method. *Review of Financial Studies*, 9(1):277–300, 1996.
- [61] John Hull. *Options, Futures, and Other Derivatives, 7/e (With CD)*. Pearson Education India, 2010.
- [62] Samuli Ikonen and Jari Toivanen. Operator splitting methods for american option pricing. *Applied Mathematics Letters*, 17(7):809–814, 2004.
- [63] Jonathan E Ingersoll. *Theory of financial decision making*, volume 3. Rowman & Littlefield, 1987.
- [64] Armin Iske. Reconstruction of functions from generalized hermite-birkhoff data. *Series in approximations and decompositions*, 6:257–264, 1995.
- [65] VP Israel and MA Rincon. Variational inequalities applied to option market problem. *Applied Mathematics and Computation*, 201(1):384–397, 2008.
- [66] Vecer Jan. A new pde approach for pricing arithmetic average asian options. *Journal of Computational Finance*, 1(2):105–113, 2001.

- [67] Nengjiu Ju. Pricing by american option by approximating its early exercise boundary as a multipiece exponential function. *Review of Financial Studies*, 11(3):627–646, 1998.
- [68] Nengjiu Ju. Pricing asian and basket options via taylor expansion. *Journal of Computational Finance*, 5(3):79–103, 2002.
- [69] Siim Kallast and Andi Kivinukk. Pricing and hedging american options using approximations by kim integral equations. *European Finance Review*, 7(3):361–383, 2003.
- [70] Edward J Kansa. Multiquadrics-a scattered data approximation scheme with applications to computational fluid-dynamics-i surface approximations and partial derivative estimates. *Computers & Mathematics with applications*, 19(8):127–145, 1990.
- [71] Edward J Kansa. Multiquadrics-a scattered data approximation scheme with applications to computational fluid-dynamics-ii solutions to parabolic, hyperbolic and elliptic partial differential equations. *Computers & mathematics with applications*, 19(8):147–161, 1990.
- [72] EJ Kansa and RE Carlson. Improved accuracy of multiquadric interpolation using variable shape parameters. *Computers & Mathematics with Applications*, 24(12):99–120, 1992.
- [73] Angeliem G Z Kemna and A C F Vorst. A pricing method for options based on average asset values. *Journal of Banking & Finance*, 14(1):113–129, 1990.
- [74] Mohmed Hassan Mohmed Khabir. *Numerical singular perturbation approaches based on spline approximation methods for solving problems in computational finance*. PhD thesis, Department of Mathematics and Applied Mathematics at the Faculty of Natural Sciences, University of the Western Cape, 2011.

- [75] Mohmed HM Khabir and Kailash C Patidar. Spline approximation method to solve an option pricing problem. *Journal of Difference Equations and Applications*, 18(11):1801–1816, 2012.
 - [76] A Q M Khaliq, E H Twizell, and D A Voss. On parallel algorithms for semidiscretized parabolic partial differential equations based on subdiagonal padé approximations. *Numerical Methods for Partial Differential Equations*, 9(2):107–116, 1993.
 - [77] A Q M Khaliq, D A Voss, and S H K Kazmi. A linearly implicit predictor–corrector scheme for pricing american options using a penalty method approach. *Journal of Banking & Finance*, 30(2):489–502, 2006.
 - [78] A Q M Khaliq, D A Voss, and M Yousuf. Pricing exotic options with l-stable padé schemes. *Journal of Banking & Finance*, 31(11):3438–3461, 2007.
 - [79] A Q M Khaliq, B A Wade, M Yousuf, and Jesús Vigo-Aguiar. High order smoothing schemes for inhomogeneous parabolic problems with applications in option pricing. *Numerical Methods for Partial Differential Equations*, 23(5):1249–1276, 2007.
 - [80] A Q M Khaliq, D A Voss, and K Kazmi. Adaptive θ -methods for pricing american options. *Journal of Computational and Applied Mathematics*, 222(1):210–227, 2008.
 - [81] Steven G Kou. A jump-diffusion model for option pricing. *Management science*, 48(8):1086–1101, 2002.
 - [82] YongHoon Kwon and Younhee Lee. A second-order tridiagonal method for american options under jump-diffusion models. *SIAM Journal on Scientific Computing*, 33(4):1860–1872, 2011.
 - [83] YongHoon Kwon and Younhee Lee. A second-order finite difference method for option pricing under jump-diffusion models. *SIAM Journal on Numerical Analysis*, 49(6):2598–2617, 2011.
-

- [84] Elisabeth Larsson, Krister Åhlander, and Andreas Hall. Multi-dimensional option pricing using radial basis functions and the generalized fourier transform. *Journal of Computational and Applied Mathematics*, 222(1):175–192, 2008.
- [85] Jean Bernard Lasserre, Tomas Prieto-Rumeau, and Mihail Zervos. Pricing a class of exotic options via moments and sdp relaxations. *Mathematical Finance*, 16(3): 469–494, 2006.
- [86] Snorre Lindset and Arne-Christian Lund. A monte carlo approach for the american put under stochastic interest rates. *Journal of Economic Dynamics and Control*, 31 (4):1081–1105, 2007.
- [87] WR Madych. Miscellaneous error bounds for multiquadric and related interpolators. *Computers & Mathematics with Applications*, 24(12):121–138, 1992.
- [88] WR Madych and SA Nelson. Bounds on multivariate polynomials and exponential error estimates for multiquadric interpolation. *Journal of Approximation Theory*, 70 (1):94–114, 1992.
- [89] John C Mairhuber. On haar’s theorem concerning chebychev approximation problems having unique solutions. In *Proceedings of the American Mathematical Society*, volume 7, pages 609–615, 1956.
- [90] Stilianos Markolefas. Standard galerkin formulation with high order lagrange finite elements for option markets pricing. *Applied Mathematics and Computation*, 195(2): 707–720, 2008.
- [91] H.P. McKean. Appendix: A free boundary problem for the heat equation arising from a problem in mathematical economics. *Industrial Management Review*, (2): 32–39, 1965.
- [92] Robert C Merton. Option pricing when underlying stock returns are discontinuous. *Journal of financial economics*, 3(1):125–144, 1976.

- [93] Robert C Merton, Michael J Brennan, and Eduardo S Schwartz. The valuation of american put options. *The Journal of Finance*, 32(2):449–462, 1977.
 - [94] Charles A Micchelli. *Interpolation of scattered data: distance matrices and conditionally positive definite functions*. Springer, 1984.
 - [95] Pierre Moerbeke. On optimal stopping and free boundary problems. *Archive for Rational Mechanics and Analysis*, 60(2):101–148, 1976.
 - [96] W Mudzimbabwe, Kailash C Patidar, and Peter J Witbooi. A reliable numerical method to price arithmetic asian options. *Applied Mathematics and Computation*, 218(22):10934–10942, 2012.
 - [97] Francis J Narcowich and Joseph D Ward. Norm estimates for the inverses of a general class of scattered-data radial-function interpolation matrices. *Journal of Approximation Theory*, 69(1):84–109, 1992.
 - [98] Edgard Ngounda, Kailash C Patidar, and Edson Pindza. Contour integral method for european options with jumps. *Communications in Nonlinear Science and Numerical Simulation*, 2012.
 - [99] Bjørn Fredrik Nielsen, Ola Skavhaug, and Aslak Tveito. Penalty and front-fixing methods for the numerical solution of american option problems. *Journal of Computational Finance*, 5(4):69–98, 2002.
 - [100] Bjørn Fredrik Nielsen, Ola Skavhaug, and Aslak Tveito. Penalty methods for the numerical solution of american multi-asset option problems. *Journal of Computational and Applied Mathematics*, 222(1):3–16, 2008.
 - [101] Konstantinos N Pantazopoulos. *Numerical methods and software for the pricing of American financial derivatives*. PhD thesis, Computer Science Department, Purdue University, 1998.
-

- [102] Ulrika Pettersson, Elisabeth Larsson, Gunnar Marcusson, and Jonas Persson. Improved radial basis function methods for multi-dimensional option pricing. *Journal of Computational and Applied Mathematics*, 222(1):82–93, 2008.
- [103] David M Pooley, Kenneth R Vetzal, and Peter A Forsyth. Convergence remedies for non-smooth payoffs in option pricing. *Journal of Computational Finance*, 6(4):25–40, 2003.
- [104] Michael JD Powell. The theory of radial basis function approximation in 1990. *Advances in numerical analysis*, 2:105–210, 1992.
- [105] N Rambeerich, DY Tangman, A Gopaul, and M Bhuruth. Exponential time integration for fast finite element solutions of some financial engineering problems. *Journal of Computational and Applied Mathematics*, 224(2):668–678, 2009.
- [106] Rolf Rannacher. Finite element solution of diffusion problems with irregular data. *Numerische Mathematik*, 43(2):309–327, 1984.
- [107] Shmuel Rippa. An algorithm for selecting a good value for the parameter c in radial basis function interpolation. *Advances in Computational Mathematics*, 11(2-3):193–210, 1999.
- [108] L C G Rogers and Z Shi. The value of an asian option. *Journal of Applied Probability*, pages 1077–1088, 1995.
- [109] AAEF Saib, Desire Yannick Tangman, and Muddun Bhuruth. A new radial basis functions method for pricing american options under merton’s jump-diffusion model. *International Journal of Computer Mathematics*, 89(9):1164–1185, 2012.
- [110] YVSS Sanyasiraju and G Chandhini. Local radial basis function based gridfree scheme for unsteady incompressible viscous flows. *Journal of Computational Physics*, 227(20):8922–8948, 2008.

- [111] YVSS Sanyasiraju and Chirala Satyanarayana. Rbf based grid-free local scheme with spatially variable optimal shape parameter for steady convection-diffusion equations. *CFD Letters*, 4(4):152–172, 2012.
 - [112] YVSS Sanyasiraju and Chirala Satyanarayana. On optimization of the rbf shape parameter in a grid-free local scheme for convection dominated problems over non-uniform centers. *Applied Mathematical Modelling*, 37(12):7245–7272, 2013.
 - [113] Scott A Sarra and Derek Sturgill. A random variable shape parameter strategy for radial basis function approximation methods. *Engineering analysis with boundary elements*, 33(11):1239–1245, 2009.
 - [114] Robert Schaback. Error estimates and condition numbers for radial basis function interpolation. *Advances in Computational Mathematics*, 3(3):251–264, 1995.
 - [115] IJ Schoenberg. Metric spaces and completely monotone functions. *Annals of Mathematics*, 39:811–841, 1938.
 - [116] Eduardo S Schwartz. The valuation of warrants: implementing a new approach. *Journal of Financial Economics*, 4(1):79–93, 1977.
 - [117] Rüdiger Seydel. *Tools for computational finance*. Springer, 2012.
 - [118] Li ShuJin and Li ShengHong. Pricing american interest rate option on zero-coupon bond numerically. *Applied Mathematics and Computation*, 175(1):834–850, 2006.
 - [119] Abdelmgid Osman Mohammed Sidahmed. *Mesh Free Methods for Differential Models in Financial Mathematics*. PhD thesis, Department of Mathematics and Applied Mathematics at the Faculty of Natural Sciences, University of the Western Cape, 2011.
 - [120] Ronald Smith. Optimal and near-optimal advection-diffusion finite-difference schemes. ii. unsteadiness and non-uniform grid. *Proceedings of the Royal Society*
-

- of London. Series A: Mathematical, Physical and Engineering Sciences*, 456(1995): 489–502, 2000.
- [121] Ghulam Sorwar, Giovanni Barone-Adesi, and Walter Allegretto. Valuation of derivatives based on single-factor interest rate models. *Global Finance Journal*, 18(2): 251–269, 2007.
- [122] Xingping Sun. Scattered hermite interpolation using radial basis functions. *Linear algebra and its applications*, 207:135–146, 1994.
- [123] DY Tangman, A Gopaul, and M Bhuruth. Exponential time integration and chebyshev discretisation schemes for fast pricing of options. *Applied Numerical Mathematics*, 58(9):1309–1319, 2008.
- [124] DY Tangman, A Gopaul, and M Bhuruth. A fast high-order finite difference algorithm for pricing american options. *Journal of Computational and Applied Mathematics*, 222(1):17–29, 2008.
- [125] DY Tangman, N Thakoor, K Dookhitram, and M Bhuruth. Fast approximations of bond option prices under ckl models. *Finance Research Letters*, 8(4):206–212, 2011.
- [126] GWP Thompson. *Fast narrow bounds on the value of Asian options*. Judge Institute of Management Studies, 2002.
- [127] Jari Toivanen. Numerical valuation of european and american options under kou’s jump-diffusion model. *SIAM Journal on Scientific Computing*, 30(4):1949–1970, 2008.
- [128] Carlos Vázquez. An upwind numerical approach for an american and european option pricing model. *Applied Mathematics and Computation*, 97(2):273–286, 1998.
- [129] BA Wade, AQM Khaliq, M Yousuf, Jesús Vigo-Aguiar, and R Deininger. On smoothing of the crank–nicolson scheme and higher order schemes for pricing barrier options. *Journal of Computational and Applied Mathematics*, 204(1):144–158, 2007.
-

- [130] Holger Wendland. Piecewise polynomial, positive definite and compactly supported radial functions of minimal degree. *Advances in computational Mathematics*, 4(1): 389–396, 1995.
- [131] Holger Wendland. Error estimates for interpolation by compactly supported radial basis functions of minimal degree. *Journal of approximation theory*, 93(2):258–272, 1998.
- [132] Paul Wilmott. *The mathematics of financial derivatives: a student introduction*. Cambridge University Press, 1995.
- [133] Grady B Wright and Bengt Fornberg. Scattered node compact finite difference-type formulas generated from radial basis functions. *Journal of Computational Physics*, 212(1):99–123, 2006.
- [134] Lixin Wu and Yue-Kuen Kwok. A front-fixing finite difference method for the valuation of american options. *Journal of Financial Engineering*, 6(4):83–97, 1997.
- [135] Zong-min Wu and Robert Schaback. Local error estimates for radial basis function interpolation of scattered data. *IMA journal of Numerical Analysis*, 13(1):13–27, 1993.
- [136] Zongmin Wu. Compactly supported positive definite radial functions. *Advances in Computational Mathematics*, 4(1):283–292, 1995.
- [137] Jungho Yoon. Spectral approximation orders of radial basis function interpolation on the sobolev space. *SIAM journal on mathematical analysis*, 33(4):946–958, 2001.
- [138] M Yousuf. Efficient smoothing of crank-nicolson method for pricing barrier options under stochastic volatility. *Proceedings in Applied Mathematics and Mechanics*, 7(1): 1081101–1081102, 2007.

- [139] M Yousuf. Efficient l-stable method for parabolic problems with application to pricing american options under stochastic volatility. *Applied Mathematics and Computation*, 213(1):121–136, 2009.
- [140] M Yousuf. A fourth-order smoothing scheme for pricing barrier options under stochastic volatility. *International Journal of Computer Mathematics*, 86(6):1054–1067, 2009.
- [141] Jin Zhang. A semi-analytical method for pricing and hedging continuously sampled arithmetic average rate options. *Journal of Computational Finance*, 5(1):59–80, 2001.
- [142] Jin E Zhang. Pricing continuously sampled asian options with perturbation method. *Journal of Futures Markets*, 23(6):535–560, 2003.
- [143] Kai Zhang and Song Wang. Pricing options under jump diffusion processes with fitted finite volume method. *Applied Mathematics and Computation*, 201(1):398–413, 2008.
- [144] Kai Zhang and Song Wang. Pricing american bond options using a penalty method. *Automatica*, 48(3):472–479, 2012.
- [145] Peter G Zhang. *Exotic options*. World Scientific, 1998.
- [146] Jichao Zhao, Matt Davison, and Robert M Corless. Compact finite difference method for american option pricing. *Journal of Computational and Applied Mathematics*, 206(1):306–321, 2007.
- [147] Hong Jun Zhou, Ka Fai Cedric Yiu, and Leong Kwan Li. Evaluating american put options on zero-coupon bonds by a penalty method. *Journal of computational and applied mathematics*, 235(13):3921–3931, 2011.
- [148] Wu Zongmin. Hermite-birkhoff interpolation of scattered data by radial basis functions. *Approximation Theory and its Applications*, 8(2):1–10, 1992.
- [149] Robert Zvan, Peter A Forsyth, and Kenneth Roy Vetzal. Robust numerical methods for pde models of asian options. *Journal of Computational Finance*, 1(2):39–78, 1998.

- [150] Robert Zvan, Peter A Forsyth, and Kenneth Roy Vetzal. Penalty methods for american options with stochastic volatility. *Journal of Computational and Applied Mathematics*, 91(2):199–218, 1998.
- [151] Robert Zvan, Peter A Forsyth, and Kenneth Roy Vetzal. Pde methods for pricing barrier options. *Journal of Economic Dynamics and Control*, 24(2):1563–1590, 2000.